Two-Step Nonlinear ARDL Estimation of the Relationship between R&D Intensity and Investment*

JIN SEO CHO
School of Economics, Yonsei University, Seoul, South Korea
Email: jinseocho@yonsei.ac.kr

MATTHEW GREENWOOD-NIMMO
Faculty of Business and Economics, University of Melbourne, Carlton, VIC 3053, Australia
Melbourne Centre for Data Science, University of Melbourne, Parkville, VIC 3010, Australia
Centre for Applied Macroeconomic Analysis, Australian National University, Canberra, ACT 2600, Australia
Codera Analytics, Johannesburg, GP 2193, South Africa
Email: matthew.greenwood@unimelb.edu.au

YONGCHEOL SHIN
Department of Economics and Related Studies, University of York, York, U.K.
Email: yongcheol.shin@york.ac.uk

This version: September 2023

Abstract

We investigate the relationship between R&D expenditure and investment using a nonlinear autoregressive distributed lag (NARDL) model. We propose a new and analytically tractable two-step NARDL (2SNARDL) estimation framework, in which the parameters of the long-run relationship are estimated first using the fully-modified least squares estimator before the dynamic parameters are estimated by ordinary least squares in the next step. We show that the 2SNARDL estimator is consistent for the parameters of the NARDL model under mild regularity conditions. We derive the relevant limit distributions and develop Wald test statistics for the hypotheses of short-run and long-run parameter asymmetry. We use the 2SNARDL procedure to show that R&D expenditure is asymmetrically associated with physical investment in the U.S.

Key Words: R&D Expenditure; Physical Investment; Nonlinear Autoregressive Distributed Lag (NARDL) Model; Two-step Estimation; Wald Test Statistic.

JEL Classifications: C22, E22, O32.

---

*This is a substantially revised version of an earlier manuscript circulated under the title "Two-Step Estimation of the Nonlinear Autoregressive Distributed Lag Model." We are grateful for the insightful comments of In Choi, Tae-Hwan Kim, Rui Lin, Viet Nguyen and Michael Thornton, as well as seminar participants at the Universities of Melbourne, Yonsei and York. Cho is grateful for financial support from the Ministry of Education of the Republic of Korea and the National Research Foundation of Korea (Grant number NRF-2019S1A5A2A01035568). Greenwood-Nimmo and Shin acknowledge financial support from the Economic and Social Research Council (Grant number ES/T01573X/1). The views expressed herein are those of the authors and should not be reported as the views of Codera Analytics. The usual disclaimer applies.

1 Introduction

The relationship between research and development (R&D) and physical investment has received little empirical attention, despite its importance in the study of innovation and growth. R&D expenditure is often characterized simply as an investment in knowledge creation that may lead to an innovation with some probability; that innovation then requires physical investment in order to be implemented (see Lach and Rob, 1996). However, this mechanism is overly simplistic, as it fails to distinguish among different types of R&D activity. For example, the product life cycle literature distinguishes between early-stage R&D that is often associated with new product development and later-stage R&D that tends to focus on scaling production and achieving efficiency gains (e.g., Gort and Wall, 1986; Audretsch, 1987). In this paper, we develop a novel theoretical model in which early-stage R&D and physical investment are complements, while later-stage R&D is a substitute for physical investment. Using quarterly U.S. time series data over the period 1960q1 to 2019q4, we provide empirical support for this distinction. Our results also reveal a long-run asymmetry in the relationship between aggregate R&D intensity and real physical investment that may have implications for the design and implementation of innovation policy.

We begin by proposing a novel theory relating early-stage and later-stage R&D expenditures to physical investment. For convenience of terminology, we henceforth refer to early-stage R&D as *innovative R&D* and to later-stage R&D as *managerial R&D*. In our model, the roles of innovative and managerial R&D expenditures differ. Innovative R&D expenditure determines the scope of production, as it describes a research activity that creates a new product or technology through the discovery of a novel production function. The more innovative R&D activity, the larger the scale of production, which implies that the limit of production activity is determined by the amount of innovative R&D activity. By contrast, managerial R&D activity does not create a new product, but produces an existing product more efficiently, implying that less physical capital is required per unit of output.

Our theoretical model delivers the testable hypothesis that innovative R&D expenditure and physical investment are positively related by virtue of their complementarity, while the sign of the relationship between managerial R&D expenditure and physical investment may be either positive or negative due to their nature as substitutes. To test these implications, we derive an empirical specifi-

cation that relates real physical investment to aggregate R&D intensity (defined as the ratio of R&D expenditure to GDP) using quarterly U.S. data spanning the period 1960q1 to 2019q4. Our model distinguishes between periods in which innovative and managerial R&D predominate based on the sign of the growth rate of R&D intensity. Noting that aggregate R&D expenditure incorporates the spectrum of R&D activities conducted throughout the economy and assuming that innovative (managerial) R&D expenditures are larger (smaller) than the output that they generate, it follows that the sign of Δr_t can be interpreted in terms of the relative prevalence of innovative and managerial R&D activity in the economy. If $\Delta r_t \geq 0$, then R&D expenditure is growing at least as fast as output, indicating the prevalence of innovative R&D activity. By contrast, if $\Delta r_t < 0$, then output is growing faster than R&D expenditure, indicating the prevalence of managerial R&D activity.

Our empirical specification takes the form of a nonlinear autoregressive distributed lag (NARDL) model. The NARDL model proposed by Shin, Yu, and Greenwood-Nimmo (2014, hereafter SYG) is an asymmetric generalization of the linear ARDL model of Pesaran and Shin (1998) and Pesaran et al. (2001). It is a single-equation error-correction model that has been widely applied to accommodate asymmetry in the long-run equilibrium relationship and/or the short-run dynamic coefficients via the use of partial sum decomposition of the independent variable(s). The NARDL approach has grown in popularity in recent years, with applications in fields including criminology (Box et al., 2018), economic growth (Eberhardt and Presbitero, 2015), energy economics (Hammoudeh et al., 2015), exchange rates and trade (Verheyen, 2013; Brun-Aguerre et al., 2017), financial economics (He and Zhou, 2018), health economics (Barati and Fariditavana, 2018), the economics of tourism (Süssmuth and Woitek, 2013) and political science (Ferris et al., 2020), to list only a few. See Cho et al. (2023) for an extensive survey.

The NARDL model has two attributes that make it particularly suitable for the problem at hand. First, it naturally accommodates a notable feature of our dataset, which is the mis-match in the time trends between the dependent and independent variables—physical investment is a unit root process with a clear upward time trend, while R&D intensity is trendless unit root process. In a typical cointegrating model, to capture the cointegrating relationship between these variables, one would be obliged to include a deterministic time trend as a regressor. This is a practical but somewhat unsatisfactory solution, as it implies that the cointegrating relationship cannot be fully explained by the posited model

structure. Specifically, the process that generates the time trend is not explained within the model. By contrast, in the NARDL model, the asymmetry introduced through the partial sum decomposition of R&D intensity drives the time trend in physical investment, such that the model structure itself directly explains how variables with mismatched time trends can be cointegrated. Second, the NARDL model provides a natural vehicle to test for sign-asymmetry in the relationship between R&D intensity and physical investment, in line with our theoretical model. Asymmetry can be tested analytically in either or both of the short-run and the long-run, and can be tested at any horizon by applying bootstrap inference to the cumulative dynamic multiplier effects obtained from the model parameters.

Use of the NARDL model is complicated by the fact that the theoretical foundations for estimation of and inference on the model parameters have yet to be fully developed. SYG provide simulation evidence that the parameters of the NARDL model can be consistently estimated in a single step by ordinary least squares (OLS), even though the positive and negative partial sums of the independent variables are dominated by deterministic trend terms that are asymptotically perfectly collinear. This collinearity introduces an asymptotic singularity problem that represents a barrier to the development of asymptotic theory for the single-step estimation framework. Consequently, SYG do not provide asymptotic results for the single-step OLS estimator or any associated inferential procedures.

We propose a new and analytically tractable two-step estimation procedure that overcomes this issue. First, for a bivariate model with a scalar dependent variable and a scalar explanatory variable, the asymmetric long-run relationship is expressed among the level of the dependent variable and the positive and negative cumulative partial sums of the explanatory variable, leading to the singular matrix problem. We resolve this problem by excluding one of the partial sum processes and replacing it with the original explanatory variable. We show that the long-run parameters of interest can be consistently estimated from this re-parameterized model while avoiding the singularity issue by virtue of the different convergence rates between the regressors. By applying the fully-modified OLS (FM-OLS) estimator of Phillips and Hansen (1990) to this first-step estimation problem, we obtain an estimator that asymptotically follows a mixed normal distribution. This facilitates standard inference on the long-run parameters. Given the super-consistency of the long-run parameter estimator, the error-correction term can be treated as known in the second step, where OLS estimation yields a consistent and asymptotically normal estimator of the short-run parameters.

In the multivariate case, a further singular matrix problem arises at the limit when estimating the re-parameterized long-run equation due to the collinearity of the trends in the regressors. We show that this issue can be resolved by adding an initial detrending step before applying the two-step procedure described above. Specifically, one first detrends the partial sum processes using OLS and then employs the OLS residuals as an explanatory variable together with a time trend and the original explanatory variable. This procedure allows for consistent estimation of the long-run relationship without any singularity problem in models with multiple explanatory variables.

By applying our two-step estimation procedure to analyze the relationship between R&D intensity and physical investment, we find that, in the long-run, physical investment responds positively to R&D expenditures when their growth rate exceeds the growth rate of GDP and negatively when they are growing more slowly than GDP. This supports our theoretical prediction regarding the nature of innovative (managerial) R&D expenditure as a complement to (substitute for) physical investment. Furthermore, we find that physical investment is more sensitive to changes in R&D intensity when the growth rate of R&D expenditure is less than that of GDP (i.e. when managerial R&D activity predominates).

This paper proceeds in 7 sections. In Section 2, we review the literature on R&D expenditure and investment and propose a novel theoretical model of their relationship. In Sections 3 and 4, we introduce the NARDL model and explore the asymptotic singularity problem mentioned above. We then introduce our two-step estimation framework and develop Wald tests for the null hypotheses of short-run and long-run symmetry. In Section 5, we scrutinize the finite sample properties of our estimators and test statistics by simulation. Section 6 is devoted to our empirical analysis of the relationship between R&D intensity and physical investment. We conclude in Section 7. Detailed proofs and additional results are collected in an Online Supplement.

2 Literature Review and Stylized Model

In this section, we review the literature and develop a theory that predicts an asymmetric relationship between R&D intensity and investment.

2.1 The Relationship between R&D Expenditure and Investment

Following Schumpeter's seminal 1942 work on creative destruction, a large literature has emerged on aspects of R&D activities. Important contributions include Utterback and Abernathy (1975), who find that R&D activity is conducted differently across the different stages of product life, the product life-cycle theory developed by Gort and Wall (1986) and Audretsch (1987), and the game-theoretic approach to R&D activity associated with Kamien and Schwartz (1972), Reinganum (1982), Fudenberg et al. (1983), Grossman and Shapiro (1987) and Harris and Vickers (1987).

It is common to distinguish between two different stages of R&D activity. Early-stage (innovative) R&D expenditure focuses on the development of a new product or technology, leading to a subsequent large-scale investment. By contrast, later-stage (managerial) R&D expenditure focuses on improvements to production efficiency. Consequently, managerial R&D expenditure should not exceed the expected increase in output, which results in a smaller-scale investments than innovative R&D. Overall, R&D expenditure tends to increase sharply in the early stage before leveling off or decreasing at the later stage.

A number of theoretical studies differentiate between innovative and managerial R&D activities and their effects on other economic variables, including Klepper (1996, 1997) and Agarwal and Audretsch (2001). Likewise, Comin and Philippon (2005) and Aghion et al. (2009) empirically examine the relationship between the entry and/or exit rate of firms and innovative R&D expenditure. Similar theories have been developed in other fields including engineering and management—for example, Zif and McCarthy (1997), who classify R&D activity into multiple stages following the product life-cycle theory (see also Chung and Shin, 2020).

However, one area in which the distinction between innovative and managerial R&D activity is yet to be fully investigated is the relationship between R&D expenditure and investment. Early studies (e.g. Schmookler, 1966) focus on the causal relationship between R&D expenditure and investment. Applying vector autoregressions (VARs) to firm- and industry-level data, Lach and Schankerman (1989) and Lach and Rob (1996) find that R&D expenditure Granger causes investment but not *vice versa*. However, using longer time series, Chiao (2001) documents a two-way causal relationship between the growth rates of the R&D expenditure and investment. Employing a vector error-correction (VEC) model, Baussola (2000) documents evidence in favor of unidirectional Granger causality from

R&D expenditure to investment. These existing results should be treated with care, however, as the failure to distinguish between innovative and managerial R&D activity undermines efforts to accurately capture the potentially asymmetric relationship between R&D expenditure and investment.

2.2 The Asymmetric Relationship between R&D Intensity and Investment

We propose a novel theoretical model relating innovative and managerial R&D expenditures to investment. In our model, innovative R&D expenditure determines the scope of production, as it describes a research activity that creates a new product or technology through the discovery of a novel production function. The more innovative R&D activity, the larger the scale of production, suggesting that the limit of production activity is determined by the amount of innovative R&D activity. By contrast, managerial R&D activity does not create a new product, but instead produces an existing product more efficiently, implying that less physical capital is required per unit of output.

Let k and y be the levels of physical capital and output, respectively. Furthermore, let c and s be the capital levels converted from innovative and managerial R&D expenditures, respectively. We assume that c is complementary to production activity conducted using physical capital while s is a substitute. Consider a simple production function embodying this mechanism as follows:

$$y = \min[c, k + s]. \tag{1}$$

The complementary relationship with c limits production activity, as output cannot be produced in excess of the level of innovative R&D activity. On the other hand, managerial R&D activity can produce capital s that substitutes for k.[1]

We use a dynamic optimization approach and apply the q-theory of investment to examine how physical investment responds to external shocks to R&D expenditure. First, physical capital, k_t, is formed by accumulating physical investment, i_t, through $\dot{k}_t = i_t - \delta k_t$, where δ is the depreciation rate of the physical capital. Similarly, c_t and s_t, are accumulated through $\dot{c}_t = r_t - \tau c_t$ and $\dot{s}_t = d_t - \gamma s_t$, where τ and γ denote depreciation rates of c_t and s_t, respectively. Next, consider the cost functions

[1] In the Online Supplement, we present a comparative analysis to show how the three types of capital interact in response to external shocks.

associated with converting R&D expenditures and physical investment into capital. Let $\kappa(r_t)$, $\xi(d_t)$ and $\phi(i_t)$ be the cost levels from innovative and managerial R&D expenditure and physical investment, respectively. We assume that the cost functions are convex with respect to R&D expenditures and physical investment, such that $\kappa'(\cdot) > 0$, $\xi'(\cdot) > 0$, $\phi'(\cdot) > 0$, $\kappa''(\cdot) > 0$, $\xi''(\cdot) > 0$, and $\phi''(\cdot) > 0$.[2]

To generalize the production function (1) into a differentiable function, we assume that output is given by $y_t = f(c_t, k_t + s_t)$, where $f(\cdot, \cdot)$ is a differentiable function with $f_c(c, a) > 0$, $f_a(c, a) > 0$, $f_{cc}(c, a) < 0$, $f_{aa}(c, a) < 0$, and $f_{ca}(c, a) > 0$ uniformly on the space of (c, a). Notice that k_t and s_t are strictly substitutes, while c_t and $a_t := k_t + s_t$ are weakly complements.[3]

The representative firm determines the optimal path of capital, investment and R&D expenditures by maximizing discounted aggregate profit:

$$\max_{\{c_t, k_t, s_t, r_t, i_t, d_t\}} \int_0^\infty \{f(c_t, k_t + s_t) - \kappa(r_t) - \phi(i_t) - \xi(d_t)\} e^{-\rho t} dt,$$

subject to $\dot{c}_t = r_t - \tau c_t$, $\dot{k}_t = i_t - \delta k_t$ and $\dot{s}_t = d_t - \gamma s_t$, where ρ is the discount rate. This extends the standard q-theory of investment by considering the role of capital converted from R&D expenditures as well as physical capital, with the three different accumulation rules treated as constraints.[4]

To analyze the long-run relationship between physical investment and R&D expenditures, we set up the dynamic optimization problem using the following Hamiltonian equation:

$$\begin{aligned}
&\mathcal{H}(c_t, k_t, s_t, r_t, i_t, d_t, \nu_t, \lambda_t, \mu_t) \\
&= \{f(c_t, k_t + s_t) - \phi(i_i) - \xi(d_t) - \kappa(r_t)\} e^{-\rho t} + \nu_t(r_t - \tau c_t) + \lambda_t(i_t - \delta k_t) + \mu_t(d_t - \gamma s_t), \quad (2)
\end{aligned}$$

[2]For example, incidental and/or additional costs may be incurred to convert R&D expenditures into capital for production. These include patent fees, monetary or non-monetary incentives for researchers, safety management fees, training costs, and so on. These costs and fees are assumed to form the convex functions.

[3]It is possible to define alternative production functions that exhibit a weakly substitutionary relationship between s_t and k_t. Suppose that the production function (1) can be generalized by the constant elasticity of substitution (CES) function, $\ell(x, y; \beta) := \left(x^{\frac{\beta-1}{\beta}} + y^{\frac{\beta-1}{\beta}}\right)^{\frac{\beta}{\beta-1}}$. Then, we can derive the generalized twofold CES production function: $f(c_t, k_t, s_t; \beta, \sigma) := \ell(c_t, \ell(k_t, s_t; \sigma); \beta)$, from which it follows that $\lim_{\sigma\to\infty} \lim_{\beta\to 0} f(c_t, k_t, s_t; \beta, \sigma) = \min[c_t, k_t + s_t]$. Provided that σ, $\beta > 0$, we can apply optimization theory as the production function is differentiable.

[4]The representative firm is assumed to choose the optimal time paths of r_t and d_t simultaneously, ignoring the fact that innovative R&D activity is conducted earlier than managerial R&D activity. This is not restrictive, as the firm represents a multitude of firms in the economy, where innovative and managerial R&D activities are conducted simultaneously.

from which we derive the following differential equations:

$$\dot{i}_t = \frac{1}{\phi''(i_t)}\left[(\delta+\rho)\phi'(i_t) - f_a(c_t, k_t+s_t)\right], \quad \dot{d}_t = \frac{1}{\xi''(d_t)}\left[(\gamma+\rho)\xi'(d_t) - f_a(c_t, k_t+s_t)\right],$$

$$\dot{r}_t = \frac{1}{\kappa''(i_t)}\left[(\tau+\rho)\kappa'(r_t) - f_c(c_t, k_t+s_t)\right], \quad \dot{c}_t = r_t - \tau c_t, \quad \dot{k}_t = i_t - \delta k_t, \quad \text{and} \quad \dot{s}_t = d_t - \gamma s_t,$$

where we use the first-order and transversality conditions: $\lambda_t k_t \to 0$, $\mu_t s_t \to 0$, and $c_t \nu_t \to 0$ as $t \to \infty$.

Let $(c_*, k_*, s_*, r_*, i_*, d_*)$ be the steady-state equilibrium, which must satisfy the steady-state conditions given by $f_a(c_*, k_*+s_*) = (\delta+\rho)\phi'(i_*)$, $f_a(c_*, k_*+s_*) = (\gamma+\rho)\xi'(d_*)$, $f_c(c_*, k_*+s_*) = (\tau+\rho)\kappa'(r_*)$, $i_* = \delta k_*$, $d_* = \gamma s_*$, and $r_* = \tau c_*$. To display the steady-state equilibrium, we plot a set of phase diagrams and marginal cost functions in Figure 1. The panels on the left show the phase diagrams of (r_t, c_t), (i_t, k_t), and (d_t, s_t), while those on the right display the marginal cost functions of innovative R&D expenditure, physical investment, and managerial R&D expenditure, respectively. The phase diagrams also indicate the steady-state equilibrium levels of the variables along with the stable arms denoted by the dotted lines, such that the steady-state equilibrium can be reached by moving toward the equilibrium following the arms. The equilibrium cannot be reached unless the initial levels of (r_0, c_0), (i_0, k_0), and (d_0, s_0) are on the stable arms, simultaneously, as it would violate the transversality conditions.

— Insert Figure 1 Here —

To examine how the steady-state equilibrium responds to external shocks, we conduct two experiments by changing the marginal cost functions of each type of R&D expenditure. In the first experiment, we let the marginal cost function of innovative R&D expenditure decrease from $\kappa_0'(\cdot)$ to $\kappa_1'(\cdot)$. Denote $(c_*, k_*, s_*, r_*, i_*, d_*)$ and $(c_{**}, k_{**}, s_{**}, r_{**}, i_{**}, d_{**})$ as the initial and new steady-state equilibria. The adjustment processes are displayed in the left panel of Figure 2. This decline in the marginal cost function shifts the locus of $\dot{c}_t = 0$ to the locus of $\dot{c}_t' = 0$, denoted by the dashed line in the first phase diagram. The steady-state equilibrium (r_{**}, c_{**}) is reached at a level greater than (r_*, c_*). To attain the new steady-state equilibrium, r_* jumps to the new stable arm, denoted by the dotted line. By contrast, c_t is a stock, so it cannot jump to the new stable arm. Thus, (r_t, c_t) grad-

ually tends to (r_{**}, c_{**}). Then, the loci of $\dot{i}_t = 0$ and $\dot{d}_t = 0$ move to $\dot{i}'_t = 0$ and $\dot{d}'_t = 0$, which are denoted by the dashed lines in the second and third diagrams. The steady-state equilibrium is determined at (i_{**}, k_{**}) and (d_{**}, s_{**}), which are greater than (i_*, k_*) and (d_*, s_*). Both i_t and d_t jump to the new stable arms denoted by the dotted lines, and (i_t, k_t) and (d_t, s_t) tend to the new steady-state equilibrium. This reveals that physical investment and innovative R&D expenditure move in the same direction following the change in the cost function of innovative R&D expenditure, implying that they are complements. The economic intuition is straightforward—as innovative R&D activities become relatively cheaper, the firm tends to accumulate more capital from innovative R&D activity, enhancing productivity. This allows the firm to invest more, thereby accumulating more physical capital.

— Insert Figure 2 Here —

In the second experiment, the marginal cost function of managerial R&D expenditure decreases from $\xi'_0(\cdot)$ to $\xi'_1(\cdot)$. The right panel in Figure 2 displays the adjustment process to the new equilibrium. The decrease in the marginal cost function shifts the locus of $\dot{d}_t = 0$ to the locus of $\dot{d}'_t = 0$, denoted by the dashed line in the third phase diagram. The new steady-state equilibrium (d_{**}, s_{**}) is reached at a level greater than (d_*, s_*). To attain the new steady-state equilibrium, d_* jumps to the new stable arm, denoted by the dotted line. However, as before, s_t cannot jump to the new stable arm because it is a stock. Consequently, (d_t, s_t) tends to (d_{**}, s_{**}) gradually and the locus of $\dot{i}_t = 0$ shifts to the locus of $\dot{i}'_t = 0$. The steady-state equilibrium level is determined at (i_{**}, k_{**}), where k_t, as a stock, cannot jump to a new level while i_t jumps to the stable arm denoted as the dotted line in the second phase diagram. Overall, following the decrease in the marginal cost of managerial R&D expenditure, d_* rises to d_{**} but i_* falls to i_{**}, revealing a substitutionary relationship between i_t and d_t. This implies that physical capital decreases from k_* to k_{**}, while s increases to s_* from s_{**}.

As s_t and k_t move in opposite directions, $a_{**} := k_{**} + s_{**}$ can be greater or less than $a_* := k_* + s_*$. The sign of the change depends upon the functional shapes of $f_a(\cdot, \cdot)$, $\xi'(\cdot)$, $\phi'(\cdot)$, and the depreciation rates δ and γ. In Figure 2 we assume that $a_{**} > a_*$, such that the locus of $\dot{c}_t = 0$ is shifted to $\dot{c}'_t = 0$, and a new equilibrium is achieved at (r_{**}, c_{**}), as indicated in the first phase diagram. Then, r_t jumps to the new stable arm denoted as the dotted line, and (r_t, c_t) approaches (r_{**}, c_{**}) gradually. In this case, $r_{**} > r_*$ and $c_{**} > c_*$, which is achieved mainly by virtue of the complementary relationship

between c_t and a_t. On the other hand, consider the case with a_{**} less than a_* in which case the locus of $\dot{c}_t' = 0$ is shifted to the left of $\dot{c}_t = 0$. Then, we obtain $r_{**} < r_*$ and $c_{**} < c_*$. The economic intuition of the substitutionary relationship between i_t and d_t is also straightforward. As managerial R&D activity becomes relatively cheaper, the firm tends to accumulate capital by converting managerial R&D expenditures, thereby substituting physical investment, implying that both physical investment and capital will decrease.

These experiments yield important testable implications—the relationship between physical investment and innovative R&D expenditure is expected to be positive by virtue of their complementarity, while the relationship between managerial R&D expenditure and investment is more likely to be negative due to their nature as substitutes.

3 A NARDL Model of R&D Expenditure and Investment

In this section, we develop a NARDL model to characterize the asymmetric relationship between R&D expenditure and physical investment, and propose a tractable two-step estimation procedure.

3.1 NARDL Specification

Our empirical specification is grounded in two stylized features of R&D expenditure highlighted in the literature surveyed in Section 2.1 and the theory developed in Section 2.2. First, as innovative R&D expenditures tend to focus on product innovation, their scale is often large relative to output. This suggests that R&D expenditure is expected to grow faster than output in the early stage, where start-up costs are large and the scale of production typically small. Second, managerial R&D expenditures focus on enhancing production efficiency, their scale is typically smaller than output.

Let r_t denote aggregate R&D intensity in the t-th period, defined as a ratio of aggregate R&D expenditure to GDP. Noting that aggregate R&D expenditure incorporates the spectrum of R&D activities conducted throughout the economy, the sign of Δr_t determines the relative prevalence of innovative and managerial R&D activities. If $\Delta r_t \geq 0$, then R&D expenditure grows at least as fast as output, indicating a prevalence of innovative R&D activity. By contrast, if $\Delta r_t < 0$, then output grows faster than R&D expenditure, indicating a prevalence of managerial R&D activity. Given

the different characteristics of innovative and managerial R&D, it is reasonable to expect that the relationship between R&D intensity and physical investment may be asymmetric.

To analyze the potential asymmetric impacts of r_t on the log of investment, denoted i_t, in the short-run and the long-run, we consider the following asymmetric error-correction model:

$$\Delta i_t = \gamma_* + \rho_* u_{t-1} + \sum_{j=1}^{p-1} \varphi_{j*} \Delta i_{t-j} + \sum_{j=0}^{q-1} \pi_{j*}^{+} \Delta r_{t-j}^{+} + \sum_{j=0}^{q-1} \pi_{j*}^{-} \Delta r_{t-j}^{-} + e_t, \tag{3}$$

where $u_{t-1} = i_{t-1} - \beta_*^{+} r_{t-1}^{+} - \beta_*^{-} r_{t-1}^{-}$ is the asymmetric error correction term and and e_t is a serially uncorrelated error term, given sufficiently large lag orders, p and q. Here, $\Delta r_t^{+} := \Delta r_t \mathbb{1}_{\{\Delta r_t \geq 0\}}$ and $\Delta r_t^{-} := \Delta r_t \mathbb{1}_{\{\Delta r_t < 0\}}$, where $\mathbb{1}_{\{\cdot\}}$ is an indicator function taking the value 1 if the condition in braces is satisfied, and zero otherwise.

Notice that the process in (3) is equivalent to the NARDL process, $i_t = \gamma_* + \sum_{j=1}^{p} \phi_{j*} i_{t-j} + \sum_{j=0}^{q} (\theta_{j*}^{+\prime} r_{t-j}^{+} + \theta_{j*}^{-\prime} r_{t-j}^{-}) + e_t$, advanced by SYG. The NARDL(p, q) process allows for both the long-run parameters, β_*^{+} and β_*^{-}, and the short-run parameters, π_{j*}^{+} and π_{j*}^{-}, to differ, which enables us to analyze long-run and short-run asymmetric relationships between R&D intensity and investment. Furthermore, the NARDL process can accommodate integrated time series with mismatched time drifts. Because $\Delta r_t^{+} \geq 0$ and $\Delta r_t^{-} \leq 0$ with probability one, the partial sum processes, r_t^{+} and r_t^{-}, will be integrated series with time drifts of positive and negative slopes, respectively. Hence, if there exists a cointegrating relationship between i_t and r_t, then i_t should be an integrated series with a time drift. This has the important implication that the NARDL model can establish a cointegrating relationship between two integrated variables with different time drifts without the need to include a deterministic time trend in the model.[5]

3.2 Singularity Issue in the NARDL Model

We review and develop the asymptotic theory for the NARDL (p, q) model advanced by SYG:

$$y_t = \gamma_* + \sum_{j=1}^{p} \phi_{j*} y_{t-j} + \sum_{j=0}^{q} \left(\boldsymbol{\theta}_{j*}^{+\prime} \boldsymbol{x}_{t-j}^{+} + \boldsymbol{\theta}_{j*}^{-\prime} \boldsymbol{x}_{t-j}^{-} \right) + e_t,$$

[5] In Section 6, we find that r_t is a unit-root process without a drift while i_t is a unit-root process with a drift. We establish that there exists a cointegrating relationship between them without including a deterministic time trend.

where $\boldsymbol{x}_t \in \mathbb{R}^k$, $\boldsymbol{x}_t^+ := \sum_{j=1}^t \Delta \boldsymbol{x}_j^+$, $\boldsymbol{x}_t^- := \sum_{j=1}^t \Delta \boldsymbol{x}_j^-$, $\Delta \boldsymbol{x}_t^+ := \max[\boldsymbol{0}, \Delta \boldsymbol{x}_t]$, and $\Delta \boldsymbol{x}_t^- := \min[\boldsymbol{0}, \Delta \boldsymbol{x}_t]$, and we apply the max and min operators element by element. The corresponding error-correction form is given by:

$$\Delta y_t = \rho_* y_{t-1} + \boldsymbol{\theta}_*^{+\prime} \boldsymbol{x}_{t-1}^+ + \boldsymbol{\theta}_*^{-\prime} \boldsymbol{x}_{t-1}^- + \gamma_* + \sum_{j=1}^{p-1} \varphi_{j*} \Delta y_{t-j} + \sum_{j=0}^{q-1} \left(\boldsymbol{\pi}_{j*}^{+\prime} \Delta \boldsymbol{x}_{t-j}^+ + \boldsymbol{\pi}_{j*}^{-\prime} \Delta \boldsymbol{x}_{t-j}^- \right) + e_t, \quad (4)$$

for some ρ_*, $\boldsymbol{\theta}_*^+$, $\boldsymbol{\theta}_*^-$, γ_*, φ_{j*} $(j = 1, 2, \ldots, p-1)$, $\boldsymbol{\pi}_{j*}^+$, and $\boldsymbol{\pi}_{j*}^-$ $(j = 0, 1, \ldots, q-1)$, where $\{e_t, \mathcal{F}_t\}$ is a martingale difference sequence and $\mathcal{F}_t$ is the smallest σ-algebra driven by $\{y_{t-1}, \boldsymbol{x}_t^+, \boldsymbol{x}_t^-, y_{t-2}, \boldsymbol{x}_{t-1}^+, \boldsymbol{x}_{t-1}^-, \ldots\}$. If y_t is cointegrated with $(\boldsymbol{x}_t^{+\prime}, \boldsymbol{x}_t^{-\prime})'$, then we may re-write (4) as $\Delta y_t = \rho_* u_{t-1} + \gamma_* + \sum_{j=1}^{p-1} \varphi_{j*} \Delta y_{t-j} + \sum_{j=0}^{q-1} \left(\boldsymbol{\pi}_{j*}^{+\prime} \Delta \boldsymbol{x}_{t-j}^+ + \boldsymbol{\pi}_{j*}^{-\prime} \Delta \boldsymbol{x}_{t-j}^- \right) + e_t$, where $u_{t-1} := y_{t-1} - \boldsymbol{\beta}_*^{+\prime} \boldsymbol{x}_{t-1}^+ - \boldsymbol{\beta}_*^{-\prime} \boldsymbol{x}_{t-1}^-$ is the cointegrating error correction term, $\boldsymbol{\beta}_*^+ := -(\boldsymbol{\theta}_*^+ / \rho_*)$ and $\boldsymbol{\beta}_*^- := -(\boldsymbol{\theta}_*^- / \rho_*)$. Note that u_t can be correlated with $\Delta \boldsymbol{x}_t$.

We now show that the NARDL process can capture a cointegrating relationship between a unit-root process with a deterministic time drift and another unit-root process without a time drift. First, suppose that $\mathbb{E}[\Delta \boldsymbol{x}_t] \equiv \boldsymbol{0}$, and let $\boldsymbol{\mu}_*^+ := \mathbb{E}[\Delta \boldsymbol{x}_t^+]$ and $\boldsymbol{\mu}_*^- := \mathbb{E}[\Delta \boldsymbol{x}_t^-]$. Then, it follows that $\boldsymbol{\mu}_*^+ + \boldsymbol{\mu}_*^- \equiv \boldsymbol{0}$ by construction. Define $\boldsymbol{s}_t^+ := \Delta \boldsymbol{x}_t^+ - \boldsymbol{\mu}_*^+$ and $\boldsymbol{s}_t^- := \Delta \boldsymbol{x}_t^- - \boldsymbol{\mu}_*^-$. Then, $\boldsymbol{x}_t^+ = \boldsymbol{\mu}_*^+ t + \sum_{j=1}^t \boldsymbol{s}_j^+$ and $\boldsymbol{x}_t^- = \boldsymbol{\mu}_*^- t + \sum_{j=1}^t \boldsymbol{s}_j^-$, showing that $\boldsymbol{x}_t^+$ and $\boldsymbol{x}_t^-$ are unit-root processes with deterministic time drifts. Note, however, that Δy_t is not necessarily distributed around zero even if $\boldsymbol{x}_t$ is a unit-root process without a deterministic trend. From the NARDL(p, q) process, it is easily seen that $\delta_* := \mathbb{E}[\Delta y_t] = -\frac{1}{\rho_*} [\sum_{j=0}^q (\boldsymbol{\theta}_{j*}^+)' \boldsymbol{\mu}_*^+ + \sum_{j=0}^q (\boldsymbol{\theta}_{j*}^-)' \boldsymbol{\mu}_*^-]$ by $\mathbb{E}[u_t] = 0$, where $\rho_* := 1 - \sum_{j=1}^p \phi_{j*}$. Let $d_t := \Delta y_t - \delta_*$. Then, $y_t = \delta_* t + \sum_{j=1}^t d_j$, showing that y_t can be a unit-root process with a deterministic time drift unless $\delta_* = 0$.

SYG propose to estimate the parameters of the NARDL model in a single step by OLS. While it is possible to establish the consistency of the single-step estimator of the long-run and short-run parameters by simulation, efforts to develop the requisite asymptotic theory are frustrated by the asymptotic singularity of the inverse matrix associated with the one-step NARDL estimator, as shown in Lemma 1. We make the following assumptions:

Assumption 1. *(i)* $\{(\Delta \boldsymbol{x}_t', u_t)'\}$ *is a globally covariance stationary mixing process of* $(k+1) \times 1$ *vectors of* ϕ *of size* $-r/(2(r-1))$ *or* α *of size* $-r/(r-2)$ *and* $r > 2$*; (ii)* $\mathbb{E}[\Delta \boldsymbol{x}_t] = \boldsymbol{0}$, $\mathbb{E}[|\Delta \boldsymbol{x}_{ti}|^r] < \infty$

$(i = 1, 2, \ldots, k)$, $\mathbb{E}[|u_t|^r] < \infty$, *and* $\mathbb{E}[|e_t|^2] < \infty$; *(iii)* $\lim_{T\to\infty}$ *Var*$[T^{-1/2}\sum_{t=1}^{T}(\Delta \boldsymbol{x}_t', u_t)']$ *exists and is positive definite (PD); and (iv) for some* $(\rho_*, \boldsymbol{\theta}_*^{+\prime}, \boldsymbol{\theta}_*^{-\prime}, \gamma_*, \varphi_{1*}, \ldots, \varphi_{p-1*}, \boldsymbol{\pi}_{0*}^{+\prime}, \ldots, \boldsymbol{\pi}_{q-1*}^{+\prime}, \boldsymbol{\pi}_{0*}^{-\prime}, \ldots, \boldsymbol{\pi}_{q-1*}^{-\prime})'$, Δy_t *is generated by* (4)*, such that* $\{e_t, \mathcal{F}_t\}$ *is a martingale difference sequence and* $\mathcal{F}_t$ *is the smallest* σ*-algebra driven by* $\{y_{t-1}, \boldsymbol{x}_t^+, \boldsymbol{x}_t^-, y_{t-2}, \boldsymbol{x}_{t-1}^+, \boldsymbol{x}_{t-1}^-, \ldots\}$. □

For notational simplicity, we define $\boldsymbol{z}_t := [\boldsymbol{z}_{1t}' \vdots \boldsymbol{z}_{2t}']' := [y_{t-1}, \boldsymbol{x}_{t-1}^{+\prime}, \boldsymbol{x}_{t-1}^{-\prime} \vdots 1, \Delta \boldsymbol{y}_{t-1}', \Delta \boldsymbol{x}_t^{+\prime}, \ldots, \Delta \boldsymbol{x}_{t-q+1}^{+\prime}, \Delta \boldsymbol{x}_t^{-\prime}, \ldots, \Delta \boldsymbol{x}_{t-q+1}^{-\prime}]'$, where $\Delta \boldsymbol{y}_{t-1} := [\Delta y_{t-1}, \Delta y_{t-2}, \ldots, \Delta y_{t-p+1}]'$. Note that $\boldsymbol{z}_t$ is partitioned into nonstationary and stationary variables. Next, we partition $\boldsymbol{z}_{2t}$ as $\boldsymbol{z}_{2t} := [1 \vdots \boldsymbol{w}_t']' := [1 \vdots \boldsymbol{w}_{1t}' \vdots \boldsymbol{w}_{2t}' \vdots \ \boldsymbol{w}_{3t}']' := [1 \vdots \Delta \boldsymbol{y}_{t-1}' \vdots \Delta \boldsymbol{x}_t^{+\prime}, \ \ldots \ , \Delta \boldsymbol{x}_{t-q+1}^{+\prime} \vdots \Delta \boldsymbol{x}_t^{-\prime}, \ \ldots \ , \Delta \boldsymbol{x}_{t-q+1}^{-\prime}]'$. In addition, we define $\boldsymbol{\alpha}_* := [\boldsymbol{\alpha}_{1*}' \vdots \boldsymbol{\alpha}_{2*}']' := [\rho_*, \boldsymbol{\theta}_*^{+\prime}, \boldsymbol{\theta}_*^{-\prime} \vdots \gamma_*, \boldsymbol{\varphi}_*', \boldsymbol{\pi}_{0*}^{+\prime}, \ldots, \boldsymbol{\pi}_{q-1*}^{+\prime}, \boldsymbol{\pi}_{0*}^{-\prime}, \ldots, \boldsymbol{\pi}_{q-1*}^{-\prime}]'$, where $\boldsymbol{\varphi}_* := [\varphi_{1*}, \varphi_{2*}, \ldots, \varphi_{p-1*}]'$. Using this notation, the single-step NARDL estimator is given by $\widehat{\boldsymbol{\alpha}}_T := (\sum_{t=1}^{T} \boldsymbol{z}_t \boldsymbol{z}_t')^{-1} \sum_{t=1}^{T} \boldsymbol{z}_t \Delta y_t = \boldsymbol{\alpha}_* + (\sum_{t=1}^{T} \boldsymbol{z}_t \boldsymbol{z}_t')^{-1} \sum_{t=1}^{T} \boldsymbol{z}_t e_t$.

Lemma 1 shows that inference on the unknown parameters using $\widehat{\boldsymbol{\alpha}}_T$ is challenging because $\sum_{t=1}^{T} \boldsymbol{z}_t \boldsymbol{z}_t'$ is asymptotically singular.

Lemma 1. *Under Assumption 1, (i)* $T^{-3}\sum_{t=1}^{T} \boldsymbol{z}_{t1}\boldsymbol{z}_{t1}' \xrightarrow{\mathbb{P}} \mathbf{M}_{11} := \frac{1}{3}\boldsymbol{n}_1\boldsymbol{n}_1'$*; (ii)* $T^{-2}\sum_{t=1}^{T} \boldsymbol{z}_{1t}\, \boldsymbol{z}_{2t}' \xrightarrow{\mathbb{P}} \mathbf{M}_{12} := \frac{1}{2}\boldsymbol{n}_1\boldsymbol{n}_2'$*; and (iii)* $T^{-1}\sum_{t=1}^{T} \boldsymbol{z}_{2t}\boldsymbol{z}_{2t}' \xrightarrow{\mathbb{P}} \mathbf{M}_{22} := \begin{bmatrix} 1 & \boldsymbol{n}_2^{(1)\prime} \\ \boldsymbol{n}_2^{(1)} & \mathbb{E}[\boldsymbol{w}_t\boldsymbol{w}_t'] \end{bmatrix}$*, where* $\boldsymbol{n}_1 := [\delta_*, \boldsymbol{\mu}_*^{+\prime}, \boldsymbol{\mu}_*^{-\prime}]'$, $\boldsymbol{n}_2 := [1, \boldsymbol{n}_2^{(1)}]$ *and* $\boldsymbol{n}_2^{(1)} := [\delta_* \boldsymbol{\iota}_{p-1}', \boldsymbol{\iota}_q' \otimes \boldsymbol{\mu}_*^{+\prime}, \boldsymbol{\iota}_q' \otimes \boldsymbol{\mu}_*^{-\prime}]'$ *with* $\boldsymbol{\iota}_a$ *being an* $a \times 1$ *vector of ones.* □

Lemma 1 implies that $\mathbf{D}_T^{-1}(\sum_{t=1}^{T} \boldsymbol{z}_t\boldsymbol{z}_t')\, \mathbf{D}_T^{-1} \xrightarrow{\mathbb{P}} \mathbf{M}_*$, where $\mathbf{D}_T := \text{diag}[T^{3/2}\mathbf{I}_{2+2k}, T^{1/2}\mathbf{I}_{p+2qk}]$, and $\mathbf{M}_*$ is a 2×2 block matrix whose i-th row and j-th column block is $\mathbf{M}_{ij}$, with $\mathbf{M}_{21} = \mathbf{M}_{12}'$. As $\mathbf{M}_*$ is singular, it is difficult to derive the limit distribution of $\widehat{\boldsymbol{\alpha}}_T$ directly, unless we can derive the limit distribution of the determinant of $\sum_{t=1}^{T} \boldsymbol{z}_t\boldsymbol{z}_t'$, which is analytically challenging.

3.3 Two-step NARDL Estimation

3.3.1 Long-Run Parameter Estimation with $k = 1$

First-Step Estimation by OLS Following the two-step estimation framework of Engle and Granger (1987), we first estimate the parameters of the long-run relationship, $y_t = \alpha_* + \beta_*^+ x_t^+ + \beta_*^- x_t^- + u_t$ by OLS. Let $\bar{\mathbf{D}}_T := \text{diag}[T^{1/2}, T^{3/2}\mathbf{I}_2]$ and $\boldsymbol{v}_t := (1, x_t^+, x_t^-)'$. Then, $\bar{\mathbf{D}}_T^{-1}\left(\sum_{t=1}^{T} \boldsymbol{v}_t\boldsymbol{v}_t'\right)\bar{\mathbf{D}}_T^{-1} \xrightarrow{\mathbb{P}} \mathbf{M}_{11}$. By Lemma 1(*i*), this is a singular matrix due to the collinearity of the trends in x_t^+ and x_t^-.

We propose to reparameterize the long-run relationship as $y_t = \alpha_* + \lambda_* x_t^+ + \eta_* x_t + u_t$, where $x_t \equiv x_t^+ + x_t^-$, $\lambda_* = \beta_*^+ - \beta_*^-$ and $\eta_* = \beta_*^-$. The long-run parameters can then be estimated as $\beta_*^+ = \lambda_* + \eta_*$ and $\beta_*^- = \eta_*$. The OLS estimator of $\boldsymbol{\varrho}_* := (\alpha_*, \lambda_*, \eta_*)'$ is obtained by $\widehat{\boldsymbol{\varrho}}_T := (\widehat{\alpha}_T, \widehat{\lambda}_T, \widehat{\eta}_T)' := \arg\min_{\alpha,\,\lambda,\,\eta} \sum_{t=1}^T (y_t - \alpha - \lambda x_t^+ - \eta x_t)^2$, where $\widehat{\beta}_T^+ := \widehat{\lambda}_T + \widehat{\eta}_T$ and $\widehat{\beta}_T^- = \widehat{\eta}_T$. Letting $\boldsymbol{q}_t := (1, x_t^+, x_t)'$, then $\widehat{\boldsymbol{\varrho}}_T = \boldsymbol{\varrho}_* + (\sum_{t=1}^T \boldsymbol{q}_t \boldsymbol{q}_t')^{-1} (\sum_{t=1}^T \boldsymbol{q}_t u_t)$. Define $\boldsymbol{\Sigma}_* := \lim_{T\to\infty} T^{-1} \sum_{t=1}^T \sum_{s=1}^T \mathbb{E}[\boldsymbol{g}_t \boldsymbol{g}_s]$ and $[\mathcal{B}_x(\cdot), \mathcal{B}_u(\cdot)]' := \boldsymbol{\Sigma}_*^{1/2} [\mathcal{W}_x(\cdot), \mathcal{W}_u(\cdot)]'$, where $\boldsymbol{g}_t := [\Delta x_t, u_t]'$ and where $[\mathcal{W}_x(\cdot), \mathcal{W}_u(\cdot)]'$ is a 2×1 vector of independent Wiener processes. Let $\sigma_*^{(i,j)}$ be the (i,j)-th element of $\boldsymbol{\Sigma}_*$. If $\{u_t\}$ is serially uncorrelated and independent of $\{\Delta x_t\}$, then $\boldsymbol{\Sigma}_*$ and $[\mathcal{B}_x(\cdot), \mathcal{B}_u(\cdot)]'$ are reduced to diag $[\sigma_x^2, \sigma_u^2]$ and $[\sigma_x \mathcal{W}_x(\cdot), \sigma_u \mathcal{W}_u(\cdot)]'$, where $\sigma_x^2 := \lim_{T\to\infty} T^{-1} \sum_{t=1}^T \sum_{s=1}^T \mathbb{E}[\Delta x_t \Delta x_s]$ and $\sigma_u^2 := \mathbb{E}[u_t^2]$.

Lemma 2 provides the limit behaviors of the components constituting the OLS estimator:

Lemma 2. *Under Assumption 1, if $k = 1$ and $\boldsymbol{\Sigma}_*$ is PD, then (i)*

$$\widehat{\mathbf{Q}}_T := \widetilde{\mathbf{D}}_T^{-1} \left(\sum_{t=1}^T \boldsymbol{q}_t \boldsymbol{q}_t' \right) \widetilde{\mathbf{D}}_T^{-1} \Rightarrow \boldsymbol{\mathcal{Q}} := \begin{bmatrix} 1 & \frac{1}{2}\mu_*^+ & \int \mathcal{B}_x \\ \frac{1}{2}\mu_*^+ & \frac{1}{3}\mu_*^+ \mu_*^+ & \mu_*^+ \int r\mathcal{B}_x \\ \int \mathcal{B}_x & \int r\mathcal{B}_x \mu_*^+ & \int \mathcal{B}_x \mathcal{B}_x \end{bmatrix},$$

where $\widetilde{\mathbf{D}}_T := diag[T^{1/2}, T^{3/2}, T]$; and (ii) if $\upsilon_* := \lim_{T\to\infty} T^{-1} \sum_{t=1}^T \sum_{i=1}^t \mathbb{E}[\Delta x_i u_t]$ is finite, then $\widehat{\mathbf{U}}_T := \widetilde{\mathbf{D}}_T^{-1} (\sum_{t=1}^T \boldsymbol{q}_t u_t) \Rightarrow \boldsymbol{\mathcal{U}} := [\int d\mathcal{B}_u, \mu_*^+ \int r d\mathcal{B}_u, \int \mathcal{B}_x d\mathcal{B}_u + \upsilon_*]$.[6] □

Note that $\boldsymbol{\mathcal{Q}}$ is nonsingular with probability 1, so the limit distribution of $\widehat{\boldsymbol{\varrho}}_T$ is obtained as a product of $\boldsymbol{\mathcal{Q}}^{-1}$ and $\boldsymbol{\mathcal{U}}$, as stated in the following corollary:

Corollary 1. *Under Assumption 1, if $k = 1$ and $\boldsymbol{\Sigma}_*$ is PD, then $\widetilde{\mathbf{D}}_T (\widehat{\boldsymbol{\varrho}}_T - \boldsymbol{\varrho}_*) \Rightarrow \boldsymbol{\mathcal{Q}}^{-1} \boldsymbol{\mathcal{U}}$.* □

Corollary 1 has important implications. First, by virtue of the reparameterization, the collinearity between x_t^+ and x_t^- can be removed by the fact that $\sum_{t=1}^T x_t = O_{\mathbb{P}}(T^{3/2})$ and $\sum_{t=1}^T x_t^+ = O_{\mathbb{P}}(T^2)$ lead to different convergence rates for $\widehat{\lambda}_T$ and $\widehat{\eta}_T$, viz., $\widehat{\lambda}_T - \lambda_* = O_{\mathbb{P}}(T^{-3/2})$ and $\widehat{\eta}_T - \eta_* = O_{\mathbb{P}}(T^{-1})$. Second, to derive the limit distribution of $\widehat{\boldsymbol{\varrho}}_T$, we apply the FCLT only to $\sum_{t=1}^{T(\cdot)} \boldsymbol{g}_t$ where $\boldsymbol{g}_t := [\Delta x_t, u_t]'$, not to $\sum_{t=1}^{[T(\cdot)]} (x_t^+ - \mu_*^+)$. Third, using the definition of $\widehat{\lambda}_T$, we have: $T\{(\widehat{\beta}_T^+ - \widehat{\beta}_T^-) -$

[6] Here, all integrals are computed with respect to $r \in [0,1]$. For example, $\int r\mathcal{B}_x$ denotes $\int_0^1 r\mathcal{B}_x(r) dr$.

$(\beta_*^+ - \beta_*^-)\} = O_{\mathbb{P}}(T^{-1/2})$. Hence, $T(\widehat{\beta}_T^+ - \beta_*^+) = T(\widehat{\beta}_T^- - \beta_*^-) + o_{\mathbb{P}}(1)$, implying that the limit distributions of $T(\widehat{\beta}_T^+ - \beta_*^+)$ and $T(\widehat{\beta}_T^- - \beta_*^-)$ are equivalent. Finally, as the convergence rate of the long-run parameter estimator is faster than $T^{1/2}$, $\widehat{\beta}_T^+$ and $\widehat{\beta}_T^-$ can be treated as known when estimating the short-run dynamic parameters.

Theorem 1. *Under Assumption 1, if* $k = 1$, *then* $T[(\widehat{\beta}_T^+ - \beta_*^+), (\widehat{\beta}_T^- - \beta_*^-)]' \Rightarrow \boldsymbol{\iota}_2 \otimes \mathbf{S}\boldsymbol{\mathcal{Q}}^{-1}\boldsymbol{\mathcal{U}}$, *where* $\mathbf{S} := [\mathbf{0}_{1\times 2}, 1]$. □

First-Step Estimation by FM-OLS Note that the limit distribution in Theorem 1 is non-normal due to its dependence on the nuisance parameters $\boldsymbol{\Sigma}_*$ and υ_*. Consequently, it cannot be readily exploited for inference on the long-run parameters. Furthermore, except in the special case where $\{u_t\}$ is independent of $\{\Delta x_t\}$ and/or serially uncorrelated, the OLS estimator of the long-run parameter exhibits an asymptotic bias determined by υ_*. Phillips and Hansen (1990) propose the FM-OLS estimator, which is shown to be free from asymptotic biases even in the presence of endogenous regressors and/or serial correlation, and which follows an asymptotic mixed normal distribution. Hence, we advocate the use of FM-OLS to estimate the long-run parameters in the first step.

Suppose that $\boldsymbol{\Sigma}_*$ is consistently estimated by a heteroskedasticity and autocorrelation consistent covariance matrix estimator, $\widetilde{\boldsymbol{\Sigma}}_T$, whose (i,j)-th element is denoted by $\widetilde{\sigma}_T^{(i,j)}$. For example, following Newey and West (1987), we have $\widetilde{\boldsymbol{\Sigma}}_T := \frac{1}{T}\sum_{t=1}^T \widehat{\boldsymbol{g}}_t\widehat{\boldsymbol{g}}_t' + \frac{1}{T}\sum_{k=1}^{\ell}\omega_{\ell k}\sum_{t=k+1}^T\{\widehat{\boldsymbol{g}}_{t-k}\widehat{\boldsymbol{g}}_t' + \widehat{\boldsymbol{g}}_t\widehat{\boldsymbol{g}}_{t-k}'\}$, where $\widehat{\boldsymbol{g}}_t := [\Delta x_t, \widehat{u}_t]'$, $\omega_{\ell k} := 1 - k/(1+\ell)$, $\ell = O(T^{1/4})$ and $\widehat{u}_t := y_t - \widehat{\alpha}_T - \widehat{\beta}_T^+ x_t^+ - \widehat{\beta}_T^- x_t^-$. Under mild regularity conditions, it is straightforward to show that the asymptotic bias, υ_* in $\boldsymbol{\mathcal{U}}$, can be consistently estimated by $\widetilde{\boldsymbol{\Pi}}_T := \frac{1}{T}\sum_{k=0}^{\ell}\sum_{t=k+1}^T \widehat{\boldsymbol{g}}_{t-k}\widehat{\boldsymbol{g}}_t'$. Let $\widetilde{\pi}_T^{(i,j)}$ be the (i,j)-th element of $\widetilde{\boldsymbol{\Pi}}_T$. Define the following long-run parameter estimator: $\widetilde{\boldsymbol{\varrho}}_T := (\widetilde{\alpha}_T, \widetilde{\lambda}_T, \widetilde{\eta}_T)' := (\sum_{t=1}^T \boldsymbol{q}_t\boldsymbol{q}_t')^{-1}$ $(\sum_{t=1}^T \boldsymbol{q}_t\widetilde{y}_t - T\mathbf{S}'\widetilde{\upsilon}_T)$, where $\widetilde{y}_t := y_t - \Delta x_t(\widetilde{\sigma}_T^{(1,1)})^{-1}\widetilde{\sigma}_T^{(1,2)}$ and $\widetilde{\upsilon}_T := \widetilde{\pi}_T^{(1,2)} - \widetilde{\pi}_T^{(1,1)}(\widetilde{\sigma}_T^{(1,1)})^{-1}\,\widetilde{\sigma}_T^{(1,2)}$. Finally, the FM-OLS estimators of the long-run parameters are obtained as $\widetilde{\beta}_T^+ := \widetilde{\lambda}_T + \widetilde{\eta}_T$ and $\widetilde{\beta}_T^- := \widetilde{\eta}_T$.

To derive the limit distribution of the FM-OLS estimator, we make the following assumptions.

Assumption 2. *(i)* $\boldsymbol{\Sigma}_*$ *is finite and PD and* $\widetilde{\boldsymbol{\Sigma}}_T \xrightarrow{\mathbb{P}} \boldsymbol{\Sigma}_*$; *and (ii)* $\boldsymbol{\Pi}_*$ *is finite and* $\widetilde{\boldsymbol{\Pi}}_T \xrightarrow{\mathbb{P}} \boldsymbol{\Pi}_*$, *where* $\boldsymbol{\Pi}_* := \lim_{T\to\infty}\frac{1}{T}\sum_{t=1}^T\sum_{i=1}^t \mathbb{E}[\boldsymbol{g}_i\boldsymbol{g}_t']$.

Let $\pi_*^{(i,j)}$ be the (i,j)-th element of $\boldsymbol{\Pi}_*$. Then, $\pi_*^{(1,2)}$ is identical to υ_*.

Lemma 3. *Under Assumptions 1 and 2, and for* $k = 1$, $\widetilde{\mathbf{U}}_T := \widetilde{\mathbf{D}}_T^{-1}\{\sum_{t=1}^{T} \boldsymbol{q}_t(u_t - \Delta x_t(\widetilde{\sigma}_T^{(1,1)})^{-1}\widetilde{\sigma}_T^{(1,2)}) - T\mathbf{S}'\widetilde{\upsilon}_T\} \Rightarrow \widetilde{\boldsymbol{\mathcal{U}}} := \tau_*[\int d\mathcal{W}_u, \mu_*^+ \int r d\mathcal{W}_u, \int \mathcal{B}_x d\mathcal{W}_u]'$, *where* $\tau_*^2 := plim_{T\to\infty}\widetilde{\tau}_T^2$ *and* $\widetilde{\tau}_T^2 := \widetilde{\sigma}_T^{(2,2)} - \widetilde{\sigma}_T^{(2,1)}(\widetilde{\sigma}_T^{(1,1)})^{-1}\widetilde{\sigma}_T^{(1,2)}$. □

By Lemma 2(*i*), $\widehat{\mathbf{Q}}_T \Rightarrow \boldsymbol{\mathcal{Q}}$, which is nonsingular with probability 1. The limit distribution of $\widetilde{\boldsymbol{\varrho}}_T$ can be obtained as the product of $\boldsymbol{\mathcal{Q}}^{-1}$ and $\widetilde{\boldsymbol{\mathcal{U}}}$:

Corollary 2. *Under Assumption 1 and for* $k = 1$, $\widetilde{\mathbf{D}}_T(\widetilde{\boldsymbol{\varrho}}_T - \boldsymbol{\varrho}_*) \Rightarrow \boldsymbol{\mathcal{Q}}^{-1}\widetilde{\boldsymbol{\mathcal{U}}}$. □

Corollary 2 has several implications. First, the limit distribution of the FM-OLS estimator is mixed normal. Conditional on $\sigma\{\mathcal{B}_x(r), r \in (0,1]\}$, the limit distribution of $\widetilde{\mathbf{D}}_T(\widetilde{\boldsymbol{\varrho}}_T - \boldsymbol{\varrho}_*)$ is $N(\mathbf{0}, \tau_*^2\boldsymbol{\mathcal{Q}}^{-1})$. Consequently, the null limit distribution of a Wald test statistic constructed using the FM-OLS estimator will be chi-squared. Second, we have: $T(\widetilde{\beta}_T^+ - \beta_*^+) = T(\widetilde{\beta}_T^- - \beta_*^-) + o_{\mathbb{P}}(1)$, implying that the limit distribution of $\widetilde{\beta}_T^+$ is equivalent to that of $\widetilde{\beta}_T^-$, where the limit distribution of $\widetilde{\beta}_T^-$ is given by that of $\widetilde{\eta}_T$. Third, the convergence rates of $\widetilde{\beta}_T^+$ and $\widetilde{\beta}_T^-$ are both T, enabling us to estimate the short-run parameters in the second stage by replacing u_{t-1} with $\widetilde{u}_{t-1} := y_{t-1} - \widetilde{\alpha}_T - \widetilde{\beta}_T^+ x_{t-1}^+ - \widetilde{\beta}_T^- x_{t-1}^-$.

Theorem 2 presents the limit distribution of the FM-OLS estimator:

Theorem 2. *Under Assumptions 1 and 2, and for* $k = 1$, $T[(\widetilde{\beta}_T^+ - \beta_*^+), (\widetilde{\beta}_T^- - \beta_*^-)]' \Rightarrow \boldsymbol{\iota}_2 \otimes \mathbf{S}\boldsymbol{\mathcal{Q}}^{-1}\widetilde{\boldsymbol{\mathcal{U}}}$. □

3.3.2 Short-Run Parameter Estimation with $k = 1$

As the long-run coefficients can be estimated by an estimator with a convergence rate faster than $T^{1/2}$, we can treat them as known when estimating the short-run parameters. Let $u_{t-1} := y_{t-1} - \beta_*^+ x_{t-1}^+ - \beta_*^- x_{t-1}^-$. Then, we can rewrite (4) as:

$$\Delta y_t = \rho_* u_{t-1} + \gamma_* + \sum_{j=1}^{p-1} \varphi_{j*}\Delta y_{t-j} + \sum_{j=0}^{q-1} \left(\pi_{j*}^{+\prime}\Delta x_{t-j}^+ + \pi_{j*}^{-\prime}\Delta x_{t-j}^-\right) + e_t,$$

which can be expressed simply as $\Delta y_t = \boldsymbol{\zeta}_*'\boldsymbol{h}_t + e_t$, where $\boldsymbol{\zeta}_* := (\rho_*, \boldsymbol{\beta}_{2*}')'$, $\boldsymbol{\beta}_{2*} := (\gamma_*, \varphi_{1*}, \ldots, \varphi_{p-1*}, \pi_{0*}^{+\prime}, \ldots, \pi_{q-1*}^{+\prime}, \pi_{0*}^{-\prime}, \ldots, \pi_{q-1*}^{-\prime},)'$ and $\boldsymbol{h}_t := (u_{t-1}, \boldsymbol{z}_{2t}')'$. Because every variable in this equation is stationary, the unknown parameters can be estimated by the OLS estimator: $\widehat{\boldsymbol{\zeta}}_T := (\sum_{t=1}^{T} \boldsymbol{h}_t\boldsymbol{h}_t')^{-1}\sum_{t=1}^{T} \boldsymbol{h}_t\Delta y_t = \boldsymbol{\zeta}_* + (\sum_{t=1}^{T} \boldsymbol{h}_t\boldsymbol{h}_t')^{-1}\sum_{t=1}^{T} \boldsymbol{h}_t e_t$.

Lemma 4. *Given Assumption 1, (i)* $\widehat{\mathbf{\Gamma}}_T := T^{-1}\sum_{t=1}^{T}\boldsymbol{h}_t\boldsymbol{h}_t' \xrightarrow{\mathbb{P}} \mathbf{\Gamma}_* := \mathbb{E}[\boldsymbol{h}_t\boldsymbol{h}_t']$*; (ii)* $T^{-1/2}\sum_{t=1}^{T}\boldsymbol{h}_t e_t \overset{A}{\sim} N[\mathbf{0}, \mathbf{\Omega}_*]$*, where* $\mathbf{\Omega}_* := \mathbb{E}[e_t^2\boldsymbol{h}_t\boldsymbol{h}_t']$*; and (iii) in the special case where* $\mathbb{E}[e_t^2|\boldsymbol{h}_t] = \sigma_*^2$*,* $\mathbf{\Omega}_*$ *simplifies to* $\sigma_*^2\mathbf{\Gamma}_*$. □

Using Lemma 4, it is possible to derive the limit distribution of $\widehat{\boldsymbol{\zeta}}_T$, as stated in Theorem 3:

Theorem 3. *Under Assumption 1, and if* $\mathbf{\Gamma}_*$ *and* $\mathbf{\Omega}_*$ *are PD, then (i)* $\sqrt{T}(\widehat{\boldsymbol{\zeta}}_T - \boldsymbol{\zeta}_*) \overset{A}{\sim} N(\mathbf{0}, \mathbf{\Gamma}_*^{-1}\mathbf{\Omega}_*\mathbf{\Gamma}_*^{-1})$*; and (ii) if it further holds that* $\mathbb{E}[e_t^2|\boldsymbol{h}_t] = \sigma_*^2$*, then* $\sqrt{T}(\widehat{\boldsymbol{\zeta}}_T - \boldsymbol{\zeta}_*) \overset{A}{\sim} N(\mathbf{0}, \sigma_*^2\mathbf{\Gamma}_*^{-1})$. □

3.3.3 Long-Run Parameter Estimation with $k > 1$

First-Step Transformed OLS If there are multiple explanatory variables in the NARDL model, then the above two-step estimation procedure can be shown to be inappropriate. Let $\boldsymbol{x}_t \equiv \boldsymbol{x}_t^+ + \boldsymbol{x}_t^-$, $\boldsymbol{\lambda}_* = \boldsymbol{\beta}_*^+ - \boldsymbol{\beta}_*^-$ and $\boldsymbol{\eta}_* = \boldsymbol{\beta}_*^-$ with $k > 1$. Then, we have: $y_t = \alpha_* + \boldsymbol{\lambda}_*'\boldsymbol{x}_t^+ + \boldsymbol{\eta}_*'\boldsymbol{x}_t + u_t$. By extending Lemma 2, it follows that:

$$\widehat{\mathbf{Q}}_T := \widetilde{\mathbf{D}}_T^{-1}\left(\sum_{t=1}^{T}\boldsymbol{q}_t\boldsymbol{q}_t'\right)\widetilde{\mathbf{D}}_T^{-1} \Rightarrow \boldsymbol{\mathcal{Q}} := \begin{bmatrix} 1 & \frac{1}{2}\boldsymbol{\mu}_*^+ & \int \boldsymbol{\mathcal{B}}_x' \\ \frac{1}{2}\boldsymbol{\mu}_*^+ & \frac{1}{3}\boldsymbol{\mu}_*^+\boldsymbol{\mu}_*^{+\prime} & \boldsymbol{\mu}_*^+\int r\boldsymbol{\mathcal{B}}_x' \\ \int \boldsymbol{\mathcal{B}}_x dr & \int r\boldsymbol{\mathcal{B}}_x\boldsymbol{\mu}_*^{+\prime} & \int \boldsymbol{\mathcal{B}}_x\boldsymbol{\mathcal{B}}_x' \end{bmatrix},$$

where $\boldsymbol{q}_t := (1, \boldsymbol{x}_t^{+\prime}, \boldsymbol{x}_t')'$, $\widetilde{\mathbf{D}}_T := \text{diag}[T^{1/2}, T^{3/2}\mathbf{I}_k, T\mathbf{I}_k]$, $\boldsymbol{\mathcal{B}}_x(\cdot)$ is a $k \times 1$ vector of Brownian motions, such that $[\boldsymbol{\mathcal{B}}_x(\cdot)', \mathcal{B}_u(\cdot)]' := \mathbf{\Sigma}_*^{1/2}[\boldsymbol{\mathcal{W}}_x(\cdot)', \mathcal{W}_u(\cdot)']'$ and $\mathbf{\Sigma}_* := \lim_{T\to\infty} T^{-1}\sum_{t=1}^{T}\sum_{s=1}^{T}\mathbb{E}[\boldsymbol{g}_t\boldsymbol{g}_s]$, with $\boldsymbol{g}_t := [\Delta\boldsymbol{x}_t, u_t]'$ and $[\boldsymbol{\mathcal{W}}_x(\cdot)', \mathcal{W}_u(\cdot)]'$ being a $(k+1) \times 1$ vector of independent Wiener processes. Note that the blocks on the second row of $\boldsymbol{\mathcal{Q}}$ form a sub-matrix with rank equal to unity. That is, $[\frac{1}{2}\boldsymbol{\mu}_*^+, \frac{1}{3}\boldsymbol{\mu}_*^+\boldsymbol{\mu}_*^{+\prime}, \boldsymbol{\mu}_*^+\int r\boldsymbol{\mathcal{B}}_x'] = \boldsymbol{\mu}_*^+[\frac{1}{2}, \frac{1}{3}\boldsymbol{\mu}_*^{+\prime}, \int r\boldsymbol{\mathcal{B}}_x']$, which implies that $\boldsymbol{\mathcal{Q}}$ is a singular matrix with probability 1. Consequently, the two-step procedure cannot be used to estimate the long-run parameters in this case.

We propose a modification to our estimation procedure to address this issue. Define $\boldsymbol{m}_t := \sum_{j=1}^{t}\boldsymbol{s}_j^+$, which is a unit-root process with zero-mean increments. Therefore, if $\boldsymbol{x}_t^+$ is regressed against t, then $\boldsymbol{\mu}_*^+$ can be estimated by $\widehat{\boldsymbol{\mu}}_T^+ := (\sum_{t=1}^{T}t^2)^{-1}\sum_{t=1}^{T}t\boldsymbol{x}_t^+ = \boldsymbol{\mu}_*^+ + (\sum_{t=1}^{T}t^2)^{-1}\sum_{t=1}^{T}t\boldsymbol{m}_t$, where $\widehat{\boldsymbol{m}}_t := \boldsymbol{x}_t^+ - \widehat{\boldsymbol{\mu}}_T^+ t$ is the regression residual. Consequently, $\boldsymbol{m}_t = \widehat{\boldsymbol{m}}_t + t\boldsymbol{d}_T$, such that $\boldsymbol{x}_t^+ = \widehat{\boldsymbol{m}}_t + (\boldsymbol{\mu}_*^+ + \boldsymbol{d}_T)t$, where $\boldsymbol{d}_T := (\sum_{t=1}^{T}t^2)^{-1}\sum_{t=1}^{T}t\boldsymbol{m}_t$. Under mild regularity conditions,

$\boldsymbol{d}_T = O_{\mathbb{P}}(T^{-1/2})$. Consequently, let $\boldsymbol{\delta}_{*T} := \boldsymbol{\mu}_*^+ + \boldsymbol{d}_T$. Then, $\boldsymbol{\delta}_{*T} = \boldsymbol{\mu}_* + O_{\mathbb{P}}(T^{-1/2})$. We now rewrite the equation for y_t using the equation for $\boldsymbol{x}_t^+$ to obtain $y_t = \alpha_* + \boldsymbol{\lambda}_*'(\boldsymbol{\mu}_*^+ + \boldsymbol{d}_T)t + \boldsymbol{\lambda}_*'\widehat{\boldsymbol{m}}_t + \boldsymbol{\eta}_*'\boldsymbol{x}_t + u_t$. Next, we can consistently estimate $\boldsymbol{\lambda}_*$ and $\boldsymbol{\eta}_*$ by regressing y_t on $\boldsymbol{r}_t := (1, t, \widehat{\boldsymbol{m}}_t', \boldsymbol{x}_t')'$. Let $\ddot{\boldsymbol{\varpi}}_T := (\ddot{\alpha}_T, \ddot{\xi}_{*T}, \ddot{\boldsymbol{\lambda}}_T', \ddot{\boldsymbol{\eta}}_T')'$ be the OLS estimator of $\varpi_{*T} := (\alpha_*, \xi_{*T}, \boldsymbol{\lambda}_*', \boldsymbol{\eta}_*')'$, where $\xi_{*T} := \boldsymbol{\lambda}_*'\boldsymbol{\delta}_{*T}$. The long-run estimators of $\boldsymbol{\beta}_*^+$ and $\boldsymbol{\beta}_*^-$ can be obtained as $\ddot{\boldsymbol{\beta}}_T^+ := \ddot{\boldsymbol{\lambda}}_T + \ddot{\boldsymbol{\eta}}_T$ and $\ddot{\boldsymbol{\beta}}_T^- := \ddot{\boldsymbol{\eta}}_T$. Let:

$$\ddot{\mathbf{S}} := \begin{bmatrix} \mathbf{0}_{k\times 1} & \mathbf{0}_{k\times 1} & \mathbf{I}_k & \mathbf{I}_k \\ \mathbf{0}_{k\times 1} & \mathbf{0}_{k\times 1} & \mathbf{0}_{k\times k} & \mathbf{I}_k \end{bmatrix}, \quad \text{then} \quad \begin{bmatrix} \widehat{\boldsymbol{\beta}}_T^+ \\ \widehat{\boldsymbol{\beta}}_T^- \end{bmatrix} = \ddot{\mathbf{S}}\ddot{\boldsymbol{\varpi}}_T.$$

We refer to this as the *first-step transformed OLS (TOLS) estimator*. The intuition is straightforward—as it is the collinear trend in $\boldsymbol{x}_t^+$ that results in the singularity of $\boldsymbol{\mathcal{Q}}$, we detrend $\boldsymbol{x}_t^+$ prior to estimation.

The limit distribution of the first-step TOLS estimator is obtained in a similar fashion to the limit distribution of the first-step OLS estimator. First, note that $\ddot{\boldsymbol{\varpi}}_T = \boldsymbol{\varpi}_{*T} + (\sum_{t=1}^T \boldsymbol{r}_t\boldsymbol{r}_t')^{-1}\sum_{t=1}^T \boldsymbol{r}_t u_t$. To characterize the limit behaviors of the components, we define $\ddot{\boldsymbol{\Sigma}}_* := \lim_{T\to\infty}\frac{1}{T}\sum_{t=1}^T\sum_{s=1}^T \mathbb{E}[\ddot{\boldsymbol{g}}_t\ddot{\boldsymbol{g}}_t']$ and $[\boldsymbol{\mathcal{B}}_m(\cdot)', \boldsymbol{\mathcal{B}}_x(\cdot)', \mathcal{B}_u(\cdot)]' := \ddot{\boldsymbol{\Sigma}}_*^{1/2}[\boldsymbol{\mathcal{W}}_m(\cdot)', \boldsymbol{\mathcal{W}}_x(\cdot)', \mathcal{W}_u(\cdot)]'$, where we let $\ddot{\boldsymbol{g}}_t := [\Delta\boldsymbol{m}_t', \Delta\boldsymbol{x}_t, u_t]'$ and $[\boldsymbol{\mathcal{W}}_m(\cdot)', \boldsymbol{\mathcal{W}}_x(\cdot)', \mathcal{W}_u(\cdot)]'$ is a $(2k+1)\times 1$ vector of independent Wiener processes.

Lemma 5. *Under Assumption 1, if $\ddot{\boldsymbol{\Sigma}}_*$ is PD, then (i) $\ddot{\mathbf{R}}_T := \ddot{\mathbf{D}}_T^{-1}(\sum_{t=1}^T \boldsymbol{r}_t\boldsymbol{r}_t')\ddot{\mathbf{D}}_T^{-1} \Rightarrow \boldsymbol{\mathcal{R}}$, where:*

$$\boldsymbol{\mathcal{R}} = \begin{bmatrix} 1 & \frac{1}{2} & \int(1-\frac{3}{2}r)\boldsymbol{\mathcal{B}}_m' & \int \boldsymbol{\mathcal{B}}_x' \\ \frac{1}{2} & \frac{1}{3} & \mathbf{0}_{1\times k} & \int r\boldsymbol{\mathcal{B}}_x' \\ \int(1-\frac{3}{2}r)\boldsymbol{\mathcal{B}}_m & \mathbf{0}_{k\times 1} & \int \boldsymbol{\mathcal{B}}_m\boldsymbol{\mathcal{B}}_m' - 3\int r\boldsymbol{\mathcal{B}}_m\int r\boldsymbol{\mathcal{B}}_m' & \int \boldsymbol{\mathcal{B}}_m\boldsymbol{\mathcal{B}}_x' - 3\int r\boldsymbol{\mathcal{B}}_m\int r\boldsymbol{\mathcal{B}}_x' \\ \int \boldsymbol{\mathcal{B}}_x & \int r\boldsymbol{\mathcal{B}}_x & \int \boldsymbol{\mathcal{B}}_x\boldsymbol{\mathcal{B}}_m' - 3\int r\boldsymbol{\mathcal{B}}_x\int r\boldsymbol{\mathcal{B}}_m' & \int \boldsymbol{\mathcal{B}}_x\boldsymbol{\mathcal{B}}_x' \end{bmatrix},$$

and $\ddot{\mathbf{D}}_T := diag[T^{1/2}, T^{3/2}, T\mathbf{I}_{2k}]$; and (ii) if $\boldsymbol{\upsilon}_{x*} := \lim_{T\to\infty} T^{-1}\sum_{t=1}^T\sum_{i=1}^t \mathbb{E}[\Delta\boldsymbol{x}_i u_t]$ and $\boldsymbol{\upsilon}_{m*} := \lim_{T\to\infty} T^{-1}\sum_{t=1}^T\sum_{i=1}^t \mathbb{E}[\Delta\boldsymbol{m}_i u_t]$ are finite, then $\ddot{\mathbf{U}}_T := \ddot{\mathbf{D}}_T^{-1}(\sum_{t=1}^T \boldsymbol{r}_t u_t) \Rightarrow \ddot{\boldsymbol{\mathcal{U}}} := [\int d\mathcal{B}_u, \int r d\mathcal{B}_u, \int \boldsymbol{\mathcal{B}}_m' d\mathcal{B}_u - 3\int r d\mathcal{B}_u \int r\boldsymbol{\mathcal{B}}_m' + \boldsymbol{\upsilon}_{m*}', \int \boldsymbol{\mathcal{B}}_x' d\mathcal{B}_u + \boldsymbol{\upsilon}_{x*}']'$. □

$\boldsymbol{\mathcal{R}}$ is no longer singular, because $\sum_{t=1}^{[T(\cdot)]} \ddot{\boldsymbol{g}}_t$ obeys the FCLT using partially correlated increments.

Corollary 3. *Given Assumption 1, $\ddot{\mathbf{D}}_T(\ddot{\boldsymbol{\varpi}}_T - \boldsymbol{\varpi}_{*T}) \Rightarrow \boldsymbol{\mathcal{R}}^{-1}\ddot{\boldsymbol{\mathcal{U}}}$ and $T^{1/2}(\widehat{\xi}_T - \boldsymbol{\lambda}_*'\boldsymbol{\mu}_*^+) \Rightarrow 3\boldsymbol{\lambda}_*'\int r\boldsymbol{\mathcal{B}}_m$.*

□

The first part of Corollary 3 follows from the first-step TOLS estimator. For the second part, $\widehat{\xi}_T$ is not of primary interest. Although the convergence rate of $(\widehat{\xi}_T - \xi_{*T})$ is $T^{3/2}$, as given in the first part, $\xi_{*T} := \boldsymbol{\lambda}_*'\boldsymbol{\delta}_{*T}$ converges to $\boldsymbol{\lambda}_*'\boldsymbol{\mu}_*^+$ at the rate $T^{1/2}$. This implies that $T^{1/2}(\widehat{\xi}_T - \boldsymbol{\lambda}_*'\boldsymbol{\mu}_*^+)$ is asymptotically bounded in probability.

Theorem 4. *Under Assumption 1, and if $\ddot{\boldsymbol{\Sigma}}_*$ is PD, then $T[(\ddot{\boldsymbol{\beta}}_T^+ - \boldsymbol{\beta}_*^+)', (\ddot{\boldsymbol{\beta}}_T^- - \boldsymbol{\beta}_*^-)']' \Rightarrow \ddot{\mathbf{S}}\boldsymbol{\mathcal{R}}^{-1}\ddot{\boldsymbol{\mathcal{U}}}$.* □

First-Step FM-TOLS The limit distribution the TOLS estimator in Theorem 4 does not provide a basis for inference, as it is non-standard and exhibits asymptotic bias driven by $\boldsymbol{\upsilon}_{*m}$ and $\boldsymbol{\upsilon}_{*x}$. Thus, we provide an alternative first-step FM-OLS estimator. We make the following assumptions:

Assumption 3. *(i) $\ddot{\boldsymbol{\Sigma}}_*$ is finite and PD, such that there is a consistent estimator for $\ddot{\boldsymbol{\Sigma}}_*$:*

$$\bar{\boldsymbol{\Sigma}}_T := \begin{bmatrix} \bar{\boldsymbol{\Sigma}}_T^{(1,1)} & \bar{\boldsymbol{\sigma}}_T^{(1,2)} \\ \bar{\boldsymbol{\sigma}}_T^{(2,1)} & \bar{\sigma}_T^{(2,2)} \end{bmatrix} \xrightarrow{\mathbb{P}} \ddot{\boldsymbol{\Sigma}}_* := \begin{bmatrix} \ddot{\boldsymbol{\Sigma}}_*^{(1,1)} & \ddot{\boldsymbol{\sigma}}_*^{(1,2)} \\ \ddot{\boldsymbol{\sigma}}_*^{(2,1)} & \sigma_*^{(2,2)} \end{bmatrix};$$

and (ii) if we let $\bar{\boldsymbol{\Pi}}_T := T^{-1}\sum_{k=0}^{\ell}\sum_{t=k+1}^{T}\bar{\boldsymbol{g}}_{t-k}\bar{\boldsymbol{g}}_t'$, then:

$$\begin{bmatrix} \bar{\boldsymbol{\Pi}}_T^{(1,1)} & \bar{\boldsymbol{\pi}}_T^{(1,2)} \\ \bar{\boldsymbol{\pi}}_T^{(2,1)} & \bar{\pi}_T^{(2,2)} \end{bmatrix} := \bar{\boldsymbol{\Pi}}_T \xrightarrow{\mathbb{P}} \ddot{\boldsymbol{\Pi}}_* := \begin{bmatrix} \ddot{\boldsymbol{\Pi}}_*^{(1,1)} & \ddot{\boldsymbol{\pi}}_*^{(1,2)} \\ \ddot{\boldsymbol{\pi}}_*^{(2,1)} & \pi_*^{(2,2)} \end{bmatrix} := \lim_{T\to\infty}\frac{1}{T}\sum_{t=1}^{T}\sum_{i=1}^{t}\mathbb{E}[\ddot{\boldsymbol{g}}_t\ddot{\boldsymbol{g}}_t'],$$

which is finite, where $\bar{\boldsymbol{g}}_t := [\Delta\widehat{\boldsymbol{m}}_t', \Delta\boldsymbol{x}_t', \ddot{u}_t]'$ and $\ddot{u}_t := y_t - \ddot{\alpha}_T - \ddot{\boldsymbol{\beta}}_T^{+\prime}\boldsymbol{x}_t^+ - \ddot{\boldsymbol{\beta}}_T^{-\prime}\boldsymbol{x}_t^-$. □

Assumption 3 corresponds to Assumption 2 in the case with $k > 1$. The *fully-modified TOLS (FM-TOLS) estimator* is defined as $\bar{\boldsymbol{\varpi}}_T := (\sum_{t=1}^{T}\boldsymbol{r}_t\boldsymbol{r}_t')^{-1}(\sum_{t=1}^{T}\boldsymbol{r}_t\bar{y}_t - T\bar{\mathbf{S}}'\bar{\boldsymbol{\upsilon}}_T)$, where $\bar{y}_t := y_t - \boldsymbol{\ell}_t'(\bar{\boldsymbol{\Sigma}}_T^{(1,1)})^{-1}\bar{\boldsymbol{\sigma}}_T^{(1,2)}$, $\boldsymbol{\ell}_t := (\Delta\widehat{\boldsymbol{m}}_t', \Delta\boldsymbol{x}_t')'$, $\bar{\boldsymbol{\upsilon}}_T := \bar{\boldsymbol{\pi}}_T^{(1,2)} - \bar{\boldsymbol{\Pi}}_T^{(1,1)}(\bar{\boldsymbol{\Sigma}}_T^{(1,1)})^{-1}\bar{\boldsymbol{\sigma}}_T^{(1,2)}$ and $\bar{\mathbf{S}} := [\mathbf{0}_{2k\times 2}, \mathbf{I}_{2k}]$.

The following lemma corresponds to Lemma 3 for the case with $k > 1$:

Lemma 6. *Under Assumptions 1 and 3, $\bar{\mathbf{U}}_T := \ddot{\mathbf{D}}_T^{-1}\{\sum_{t=1}^{T}\boldsymbol{r}_t(u_t - \boldsymbol{\ell}_t'(\bar{\boldsymbol{\Sigma}}_T^{(1,1)})^{-1}\bar{\boldsymbol{\sigma}}_T^{(1,2)}) - T\bar{\mathbf{S}}'\bar{\boldsymbol{\upsilon}}_T\} \Rightarrow \bar{\boldsymbol{\mathcal{U}}} := \ddot{\tau}[\int d\mathcal{W}_u, \int r d\mathcal{W}_u, \int \boldsymbol{\mathcal{B}}_m' d\mathcal{W}_u - 3\int r d\mathcal{W}_u \int r\boldsymbol{\mathcal{B}}_m', \int \boldsymbol{\mathcal{B}}_x' d\mathcal{W}_u]'$, where $\ddot{\tau}^2 := plim_{T\to\infty}\bar{\tau}_T^2$ and $\bar{\tau}_T^2 := \bar{\sigma}_T^{(2,2)} - \bar{\boldsymbol{\sigma}}_T^{(2,1)}(\bar{\boldsymbol{\Sigma}}_T^{(1,1)})^{-1}\bar{\boldsymbol{\sigma}}_T^{(1,2)}$.* □

By Lemmas 5 and 6, the limit distribution of the FM-TOLS estimator is obtained as the product of $\boldsymbol{\mathcal{R}}^{-1}$ and $\bar{\boldsymbol{\mathcal{U}}}$. Letting $[\bar{\boldsymbol{\beta}}_T^{+\prime}, \bar{\boldsymbol{\beta}}_T^{-\prime}]' := \ddot{\mathbf{S}}\bar{\boldsymbol{\varpi}}_T$, we obtain its weak limit as follows:

Theorem 5. *Under Assumptions 1 and 3,* $\ddot{\mathbf{D}}_T(\bar{\boldsymbol{\varpi}}_T - \bar{\boldsymbol{\varpi}}_{*T}) \Rightarrow \boldsymbol{\mathcal{R}}^{-1}\bar{\boldsymbol{\mathcal{U}}}$ *and* $T[(\bar{\boldsymbol{\beta}}_T^+ - \boldsymbol{\beta}_*^+)', (\bar{\boldsymbol{\beta}}_T^- - \boldsymbol{\beta}_*^-)']' \Rightarrow \ddot{\mathbf{S}}\boldsymbol{\mathcal{R}}^{-1}\bar{\boldsymbol{\mathcal{U}}}$. □

The limit distribution of the FM-TOLS estimator is mixed normal: $\bar{\mathbf{D}}_T(\bar{\boldsymbol{\varpi}}_T - \bar{\boldsymbol{\varpi}}_{*T}) \overset{\text{A}}{\sim} N(\mathbf{0}, \ddot{\tau}^2\boldsymbol{\mathcal{R}}^{-1})$ conditional on $\sigma\{(\boldsymbol{\mathcal{B}}_m(r)', \boldsymbol{\mathcal{B}}_x(r)')', r \in (0,1]\}$.

3.3.4 Short-Run Parameter Estimation with $k > 1$

We can treat the FM-TOLS estimator of the long-run parameters as known when estimating the short-run parameters in the second step, because it has a convergence rate faster than $T^{1/2}$. Let $u_{t-1} := y_{t-1} - \boldsymbol{\beta}_*^{+\prime}\boldsymbol{x}_{t-1}^+ - \boldsymbol{\beta}_*^{-\prime}\boldsymbol{x}_{t-1}^- = y_{t-1} - \boldsymbol{\lambda}_*'\boldsymbol{\mu}_*^+(t-1) - \boldsymbol{\lambda}_*'\boldsymbol{m}_{t-1} - \boldsymbol{\eta}_*'\boldsymbol{x}_{t-1}$, where $\boldsymbol{\lambda}_*$, $\boldsymbol{\mu}_*^+$, and $\boldsymbol{\eta}_*$ are assumed to be known. This allows us to rewrite (4) as described in Section 3.3.2, so that the short-run parameters can be estimated by the OLS estimator $\widehat{\boldsymbol{\zeta}}_T$ and Theorem 3 can be applied.

4 Hypothesis Testing

In this section, we develop the testing procedure for the presence of asymmetries in both the long-run and short-run.

4.1 Testing Long-Run Symmetry with $k = 1$

Consider $H_0' : (\beta_*^+ - \beta_*^-) = r$ vs. $H_1' : (\beta_*^+ - \beta_*^-) \neq r$ for some $r \in \mathbb{R}$. By setting $r = 0$, we can test whether $\beta_*^+ = \beta_*^-$. Recalling that $\lambda_* := \beta_*^+ - \beta_*^-$, we express these hypotheses as $H_0'' : \lambda_* = r$ vs. $H_1'' : \lambda_* \neq r$. It is straightforward to test this restriction if λ_* is estimated by the FM-OLS estimator, which is asymptotically mixed-normal. The corresponding Wald statistic follows a chi-squared distribution under the null asymptotically. This is a significant advantage of the FM-OLS estimator over the OLS estimator.

Corollary 2 provides the limit distribution of $\widetilde{\lambda}_T$. Letting $\mathbf{S}_\ell := [0, 1, 0]$, then $T^{3/2}(\widetilde{\lambda}_T - \lambda_*) = \mathbf{S}_\ell\widetilde{\mathbf{D}}_T(\widetilde{\boldsymbol{\varrho}}_T - \boldsymbol{\varrho}_*) \Rightarrow \mathbf{S}_\ell\boldsymbol{\mathcal{Q}}^{-1}\widetilde{\boldsymbol{\mathcal{U}}}$, implying that $T^{3/2}(\widetilde{\lambda}_T - r) \Rightarrow \mathbf{S}_\ell\boldsymbol{\mathcal{Q}}^{-1}\widetilde{\boldsymbol{\mathcal{U}}}$ under H_0''. The Wald test statistic is constructed as $\mathcal{W}_T^{(\ell)} := T^3(\widetilde{\lambda}_T - r)^2(\widetilde{\tau}_T^2\mathbf{S}_\ell\widehat{\mathbf{Q}}_T^{-1}\mathbf{S}_\ell')^{-1}$. Notice, however, that this Wald statistic may be inappropriate to test other forms of hypothesis. For example, consider $H_0''' : \mathbf{R}\boldsymbol{\beta}_* = \mathbf{r}$

vs. $H_1''' : \mathbf{R}\boldsymbol{\beta}_* \neq \mathbf{r}$ for some $\mathbf{R} \in \mathbb{R}^{r\times 2}$ and $\mathbf{r} \in \mathbb{R}^r$ ($r \in \{1,2\}$), where $\boldsymbol{\beta}_* := (\beta_*^+, \beta_*^-)'$. Let: $\widetilde{\mathbf{R}}_\ell := \begin{bmatrix} 0 & 1 & 1 \\ 0 & 0 & 1 \end{bmatrix}$. These hypotheses can be rewritten as $H_0''' : \widetilde{\mathbf{R}}\boldsymbol{\varrho}_* = \mathbf{r}$ vs. $H_1''' : \widetilde{\mathbf{R}}\boldsymbol{\varrho}_* \neq \mathbf{r}$, where $\widetilde{\mathbf{R}}\boldsymbol{\varrho}_* = \boldsymbol{\beta}_*$ and $\widetilde{\mathbf{R}} := \mathbf{R}\widetilde{\mathbf{R}}_\ell$. Then, we construct the Wald test statistic as $\widetilde{\mathcal{W}}_T^{(\ell)} := (\widetilde{\mathbf{R}}\widetilde{\boldsymbol{\varrho}}_T - \mathbf{r})'(\widetilde{\tau}_T^2\widetilde{\mathbf{R}}\mathbf{Q}_T^{-1}\widetilde{\mathbf{R}}')^{-1}(\widetilde{\mathbf{R}}\widetilde{\boldsymbol{\varrho}}_T - \mathbf{r})$, where $\mathbf{Q}_T := \sum_{t=1}^T \boldsymbol{q}_t\boldsymbol{q}_t'$.

Theorem 6. *Under Assumptions 1 and 2, $\mathcal{W}_T^{(\ell)} \overset{A}{\sim} \mathcal{X}_1^2$ under H_0'' and $\widetilde{\mathcal{W}}_T^{(\ell)} \overset{A}{\sim} \mathcal{X}_2^2$ under H_0'''. For any sequence, c_T and $\widetilde{c}_T$ such that $c_T = o(T^3)$ and $\widetilde{c}_T = o(T^2)$, $\mathbb{P}(\mathcal{W}_T^{(\ell)} > c_T) \to 1$ under H_1'' and $\mathbb{P}(\widetilde{\mathcal{W}}_T^{(\ell)} > \widetilde{c}_T) \to 1$ under H_1'''.* □

4.2 Testing Short-Run Symmetry with $k = 1$

In NARDL models, it is common to test for additive symmetry of the short-run dynamic parameters. Consider $H_0 : \mathbf{R}_s\boldsymbol{\zeta}_* = \mathbf{r}$ vs. $H_1 : \mathbf{R}_s\boldsymbol{\zeta}_* \neq \mathbf{r}$, where $\mathbf{R}_s \in \mathbb{R}^{r\times(1+p+2q)}$ and $\mathbf{r} \in \mathbb{R}^r$ ($r \in \mathbb{N}$) are selection matrices. Define $\mathbf{R}_s := \left[\mathbf{0}_{1+p}', \boldsymbol{\iota}_q', -\boldsymbol{\iota}_q'\right]$ and $\mathbf{r} = 0$. The null hypothesis of additive short-run symmetry can be tested against the alternative hypothesis of asymmetry: $H_0 : \sum_{j=0}^{q-1}\pi_{j*}^+ = \sum_{j=0}^{q-1}\pi_{j*}^-$ vs. $H_1 : \sum_{j=0}^{q-1}\pi_{j*}^+ \neq \sum_{j=0}^{q-1}\pi_{j*}^-$.[7] The Wald test statistic is constructed as $\mathcal{W}_T^{(s)} := T(\mathbf{R}_s\widehat{\boldsymbol{\zeta}}_T - \mathbf{r})'(\mathbf{R}_s\widehat{\boldsymbol{\Gamma}}_T^{-1}\widehat{\boldsymbol{\Omega}}_T\widehat{\boldsymbol{\Gamma}}_T^{-1}\mathbf{R}_s')^{-1}(\mathbf{R}_s\widehat{\boldsymbol{\zeta}}_T - \mathbf{r})$, where $\widehat{\boldsymbol{\Omega}}_T := T^{-1}\sum_{t=1}^T \widehat{e}_t^2\boldsymbol{h}_t\boldsymbol{h}_t'$ is a consistent estimator of $\boldsymbol{\Omega}_*$. Let $\widehat{e}_t := \Delta y_t - \widehat{\boldsymbol{\zeta}}_T'\boldsymbol{h}_t$, where $\widehat{\boldsymbol{\zeta}}_T$ can be constructed from the first-step regression using FM-OLS. Further, if the condition in Lemma 4(*iii*) holds, then the Wald statistic simplifies to $\mathcal{W}_T^{(s)} := T(\mathbf{R}_s\widehat{\boldsymbol{\zeta}}_T - \mathbf{r})'(\widehat{\sigma}_{e,T}^2\mathbf{R}_s\widehat{\boldsymbol{\Gamma}}_T^{-1}\mathbf{R}_s')^{-1}(\mathbf{R}_s\widehat{\boldsymbol{\zeta}}_T - \mathbf{r})$, where $\widehat{\sigma}_{e,T}^2 := T^{-1}\sum_{t=1}^T \widehat{e}_t^2$.

Theorem 7. *Given Assumption 1, if $\boldsymbol{\Gamma}_*$ and $\boldsymbol{\Omega}_*$ are PD, then $\mathcal{W}_T^{(s)} \overset{A}{\sim} \mathcal{X}_r^2$ under H_0 and, for any sequence c_T such that $c_T = o(T)$, $\mathbb{P}(\mathcal{W}_T^{(s)} > c_T) \to 1$ under H_1.* □

4.3 Testing Long-Run Symmetry with $k > 1$

Define $\boldsymbol{\beta}_* := (\boldsymbol{\beta}_*^{+\prime}, \boldsymbol{\beta}_*^{-\prime})'$ as a natural extension of the corresponding definition in Section 4.1. Consider $H_0^{(4)} : \mathbf{R}\boldsymbol{\beta}_* = \boldsymbol{r}$ vs. $H_1^{(4)} : \mathbf{R}\boldsymbol{\beta}_* \neq \boldsymbol{r}$ for some $\mathbf{R} \in \mathbb{R}^{r\times 2k}$ and $\boldsymbol{r} \in \mathbb{R}^r$ ($r \leq 2k$).

[7] In the NARDL literature, several different forms of short-run symmetry restrictions have been considered, including pairwise symmetry of $\boldsymbol{\pi}_{j*}^+$ and $\boldsymbol{\pi}_{j*}^-$ for $j = 0, \ldots, q-1$ (e.g. SYG) and impact symmetry defined by $\boldsymbol{\pi}_{0*}^+$ and $\boldsymbol{\pi}_{0*}^-$ (e.g. Greenwood-Nimmo and Shin, 2013). It is straightforward to test these alternative restrictions by specifying appropriate selection matrices, $\mathbf{R}_s$ and $\mathbf{r}$.

We then construct the Wald test as $\ddot{\mathcal{W}}_T := T^2(\mathbf{R}\bar{\boldsymbol{\beta}}_T - \boldsymbol{r})'\{\bar{\tau}_T^2\mathbf{R}\ddot{\mathbf{S}}\ddot{\mathbf{R}}_T^{-1}\ddot{\mathbf{S}}'\mathbf{R}'\}^{-1}(\mathbf{R}\bar{\boldsymbol{\beta}}_T - \boldsymbol{r})$, where $\bar{\boldsymbol{\beta}}_T := (\bar{\boldsymbol{\beta}}_T^{+\prime}, \bar{\boldsymbol{\beta}}_T^{-\prime})'$.

Theorem 8. *Given Assumptions 1 and 3, $\ddot{\mathcal{W}}_T^{(\ell)} \overset{A}{\sim} \mathcal{X}_r^2$ under $H_0^{(4)}$. Further, for any sequence c_T such that $c_T = o(T^2)$, $\mathbb{P}(\ddot{\mathcal{W}}_T^{(\ell)} > c_T) \to 1$ under $H_1^{(4)}$.* □

4.4 Testing Short-Run Symmetry with $k > 1$

To examine the test for additive symmetry of the short-run dynamic parameters, we consider $H_0 : \mathbf{R}_s\boldsymbol{\zeta}_* = \mathbf{r}$ vs. $H_1 : \mathbf{R}_s\boldsymbol{\zeta}_* \neq \mathbf{r}$, where $\mathbf{R}_s \in \mathbb{R}^{r\times(1+p+2qk)}$ and $\mathbf{r} \in \mathbb{R}^r$ are selection matrices, and $\boldsymbol{\zeta}_*$ generalizes our prior definition for $k = 1$, viz., $\boldsymbol{\zeta}_* := (\rho_*, \gamma_*, \varphi_{1*}, \ldots, \varphi_{p-1*}, \boldsymbol{\pi}_{0*}^{+\prime}, \ldots, \boldsymbol{\pi}_{q-1*}^{+\prime}, \boldsymbol{\pi}_{0*}^{-\prime}, \ldots, \boldsymbol{\pi}_{q-1*}^{-\prime})$. Let $\mathbf{R}_s := \left[\mathbf{0}_{k\times(1+p)}, \boldsymbol{\iota}_q' \otimes \mathbf{I}_k, -\boldsymbol{\iota}_q \otimes \mathbf{I}_k\right]$ and $\mathbf{r} = \mathbf{0}$. Then, we can test the null hypothesis of additive short-run symmetry: $H_0 : \sum_{j=0}^{q-1}\boldsymbol{\pi}_{j*}^{+} = \sum_{j=0}^{q-1}\boldsymbol{\pi}_{j*}^{-}$ vs. $H_1 : \sum_{j=0}^{q-1}\boldsymbol{\pi}_{j*}^{+} \neq \sum_{j=0}^{q-1}\boldsymbol{\pi}_{j*}^{-}$. If the cointegration residuals are obtained as in Section 3.3.4, then we can employ the same Wald test statistic introduced in Section 4.2 for $k > 1$.

5 Monte Carlo Simulations

In this section, we conduct stochastic simulations for the case with $k = 1$ to examine the finite sample properties of the tests described in Section 4. Additional simulation results relating to the bias and mean squared error of the estimators as well as for the case with $k > 1$ are reported in the Online Supplement.

Consider the following NARDL(1,0) data generating process (DGP): $\Delta y_t = \gamma_* + \rho_* u_{t-1} + \varphi_*\Delta y_{t-1} + \pi_*^+\Delta x_t^+ + \pi_*^-\Delta x_t^- + e_t$, where $u_{t-1} := y_{t-1} - \alpha_* - \beta_*^+ x_{t-1}^+ - \beta_*^- x_{t-1}^-$, $\Delta x_t := \kappa_*\Delta x_{t-1} + \sqrt{1-\kappa_*^2}v_t$, and $(e_t, v_t)' \sim \text{IID}N(\mathbf{0}_2, \mathbf{I}_2)$.

Testing the Long-run Parameters We confine our attention to the case where the FM-OLS estimator is used in the first step and set $(\alpha_*, \beta_*^+, \beta_*^-, \gamma_*, \rho_*, \varphi_*, \pi_*^+, \pi_*^-, \kappa_*) = (0, 2, 1, 0, -2/3, \varphi_*, 1, 1/2, 1/2)$. We test $H_0^{(\ell)} : \beta_*^+ - \beta_*^- = 0$ vs. $H_1^{(\ell)} : \beta_*^+ - \beta_*^- \neq 0$ by allowing φ_* to vary over $-1/2$, $-1/4$, 0, $1/4$ and $1/2$. The simulation results reported in Table 1 reveal some size distortion in

small samples for negative values of φ_*. Nonetheless, as T increases, the distribution of the Wald test statistic becomes well-approximated by the chi-squared distribution with one degree of freedom.

— Insert Table 1 Here —

To examine the power of the Wald test, we generate data with $(\alpha_*, \beta_*^+, \beta_*^-, \gamma_*, \rho_*, \varphi_*, \pi_*^+, \pi_*^-, \kappa_*) = (0, 1.01, 1, 0, -2/3, \varphi_*, 1/3, 1/2, 1/2)$ and allow φ_* to vary as above. The simulation results for $\mathcal{W}_T^{(\ell)}$ reported in Table 2 confirm that the Wald test statistic is consistent under the alternative hypothesis. Furthermore, its power patterns are largely insensitive to the value of φ_*.

— Insert Table 2 Here —

Testing the Short-run Parameters To examine the empirical level properties of the Wald test statistic, we set $(\alpha_*, \beta_*^+, \beta_*^-, \gamma_*, \rho_*, \varphi_*, \pi_*^+, \pi_*^-, \kappa_*) = (0, 2, 1, 0, -2/3, \varphi_*, 1/2, 1/2, 1/2)$ and allow φ_* to vary over $-1/2$, $-1/4$, 0, $1/4$ and $1/2$, as above. We first estimate the long-run parameters by FM-OLS and compute $\widehat{u}_t$ before estimating the short-run parameters by OLS. We then test $H_0^{(s)} : \pi_*^+ - \pi_*^- = 0$ vs. $H_1^{(s)} : \pi_*^+ - \pi_*^- \neq 0$ using $\mathcal{W}_T^{(s)}$ with the heteroskedasticity consistent covariance estimator, $\widehat{\mathbf{\Omega}}_T$. The Wald statistic is compared against the critical values of the chi-squared distribution with one degree of freedom at the 1%, 5%, and 10% levels of significance.

The simulation results reported in Table 3 reveal that the finite sample distribution of the Wald test statistic is well-approximated by the chi-squared distribution. For each level of significance, its empirical level tends to the nominal level once the number of observations reaches 500. Furthermore, the empirical levels display little sensitivity to the value of φ_* even for small T.

— Insert Table 3 Here —

Next, we examine the empirical power properties of the Wald test statistic. We maintain the same hypotheses but update the parameters to $(\alpha_*, \beta_*^+, \beta_*^-, \gamma_*, \rho_*, \varphi_*, \pi_*^+, \pi_*^-, \kappa_*) = (0, 2, 1, 0, -2/3, \varphi_*, 1, 1/2, 1/2)$. We compute $\mathcal{W}_T^{(s)}$ using the heteroskedasticity consistent covariance matrix estimator. Two points are noteworthy from the simulation results reported in Table 4. First, the empirical power of the Wald test rises with T, indicating that the test is consistent. Second, the power of the Wald test exhibits little sensitivity to the degree of autocorrelation captured by the value of φ_*.

— Insert Table 4 Here —

6 Estimation Results

We examine the asymmetric relationship between R&D intensity and physical investment using quarterly U.S. data covering the period from 1960q1 to 2019q4, which we collect from the Federal Reserve Economic Data service at the Federal Reserve Bank of St. Louis. R&D intensity, denoted r_t, is measured as 100 times the ratio of seasonally adjusted nominal R&D expenditure to seasonally adjusted nominal GDP. Investment, denoted i_t, is the log of seasonally adjusted real gross private domestic investment in 2012 prices (GPDI). The National Income and Product Accounts (NIPAs) separately aggregate R&D expenditure and GPDI, so there is no double-counting of R&D expenditure in our analysis.[8]

The Phillips and Perron (1988) unit root test results reported in the Online Supplement indicate that both r_t and i_t are nonstationary.[9] Because of their nonstationarity, we report descriptive statistics for the first differences of both series in the Online Supplement. While the growth rate of R&D intensity is well approximated by a normal distribution centered at zero, the GPDI growth rate exhibits a non-zero mean with negative skewness and notable excess kurtosis. The different behavior of the two series suggests that it may be inadequate to apply a linear model of the relationship between r_t and i_t. Furthermore, from the unit root test, we find that i_t is a unit-root process with a time drift, but r_t is a driftless unit-root process.[10] As described above, the NARDL model is able to capture a cointegrating relationship between i_t and r_t without the need to include a deterministic time trend.

We estimate the NARDL model using the two-step procedure proposed in Section 3, with the FM-OLS estimator used in the first step. We select the lag orders using the Akaike Information Criterion (AIC), which results in the following NARDL(2,2) error-correction specification:

$$\Delta i_t = \gamma_* + \rho_* u_{t-1} + \varphi_* \Delta i_{t-1} + \pi_{0*}^{+} \Delta r_t^{+} + \pi_{0*}^{-} \Delta r_t^{-} + \pi_{1*}^{+} \Delta r_{t-1}^{+} + \pi_{1*}^{-} \Delta r_{t-1}^{-} + e_t,$$

where $i_t = \beta_*^{+} r_t^{+} + \beta_*^{-} r_t^{-} + u_t$. When applying the Phillips and Perron (1988) unit root test to the

[8] The Bureau of Economic Analysis constructs a partial R&D satellite account and revises the NIPAs by treating R&D expenditure as part of investment (see Fraumeni and Okubo, 2005).

[9] Irrespective of the presence of a time trend, the unit-root hypothesis cannot be rejected for the two series.

[10] From the univariate time series regressions, we observe that the time trend coefficient is significantly different from zero for i_t, but not for r_t.

residuals, we reject the null hypothesis of no cointegration with a p-value of 0.010, and conclude that there exists an asymmetric long-run relationship between i_t, r_t^+ and r_t^-.

— Insert Table 5 Here —

The long-run parameter estimates, reported in Table 5, are not only different in magnitude, with $\tilde{\beta}_*^+ > \tilde{\beta}_*^-$, but they also display opposite signs: $\tilde{\beta}_*^+$ is positive and $\tilde{\beta}_*^-$ is negative, with both being highly statistically significant. Furthermore, the null hypothesis of long-run symmetry is strongly rejected.[11] This long-run asymmetry is in line with the fact that the NARDL model can capture a cointegrating relationship between a unit root process with a drift and a driftless unit root process.[12]

Our results indicate that an increase in R&D spending equivalent to 1% of GDP when R&D growth exceeds GDP growth (i.e. when innovative R&D is prevalent) is associated with an increase in real investment of 2.7% in the long-run. On the other hand, an increase in R&D spending of 1% of GDP when R&D growth is slower than GDP growth (i.e. when managerial R&D is prevalent) reduced real investment by 6.4%.[13] This is consistent with our theoretical prediction regarding the asymmetric relationship between R&D intensity and physical investment. Specifically, we expect $\beta_*^+ > 0$ due to the complementarity of innovative R&D expenditure and physical investment, while $\beta_*^- < 0$ is consistent with the nature of managerial R&D expenditure and physical investment as substitutes. Our results suggest that the substitutionary effect is much stronger than the complementary effect in the long-run over our sample period.

Next, from the short-run estimation results reported in Table 6, we find no evidence of residual autocorrelation up to order 4, with the p-value of the Breusch-Godfrey Lagrange multiplier (LM) test statistic being 0.39. However, the Breusch-Pagan LM test rejects the conditional homoskedasticity hypothesis with a p-value of 0.035. Thus, we report the robust standard errors obtained using the HAC covariance matrix estimator.

— Insert Table 6 Here —

[11] Due to the transformation applied to the FM-OLS slope parameters to obtain the long-run parameters, the Wald test of $H_0 : \beta_*^+ = \beta_*^-$ versus $H_1 : \beta_*^+ \neq \beta_*^-$ is equivalent to a t-test of the hypothesis $H_0 : \lambda_* = 0$ versus $H_1 : \lambda_* \neq 0$, which returns a p-value almost identical to zero.

[12] If $\beta_*^+ = \beta_*^-$, then i_t could not exhibit a time drift, because $\mathbb{E}[\Delta i_t] = (\beta_*^+ - \beta_*^-)\mathbb{E}[\Delta r_t^+]$ and $\mathbb{E}[\Delta r_t] = 0$. Consequently, the pattern of long-run asymmetry that we observe is consistent with the positive time drift in i_t.

[13] Note that the average value of U.S. R&D intensity over our sample period is 2.69% of GDP with a standard deviation of 0.2%. Therefore, a shock equivalent to 1% of GDP is large by historical standards.

We observe that disequilibrium errors are corrected at a statistically significant rate of 6.8% per quarter, but we find no evidence of short-run asymmetry. The Wald test of the null hypothesis of impact symmetry, $H_0 : \pi_{0*}^{+} = \pi_{0*}^{-}$, versus the alternative, $H_1 : \pi_{0*}^{+} \neq \pi_{0*}^{-}$, returns a p-value of 0.677. Moreover, the null hypothesis of additive short-run symmetry, $H_0 : \pi_{0*}^{+} + \pi_{1*}^{+} = \pi_{0*}^{-} + \pi_{1*}^{-}$, is not rejected against the alternative, $H_1 : \pi_{0*}^{+} + \pi_{1*}^{+} \neq \pi_{0*}^{-} + \pi_{1*}^{-}$, with a p-value of 0.146.

The short-run dynamic coefficients cannot be easily interpreted in isolation. Consequently, in panels (a) and (b) of Figure 3, we report the cumulative dynamic multiplier effects associated with an increase in R&D intensity equal to 1% of GDP in each regime (i.e. in the case where R&D grows faster than GDP and in the case where it grows slower than GDP). In panel (c), we display the difference between these two dynamic multipliers as a measure of asymmetry at each horizon. We also provide an empirical 95% confidence interval obtained from 5,000 iterations of a moving block bootstrap procedure with a block length of $T^{1/3}$.

— Insert Figure 3 Here —

In Figure 3(a), we find that a 1% increase in R&D intensity when R&D growth exceeds GDP growth (i.e. when innovative R&D predominates) initially reduces real physical investment, with a peak reduction of 6.7% after one quarter. From the perspective of creative destruction, this initial reduction may reflect that large innovate R&D expenditures focus on new product development, creating a degree of obsolescence in existing technologies and promoting an incentive to reduce investment in those technologies. After this initial reduction, the dynamic multiplier rises steadily and becomes positive after 8 quarters, as newly developed technologies begin to mature and scale. In the long-run, the impact of innovative R&D expenditure on real physical investment is positive, at 2.7%.

By contrast, Figure 3(b) shows that a 1% increase in R&D intensity when managerial R&D predominates leads to an immediate reduction in physical investment of -3.6%, reflecting short-term substitution. The dynamic multiplier effect is then indistinguishable from zero until horizon 11, after which it converges to a long-run value of -6.4%. Overall, the figure reveals that an economic environment that favors managerial R&D expenditure is conducive to decreased real physical investment, particularly in the long-run, as the efficiency gains derived from managerial R&D raise the return on each dollar invested.

In Figure 3(c), we characterize the asymmetry between the cumulative dynamic multipliers associated with innovative and managerial R&D expenditures. Specifically, we subtract the cumulative dynamic multiplier reported in panel (b) from that reported in panel (a) and provide a 95% bootstrap interval for this quantity that can be used to test for asymmetry at any horizon. In the short-run, we observe substantial negative asymmetry that is marginally insignificant at the 5% level but that is statistically significant at the 10% level. This suggests that real physical investment is more responsive to innovative than managerial R&D expenditures in the short-run. However, in the long-run, we observe positive asymmetry as the substitutionary effect associated with managerial R&D expenditure is stronger than the complementarity of innovative R&D expenditure. This pattern is generally in line with the product life cycle, where large innovative R&D expenditure occurs early in the cycle, often exerting a disruptive influence on existing products. Once the new product becomes established, managerial R&D expenditure focuses on scaling-up production and delivering efficiency gains. Collectively, these results have important implications for the endogenous growth literature, where linear functional forms are routinely imposed to characterize the relationship between the stock of knowledge and R&D intensity (e.g. Romer, 1990). Our main findings suggest that the imposition of a linear functional form in this case may produce misleading results.

In the Online Supplement, we present the results of a replication exercise in which the preceding analysis is repeated using the single-step OLS estimation procedure popularized by SYG. The results of this exercise are summarized compactly in Figure A.1, which presents the cumulative dynamic multipliers obtained from the single-step parameter estimates. A comparison of Figures 3 and A.1 reveals that they are very similar, which indicates that the single-step and two-step estimation procedures yield comparable outcomes.

— Insert Figure A.1 Here —

7 Concluding Remarks

In this paper, we analyze the potentially asymmetric relationship between R&D expenditure and physical investment in the U.S. using quarterly time series data over the period 1960Q1–2019Q4.

We make three contributions. First, we develop a novel theoretical model that exploits documented

differences in the characteristics of innovative and managerial R&D to establish that there exists an asymmetric relationship between physical investment and R&D expenditures. Our model yields the testable hypotheses that innovative R&D expenditure is a complement to physical investment, while managerial R&D expenditure is a substitute for physical investment.

Second, we develop a corresponding empirical specification that takes the form of a NARDL model in which real physical investment is regressed on the positive and negative partial sums of aggregate R&D intensity. While the NARDL model has been widely applied to the analysis of asymmetric relationships (see Cho et al., 2023), the asymptotic theory for the single-step NARDL estimator and the associated inferential procedures has yet to be fully developed due to an asymptotic singularity issues that frustrate efforts to derive its limit distribution. We develop a two-step estimation procedure to overcome this issue. In the first step, we estimate the parameters of a transformed long-run relationship using any consistent estimator with a convergence rate faster than $T^{1/2}$. We advocate the use of the FM-OLS estimator that accounts for serial correlation and potential endogeneity of the explanatory variables and that facilitates standard inference. In the second step, the short-run dynamic coefficients can be consistently estimated by OLS, treating the error-correction term from the first step as given. We derive the asymptotic distributions of the estimators, and develop standard Wald tests for inference on the short- and long-run parameters. A suite of Monte Carlo simulations indicates that our asymptotic results offer good approximations in finite samples.

Third, we provide comprehensive empirical evidence in favor of the asymmetric relationship between aggregate R&D intensity and investment. In the long-run, physical investment responds positively to R&D expenditures when their growth rate exceeds the growth rate of GDP and negatively when they are growing more slowly than GDP. This supports our theoretical prediction that the innovative (managerial) R&D expenditure is a complement to (substitute for) physical investment. Furthermore, we find that physical investment is more sensitive to changes in R&D intensity when the growth rate of R&D expenditure is lower than GDP growth.

Our work opens several avenues for continuing research. On the methodological side, there is scope to generalize our approach to accommodate trending regressors or to estimate an unknown threshold parameter in the construction of the partial sum processes. On the empirical side, our results motivate the study of potential asymmetries in other areas of the innovation literature, such

as in the knowledge production function that is routinely estimated in linear form in the endogenous growth literature.

References

AGARWAL, R. AND D. B. AUDRETSCH (2001): "Does Entry Size Matter? The Impact of the Life Cycle and Technology on Firm Survival," *Journal of Industrial Economics*, 49, 21–43.

AGHION, P., R. BLUNDELL, R. GRIFFTH, P. HOWITT, AND S. PRANTL (2009): "The Effects of Entry on Incumbent Innovation and Productivity," *Review of Economics and Statistics*, 91, 20–32.

AUDRETSCH, D. B. (1987): "An Empirical Test of the Industry Life Cycle," *Weltwirtschaftliches Archiv*, 123, 297–308.

BARATI, M. AND H. FARIDITAVANA (2018): "Asymmetric Effect of Income on the US Healthcare Expenditure: Evidence from the Nonlinear Autoregressive Distributed Lag (ARDL) Approach," *Empirical Economics*, in press.

BAUSSOLA, M. (2000): "The Causality Between R&D and Investment," *Economics of Innovation and New Technology*, 9, 385–399.

BOX, M., K. GRATZER, AND X. LIN (2018): "The Asymmetric Effect of Bankruptcy Fraud in Sweden: A Long-Term Perspective," *Journal of Quantitative Criminology*, in press.

BRUN-AGUERRE, R. X., A.-M. FUERTES, AND M. J. GREENWOOD-NIMMO (2017): "Heads I Win; Tails You Lose: Asymmetry in Exchange Rate Pass-Through into Import Prices," *Journal of the Royal Statistical Society: Series A (Statistics in Society)*, 180, 587–612.

CHIAO, C. (2001): "The Relationship between R&D and Physical Investment of Firms in Science-Based Industries," *Applied Economics*, 33, 23–35.

CHO, J., M. GREENWOOD-NIMMO, AND Y. SHIN (2023): "Recent Developments of the Autoregressive Distributed Lag Modelling Framework," *Journal of Economic Surveys*, 37, 7–32.

CHUNG, D. AND D. SHIN (2020): "When do Firms Invest in R&D? Two Types of Performance Feedback and Organizational Search in the Korean Shipbuilding Industry," *Asian Business & Management*, forthcoming.

COMIN, D. AND T. PHILIPPON (2005): "The Rise in Firm-level Volatility: Causes and Conse-

quences," *NBER/Macroeconomics Annual*, 20, 167–201.

EBERHARDT, M. AND A. F. PRESBITERO (2015): "Public Debt and Growth: Heterogeneity and Non-Linearity," *Journal of International Economics*, 97, 45–58.

ENGLE, R. F. AND C. W. GRANGER (1987): "Co-integration and Error Correction: Representation, Estimation and Testing," *Econometrica*, 55, 251–276.

FERRIS, J. S., S. L. WINER, AND D. E. OLMSTEAD (2020): "A Dynamic Model of Political Party Equilibrium: The Evolution of ENP in Canada, 1870 – 2015," Working Paper 8387, CESifo, Munich.

FRAUMENI, B. M. AND S. OKUBO (2005): "R&D in the National Income and Product Accounts: A First Look at Its Effect on GDP," in *Measuring Capital in the New Economy*, ed. by J. H. C. Corrado and D. Sichel, Chicago (IL): The University of Chicago Press, 275–322.

FUDENBERG, D., R. GILBERT, J. STIGLITZ, AND J. TIROLE (1983): "Preemption, Leapfrogging and Competition in Patent Races," *European Economic Review*, 22, 3–31.

GORT, M. AND R. A. WALL (1986): "The Evolution of Technologies and Investment in Innovations," *Economic Journal*, 96, 741–757.

GREENWOOD-NIMMO, M. J. AND Y. SHIN (2013): "Taxation and the Asymmetric Adjustment of Selected Retail Energy Prices in the UK," *Economics Letters*, 121, 411–416.

GROSSMAN, G. M. AND C. SHAPIRO (1987): "Dynamic R&D Competition," *Economic Journal*, 97, 372–387.

HAMMOUDEH, S., A. LAHIANI, D. K. NGUYEN, AND R. M. SOUSA (2015): "An Empirical Analysis of Energy Cost Pass-Through to CO2 Emission Prices," *Energy Economics*, 49, 149–156.

HARRIS, C. J. AND J. S. VICKERS (1987): "Racing with Uncertainty," *Review of Economic Studies*, 54, 1–21.

HE, Z. AND F. ZHOU (2018): "Time-Varying and Asymmetric Eeffects of the Oil-Specific Demand Shock on Investor Sentiment," *PLOS ONE*, 31.

KAMIEN, M. I. AND N. L. SCHWARTZ (1972): "Timing of Innovations under Rivalry," *Econometrica*, 40, 43–60.

KLEPPER, S. (1996): "Entry, Exit, Growth, and Innovation over the Product Life Cycle," *American Economic Review*, 86, 562–583.

——— (1997): "Industry Life Cycles," *Industrial and Corporate Change*, 6, 145–182.

LACH, S. AND R. ROB (1996): "R&D Investment and Industry Dynamics," *Journal of Economics and Management Strategy*, 5, 217–249.

LACH, S. AND M. SCHANKERMAN (1989): "Dynamics of R&D and Physical Investment in the Scientific Sector," *Journal of Political Economy*, 97, 880–904.

NEWEY, W. K. AND K. D. WEST (1987): "A Simple, Positive Semi-Definite, Heteroskedasticity and Autocorrelation Consistent Covariance Matrix," *Econometrica*, 55, 703–708.

PESARAN, M. H. AND Y. SHIN (1998): "An Autoregressive Distributed Lag Modelling Approach to Cointegration Analysis," in *Econometrics and Economic Theory: The Ragnar Frisch Centennial Symposium*, ed. by S. Strom, Cambridge: Cambridge University Press, Econometric Society Monographs, 371–413.

PESARAN, M. H., Y. SHIN, AND R. J. SMITH (2001): "Bounds Testing Approaches to the Analysis of Level Relationships," *Journal of Applied Econometrics*, 16, 289–326.

PHILLIPS, P. AND P. PERRON (1988): "Testing for a Unit Root in Time Series Regression," *Biometrika*, 75, 335–346.

PHILLIPS, P. C. AND B. E. HANSEN (1990): "Statistical Inference in Instrumental Variable Regression with I(1) Processes," *Review of Economic Studies*, 57, 99–125.

REINGANUM, J. F. (1982): "A Dynamic Game of R&D: Patent Protection and Competitive Behavior," *Econometrica*, 50, 671–688.

ROMER, P. M. (1990): "Endogenous Technological Change," *Journal of Political Economy*, 98, 71–102.

SCHMOOKLER, J. (1966): *Innovation and Economic Growth*, Cambridge (MA): Harvard University Press.

SCHUMPETER, J. A. (1942): *Capitalism, Socialism, and Democracy*, New York (NY): Harper & Row.

SHIN, Y., B. YU, AND M. J. GREENWOOD-NIMMO (2014): "Modelling Asymmetric Cointegration and Dynamic Multipliers in a Nonlinear ARDL Framework," in *Festschrift in Honor of Peter Schmidt: Econometric Methods and Applications*, ed. by W. Horrace and R. Sickles, New York (NY): Springer Science & Business Media, 281–314.

SÜSSMUTH, B. AND U. WOITEK (2013): "Estimating Dynamic Asymmetries in Demand at the Munich Oktoberfest," *Tourism Economics*, 19, 653–674.

UTTERBACK, J. AND W. Y. ABERNATHY (1975): "A Dynamic Model of Process and Product Innovation," *Omega*, 3, 639–659.

VERHEYEN, F. (2013): "Exchange Rate Nonlinearities in EMU Exports to the US," *Economic Modelling*, 32, 66–76.

ZIF, J. AND D. J. MCCARTHY (1997): "The R&D Cycle: The Influence of Product and Process R&D on Short-Term ROI," *IEEE Transactions on Engineering Management*, 44, 114–123.

φ_*	sample size	100	250	500	750	1,000
-0.50	1%	12.40	5.06	2.38	1.82	1.44
	5%	23.34	12.88	7.96	7.70	5.90
	10%	31.50	21.04	14.08	13.22	11.46
-0.25	1%	8.74	3.80	2.54	1.74	1.18
	5%	19.06	11.10	8.44	6.62	5.48
	10%	27.22	18.36	14.96	11.68	10.48
0.00	1%	4.96	2.92	1.84	1.72	1.42
	5%	13.86	9.76	7.20	6.60	6.12
	10%	21.40	16.28	13.02	12.20	11.34
0.25	1%	3.32	1.62	1.34	1.22	1.06
	5%	10.38	6.24	5.56	5.66	5.60
	10%	17.28	11.42	10.96	11.22	10.70
0.50	1%	1.70	0.86	0.78	0.66	0.72
	5%	5.82	4.06	4.60	4.30	4.22
	10%	10.74	8.20	9.88	9.08	9.12

Table 1: EMPIRICAL LEVELS OF THE WALD TEST FOR LONG-RUN SYMMETRY. The FM-OLS is used in the first step. The data is generated as follows: $\Delta y_t = -(2/3)u_{t-1} + \varphi_* \Delta y_{t-1} + (1/3)\Delta x_t^+ + (1/2)\Delta x_t^- + e_t$, where $u_t := y_t - x_t^+ - x_t^-$, $\Delta x_t = 0.5\Delta x_{t-1} + \sqrt{1-0.5^2}v_t$, and $(e_t, v_t)' \sim$ IID$N(\mathbf{0}_2, \mathbf{I}_2)$. $H_0^{(\ell)} : \beta_*^+ - \beta_*^- = 0$ vs. $H_1^{(\ell)} : \beta_*^+ - \beta_*^- \neq 0$. The simulation results are obtained using $R = 5,000$ replications.

φ_*	sample size	100	250	500	750	1,000
-0.50	1%	9.80	20.76	83.66	97.34	99.76
	5%	20.00	35.78	89.36	98.54	99.96
	10%	27.66	44.70	91.98	98.92	99.96
-0.25	1%	7.90	26.04	88.16	98.44	99.82
	5%	17.98	41.74	92.88	99.32	99.92
	10%	25.08	51.30	94.58	99.60	99.94
0.00	1%	5.74	32.24	91.22	99.20	99.86
	5%	14.72	49.46	95.12	99.68	99.96
	10%	22.40	58.54	96.66	99.80	99.98
0.25	1%	4.4	34.46	92.36	99.38	99.96
	5%	12.08	52.82	96.04	99.70	100.0
	10%	19.2	61.96	97.22	99.82	100.0
0.50	1%	2.92	25.40	90.96	99.16	99.98
	5%	9.44	47.06	95.40	99.70	100.0
	10%	16.08	58.68	96.98	99.82	100.0

Table 2: EMPIRICAL POWER OF THE WALD TEST FOR LONG-RUN SYMMETRY (IN PERCENT). The FM-OLS is used in the first step. The data is generated as follows: $\Delta y_t = -(2/3)u_{t-1} + \varphi_* \Delta y_{t-1} + (1/3)\Delta x_t^+ + (1/2)\Delta x_t^- + e_t$, where $u_t := y_t - 1.01x_t^+ - x_t^-$, $\Delta x_t = 0.5\Delta x_{t-1} + \sqrt{1-0.5^2}v_t$, and $(e_t, v_t)' \sim$ IID$N(\mathbf{0}_2, \mathbf{I}_2)$. $H_0^{(\ell)} : \beta_*^+ - \beta_*^- = 0$ vs. $H_1^{(\ell)} : \beta_*^+ - \beta_*^- \neq 0$. The simulation results are obtained using $R = 5,000$ replications.

φ_*	sample size	100	250	500	750	1,000
-0.50	1%	2.44	1.60	0.98	1.18	1.12
	5%	8.06	6.06	5.42	5.46	6.02
	10%	13.82	11.00	10.90	10.36	10.94
-0.25	1%	2.38	1.74	1.46	1.30	1.14
	5%	7.38	6.44	6.02	5.36	5.30
	10%	12.90	11.38	11.28	10.54	10.48
0.00	1%	2.12	1.18	1.22	1.26	0.98
	5%	7.30	5.86	5.76	6.00	5.20
	10%	13.40	11.26	10.94	11.16	10.22
0.25	1%	2.28	1.42	1.36	0.96	0.82
	5%	7.32	6.14	5.84	5.12	4.68
	10%	13.42	11.40	10.96	9.76	9.50
0.50	1%	2.02	1.80	0.98	1.10	1.22
	5%	6.64	6.44	5.44	5.52	5.54
	10%	11.84	11.54	10.62	10.60	10.74

Table 3: EMPIRICAL LEVELS OF THE WALD TEST FOR SHORT-RUN SYMMETRY (IN PERCENT). The FM-OLS is used in the first step and OLS is used in the second step. The data is generated as follows: $\Delta y_t = -(2/3)u_{t-1} + \varphi_* \Delta y_{t-1} + (1/2)\Delta x_t^+ + (1/2)\Delta x_t^- + e_t$, where $u_t := y_t - 2x_t^+ - x_t^-$, $\Delta x_t = 0.5\Delta x_{t-1} + \sqrt{1-0.5^2}v_t$, and $(e_t, v_t)' \sim \text{IID}N(\mathbf{0}_2, \mathbf{I}_2)$. $H_0^{(s)} : \pi_*^+ - \pi_*^- = 0$ vs. $H_1^{(s)} : H_0 : \pi_*^+ - \pi_*^- \neq 0$. The simulation results are obtained using $R = 5,000$ replications.

φ_*	sample size	100	250	500	750	1,000
-0.50	1%	17.86	44.00	78.48	93.50	98.40
	5%	35.38	66.66	91.82	98.44	99.76
	10%	45.56	76.70	95.76	99.34	99.92
-0.25	1%	17.58	44.84	79.40	93.70	98.32
	5%	34.96	66.66	91.90	98.26	99.72
	10%	46.04	76.64	95.96	99.14	99.86
0.00	1%	17.26	43.16	78.56	93.28	98.60
	5%	35.66	66.68	92.38	98.14	99.72
	10%	46.62	76.14	96.06	99.18	99.90
0.25	1%	17.90	43.02	78.76	93.34	98.72
	5%	35.02	66.14	92.12	98.32	99.68
	10%	45.80	76.24	95.48	99.34	99.98
0.50	1%	17.50	42.82	77.82	92.94	98.54
	5%	34.20	65.78	91.32	98.28	99.78
	10%	44.90	76.06	94.90	99.26	99.92

Table 4: EMPIRICAL POWER OF THE WALD TEST FOR SHORT-RUN SYMMETRY (IN PERCENT). The FM-OLS is used in the first step and OLS is used in the second step. The data is generated as follows: $\Delta y_t = -(2/3)u_{t-1} + \varphi_* \Delta y_{t-1} + \Delta x_t^+ + (1/2)\Delta x_t^- + e_t$, where $u_t := y_t - 2x_t^+ - x_t^-$, $\Delta x_t = 0.5\Delta x_{t-1} + \sqrt{1-0.5^2}v_t$, and $(e_t, v_t)' \sim \text{IID}N(\mathbf{0}_2, \mathbf{I}_2)$. $H_0^{(s)} : \pi_*^+ - \pi_*^- = 0$ vs. $H_1^{(s)} : H_0 : \pi_*^+ - \pi_*^- \neq 0$. The simulation results are obtained using $R = 5,000$ replications.

	Estimate	S.E.
Intercept	7.453	0.381
β_*^+	0.271	0.133
β_*^-	-0.640	0.154

Table 5: LONG-RUN PARAMETER ESTIMATES USING QUARTERLY OBSERVATIONS. This table reports the long-run parameter estimates obtained from our two-step estimation procedure applied to observations from 1960Q1 to 2019Q4, where FM-OLS is used in the first step.

	Estimate	S.E.
γ_*	0.015	0.005
ρ_*	-0.068	0.016
φ_*	0.255	0.066
π_{0*}^+	-0.555	0.179
π_{1*}^+	-0.029	0.150
π_{0*}^-	-0.359	0.344
π_{1*}^-	0.482	0.176
Adjusted R^2	0.199	
$\mathcal{X}^2_{\text{S.Corr.}}$	0.385	
$\mathcal{X}^2_{\text{Hetero.}}$	0.035	

Table 6: DYNAMIC PARAMETER ESTIMATES USING QUARTERLY OBSERVATIONS. This table reports parameter estimates for the NARDL(2,2) model in error-correction form estimated using the two-step procedure applied to observations from 1960Q1 to 2019Q4, where FM-OLS is used in the first step and OLS is used in the second step. The lag order is selected by AIC, and the standard errors are computed by HAC robust covariance matrix estimation. $\mathcal{X}^2_{\text{S.Corr.}}$ denotes the Breusch–Godfrey Lagrange multiplier test for serial correlation up to order four. $\mathcal{X}^2_{\text{Hetero.}}$ denotes the Breusch–Pagan–Godfrey Lagrange multiplier test for residual heteroskedasticity. The values reported for these two tests are asymptotic p-values.

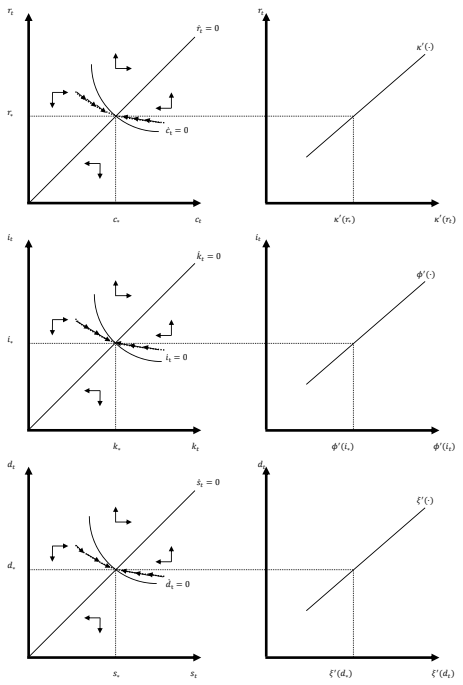

Figure 1: PHASE DIAGRAMS AND STEADY STATE. This figure shows the phase diagrams of (r_t, c_t), (i_t, k_t), and (d_t, k_t) and their relationships with the marginal cost functions.

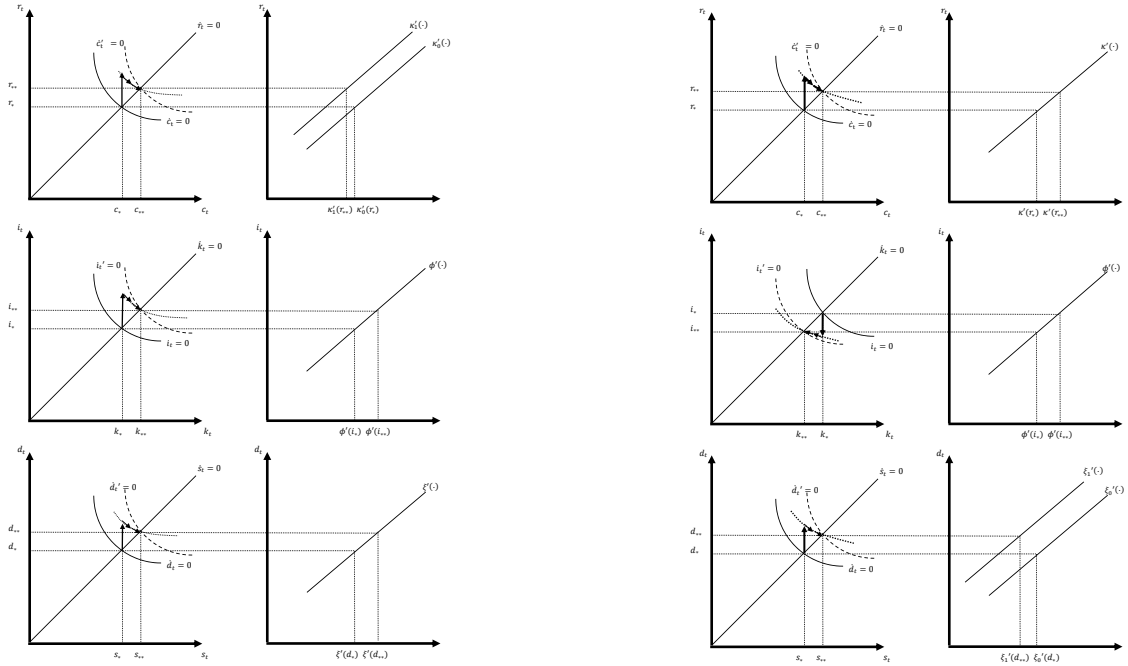

Figure 2: PHASE DIAGRAMS AND STEADY STATE. The left figure demonstrates how the steady-state levels are adjusted as the marginal cost function $\kappa'(\cdot)$ of innovative R&D expenditure decreases from $\kappa_0'(\cdot)$ to $\kappa_1'(\cdot)$. The right figure demonstrates how the steady-state levels are adjusted as the marginal cost function of managerial R&D expenditure decreases from $\xi_0'(\cdot)$ to $\xi_1'(\cdot)$.

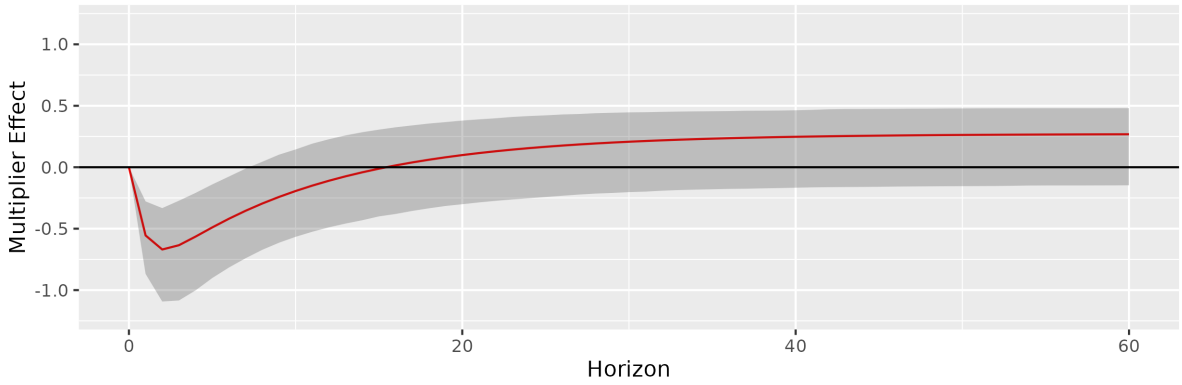

(a) Cumulative response of i_{t+h} to a +1 unit shock to r_t^+ in period 1

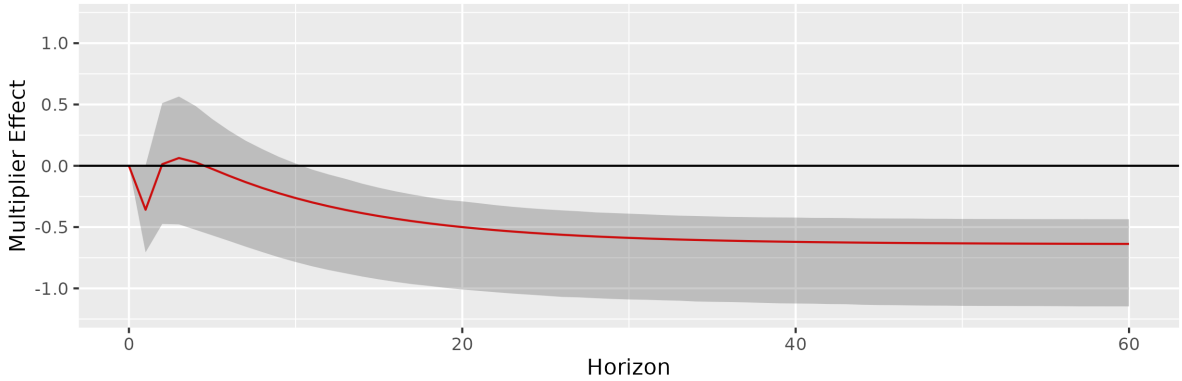

(b) Cumulative response of i_{t+h} to a +1 unit shock to r_t^- in period 1

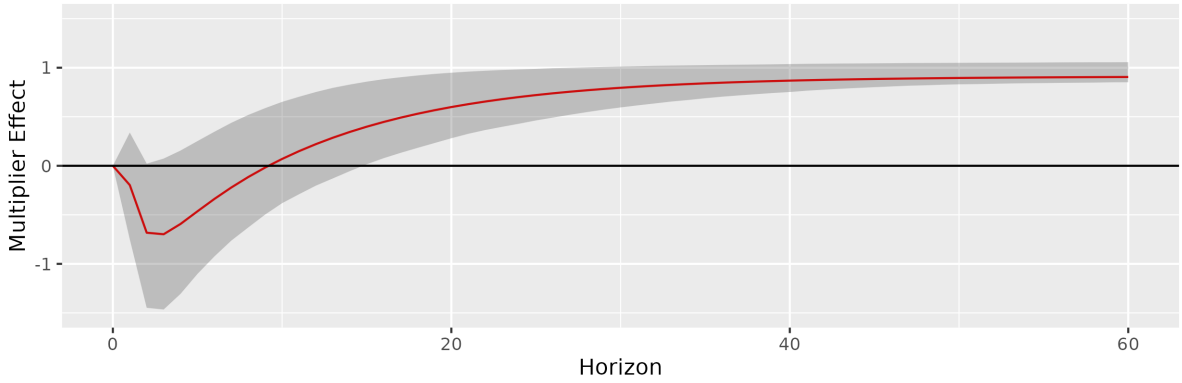

(c) Asymmetry across horizons

Figure 3: CUMULATIVE DYNAMIC MULTIPLIERS. Panels (a) and (b) present the cumulative dynamic multiplier effects with respect to unit shocks to r_t^+ and r_t^-, respectively, occurring in period 1. Panel (c) shows the asymmetry at each horizon, i.e., the value of the cumulative dynamic multiplier effect in panel (b) subtracted from the corresponding value in panel (a). Empirical 95% confidence intervals obtained from 5,000 replications of a moving block bootstrap procedure are reported throughout.

Online Supplement for 'Two-Step Nonlinear ARDL Estimation of the Relationship between R&D Intensity and Investment'[1]

by

Jin Seo Cho[a], Matthew Greenwood-Nimmo[b,c,d], and Yongcheol Shin[e]

[a]Yonsei University

[b]University of Melbourne, [c]Australian National University, [d]Codera Analytics

[e]University of York

This Online Supplement is comprised of six sections. In Sections A.1 and A.2, we provide proofs of the main claims of the manuscript. In Section A.3, we employ the extreme production function in (1) and conduct a comparative analysis to confirm the theoretical results in Section 2.2. In Section A.4, we further explore the singularity problem. Finally, in Sections A.5 and A.6, we present additional simulation and estimation results.

A.1 Preliminary Equations

We first provide some equations given in the manuscript for an efficient exposition of our proofs. As they are already explained in the manuscript, we simply provide them without reiterating their motivation and derivations.

$$\boldsymbol{x}_t^+ = \boldsymbol{\mu}_*^+ t + \sum_{j=1}^{t} \boldsymbol{s}_j^+ \quad \text{and} \quad \boldsymbol{x}_t^- = \boldsymbol{\mu}_*^- t + \sum_{j=1}^{t} \boldsymbol{s}_j^- \tag{A.1}$$

$$y_t = \delta_* t + \sum_{j=1}^{t} d_j \tag{A.2}$$

[1]This is a substantially revised version of an earlier manuscript circulated under the title "Two-Step Estimation of the Nonlinear Autoregressive Distributed Lag Model." We are grateful to In Choi, Tae-Hwan Kim, Rui Lin, Viet Nguyen, Michael Thornton, and the seminar participants at Universities of Melbourne, Yonsei and York for insightful comments. Cho is grateful for financial support from the Ministry of Education of the Republic of Korea and the National Research Foundation of Korea (Grant number NRF-2019S1A5A2A01035568). Greenwood-Nimmo and Shin acknowledge financial support from the Economic and Social Research Council (Grant number ES/T01573X/1). The views expressed herein are those of the authors and should not be reported as the views of Codera Analytics. The usual disclaimer applies.

$$\Delta y_t = \rho_* y_{t-1} + (\theta_*^+ - \theta_*^-) x_{t-1}^+ + \theta_*^- x_{t-1} + \gamma_* + \sum_{j=1}^{p-1} \varphi_{j*} \Delta y_{t-j} + \sum_{j=0}^{q-1} \left(\pi_{j*}^+ \Delta x_{t-j}^+ + \pi_{j*}^- \Delta x_{t-j}^- \right) + e_t \quad \text{(A.3)}$$

$$y_t = \alpha_* + \lambda_* x_t^+ + \eta_* x_t + u_t \quad \text{(A.4)}$$

$$u_{t-1} := y_{t-1} - \beta_*^+ x_{t-1}^+ - \beta_*^- x_{t-1}^- \quad \text{(A.5)}$$

$$\Delta y_t = \rho_* u_{t-1} + \gamma_* + \sum_{j=1}^{p-1} \varphi_{j*} \Delta y_{t-j} + \sum_{j=0}^{q-1} \left(\boldsymbol{\pi}_{j*}^{+\prime} \Delta \boldsymbol{x}_{t-j}^+ + \boldsymbol{\pi}_{j*}^{-\prime} \Delta \boldsymbol{x}_{t-j}^- \right) + e_t \quad \text{(A.6)}$$

$$\widehat{\boldsymbol{\varrho}}_T = \boldsymbol{\varrho}_* + \left(\sum_{t=1}^T \boldsymbol{q}_t \boldsymbol{q}_t' \right)^{-1} \left(\sum_{t=1}^T \boldsymbol{q}_t u_t \right) \quad \text{(A.7)}$$

$$\widehat{\boldsymbol{\zeta}}_T := \left(\sum_{t=1}^T \boldsymbol{h}_t \boldsymbol{h}_t' \right)^{-1} \left(\sum_{t=1}^T \boldsymbol{h}_t \Delta y_t \right) = \boldsymbol{\zeta}_* + \left(\sum_{t=1}^T \boldsymbol{h}_t \boldsymbol{h}_t' \right)^{-1} \left(\sum_{t=1}^T \boldsymbol{h}_t e_t \right) \quad \text{(A.8)}$$

A.2 Proofs

Proof of Lemma 1. (*i*) By (A.1) and (A.2), we obtain the following:

- $T^{-3} \sum_{t=1}^T y_{t-1}^2 = \frac{1}{3}\delta_*^2 + o_{\mathbb{P}}(1)$;
- $T^{-3} \sum_{t=1}^T y_{t-1} \boldsymbol{x}_t^{+\prime} = \frac{1}{3}\delta_* \boldsymbol{\mu}_*^{+\prime} + o_{\mathbb{P}}(1)$;
- $T^{-3} \sum_{t=1}^T y_{t-1} \boldsymbol{x}_t^{-\prime} = \frac{1}{3}\delta_* \boldsymbol{\mu}_*^{-\prime} + o_{\mathbb{P}}(1)$;
- $T^{-3} \sum_{t=1}^T \boldsymbol{x}_t^+ \boldsymbol{x}_t^{+\prime} = \frac{1}{3}\boldsymbol{\mu}_*^+ \boldsymbol{\mu}_*^{+\prime} + o_{\mathbb{P}}(1)$;
- $T^{-3} \sum_{t=1}^T \boldsymbol{x}_t^+ \boldsymbol{x}_t^{-\prime} = \frac{1}{3}\boldsymbol{\mu}_*^+ \boldsymbol{\mu}_*^{-\prime} + o_{\mathbb{P}}(1)$; and
- $T^{-3} \sum_{t=1}^T \boldsymbol{x}_t^- \boldsymbol{x}_t^{-\prime} = \frac{1}{3}\boldsymbol{\mu}_*^- \boldsymbol{\mu}_*^{-\prime} + o_{\mathbb{P}}(1)$.

These limits imply that $T^{-3} \sum_{t=1}^T \boldsymbol{z}_{1t} \boldsymbol{z}_{1t}' = \mathbf{M}_{11} + o_{\mathbb{P}}(1)$.

(*ii*) By (A.1) and (A.2), we note that:

- $T^{-2} \sum_{t=1}^T y_{t-1} = \frac{1}{2}\delta_* + o_{\mathbb{P}}(1)$;
- $T^{-2} \sum_{t=1}^T y_{t-1} \boldsymbol{w}_{1t}' = T^{-2} \sum_{t=1}^T [\delta_*^2 t, \delta_*^2 t, \ldots, \delta_*^2 t] + o_{\mathbb{P}}(1) = \frac{1}{2}\delta_*^2 \boldsymbol{\iota}_{p-1}' + o_{\mathbb{P}}(1)$;

- $T^{-2}\sum_{t=1}^{T} y_{t-1}\boldsymbol{w}_{2t}' = T^{-2}\sum_{t=1}^{T}[\delta_*\boldsymbol{\mu}_*^{+\prime}t, \delta_*\boldsymbol{\mu}_*^{+\prime}t, \ldots, \delta_*\boldsymbol{\mu}_*^{+\prime}t] + o_{\mathbb{P}}(1) = \frac{1}{2}\delta_*\boldsymbol{\iota}_q' \otimes \boldsymbol{\mu}_*^{+\prime} + o_{\mathbb{P}}(1)$;
- $T^{-2}\sum_{t=1}^{T} y_{t-1}\boldsymbol{w}_{3t}' = T^{-2}\sum_{t=1}^{T}[\delta_*\boldsymbol{\mu}_*^{-\prime}t, \delta_*\boldsymbol{\mu}_*^{-\prime}t, \ldots, \delta_*\boldsymbol{\mu}_*^{-\prime}t] + o_{\mathbb{P}}(1) = \frac{1}{2}\delta_*\boldsymbol{\iota}_q' \otimes \boldsymbol{\mu}_*^{-\prime} + o_{\mathbb{P}}(1)$;
- $T^{-2}\sum_{t=1}^{T} \boldsymbol{x}_{t-1}^{+} = \frac{1}{2}\boldsymbol{\mu}_*^{+} + o_{\mathbb{P}}(1)$;
- $T^{-2}\sum_{t=1}^{T} \boldsymbol{x}_{t-1}^{+}\boldsymbol{w}_{1t}' = T^{-2}\sum_{t=1}^{T}[\delta_*\boldsymbol{\mu}_*^{+}t, \delta_*\boldsymbol{\mu}_*^{+}t, \ldots, \delta_*\boldsymbol{\mu}_*^{+}t] + o_{\mathbb{P}}(1) = \frac{1}{2}\delta_*\boldsymbol{\mu}_*^{+}\boldsymbol{\iota}_{p-1}' + o_{\mathbb{P}}(1)$;
- $T^{-2}\sum_{t=1}^{T} \boldsymbol{x}_{t-1}^{+}\boldsymbol{w}_{2t}' = T^{-2}\sum_{t=1}^{T}[\boldsymbol{\mu}_*^{+}\boldsymbol{\mu}_*^{+\prime}t, \boldsymbol{\mu}_*^{+}\boldsymbol{\mu}_*^{+\prime}t, \ldots, \boldsymbol{\mu}_*^{+}\boldsymbol{\mu}_*^{+\prime}t] + o_{\mathbb{P}}(1) = \frac{1}{2}\boldsymbol{\iota}_q' \otimes \boldsymbol{\mu}_*^{+}\boldsymbol{\mu}_*^{+\prime} + o_{\mathbb{P}}(1)$;
- $T^{-2}\sum_{t=1}^{T} \boldsymbol{x}_{t-1}^{+}\boldsymbol{w}_{3t}' = T^{-2}\sum_{t=1}^{T}[\boldsymbol{\mu}_*^{+}\boldsymbol{\mu}_*^{-\prime}t, \boldsymbol{\mu}_*^{+}\boldsymbol{\mu}_*^{-\prime}t, \ldots, \boldsymbol{\mu}_*^{+}\boldsymbol{\mu}_*^{-\prime}t] + o_{\mathbb{P}}(1) = \frac{1}{2}\boldsymbol{\iota}_q' \otimes \boldsymbol{\mu}_*^{+}\boldsymbol{\mu}_*^{-\prime} + o_{\mathbb{P}}(1)$;
- $T^{-2}\sum_{t=1}^{T} \boldsymbol{x}_{t-1}^{-} = -\frac{1}{2}\boldsymbol{\mu}_*^{+} + o_{\mathbb{P}}(1)$;
- $T^{-2}\sum_{t=1}^{T} \boldsymbol{x}_{t-1}^{-}\boldsymbol{w}_{1t}' = T^{-2}\sum_{t=1}^{T}[\delta_*\boldsymbol{\mu}_*^{-}t, \delta_*\boldsymbol{\mu}_*^{-}t, \ldots, \delta_*\boldsymbol{\mu}_*^{-}t] + o_{\mathbb{P}}(1) = \frac{1}{2}\delta_*\boldsymbol{\mu}_*^{-}\boldsymbol{\iota}_{p-1}' + o_{\mathbb{P}}(1)$;
- $T^{-2}\sum_{t=1}^{T} \boldsymbol{x}_{t-1}^{-}\boldsymbol{w}_{2t}' = T^{-2}\sum_{t=1}^{T}[\boldsymbol{\mu}_*^{-}\boldsymbol{\mu}_*^{+\prime}t, \boldsymbol{\mu}_*^{-}\boldsymbol{\mu}_*^{+\prime}t, \ldots, \boldsymbol{\mu}_*^{-}\boldsymbol{\mu}_*^{+\prime}t] + o_{\mathbb{P}}(1) = \frac{1}{2}\boldsymbol{\iota}_q' \otimes \boldsymbol{\mu}_*^{-}\boldsymbol{\mu}_*^{+\prime} + o_{\mathbb{P}}(1)$;
- $T^{-2}\sum_{t=1}^{T} \boldsymbol{x}_{t-1}^{-}\boldsymbol{w}_{3t}' = T^{-2}\sum_{t=1}^{T}[\boldsymbol{\mu}_*^{-}\boldsymbol{\mu}_*^{-\prime}t, \boldsymbol{\mu}_*^{-}\boldsymbol{\mu}_*^{-\prime}t, \ldots, \boldsymbol{\mu}_*^{-}\boldsymbol{\mu}_*^{-\prime}t] + o_{\mathbb{P}}(1) = \frac{1}{2}\boldsymbol{\iota}_q' \otimes \boldsymbol{\mu}_*^{-}\boldsymbol{\mu}_*^{-\prime} + o_{\mathbb{P}}(1)$.

These limit results imply that $T^{-1}\sum_{t=1}^{T} \boldsymbol{z}_{1t}\boldsymbol{z}_{2t}' = \mathbf{M}_{12} + o_{\mathbb{P}}(1)$.

(*iii*) We note that:

- $T^{-1}\sum_{t=1}^{T} \boldsymbol{w}_{1t}' = \mathbb{E}[\Delta\boldsymbol{y}_{t-1}]' + o_{\mathbb{P}}(1) = \delta_*\boldsymbol{\iota}_{p-1}' + o_{\mathbb{P}}$;
- $T^{-1}\sum_{t=1}^{T} \boldsymbol{w}_{2t}' = [\mathbb{E}[\Delta\boldsymbol{x}_t^{+\prime}], \mathbb{E}[\Delta\boldsymbol{x}_{t-1}^{+\prime}], \ldots, \mathbb{E}[\Delta\boldsymbol{x}_{t-q+1}^{+\prime}]] + o_{\mathbb{P}}(1) = [\boldsymbol{\mu}_*^{+\prime}, \ldots, \boldsymbol{\mu}_*^{+\prime}] + o_{\mathbb{P}}(1) = \boldsymbol{\iota}_q' \otimes \boldsymbol{\mu}_*^{+} + o_{\mathbb{P}}(1)$;
- $T^{-1}\sum_{t=1}^{T} \boldsymbol{w}_{3t}' = [\mathbb{E}[\Delta\boldsymbol{x}_t^{-\prime}], \mathbb{E}[\Delta\boldsymbol{x}_{t-1}^{-\prime}], \ldots, \mathbb{E}[\Delta\boldsymbol{x}_{t-q+1}^{-\prime}]] + o_{\mathbb{P}}(1) = [\boldsymbol{\mu}_*^{-\prime}, \ldots, \boldsymbol{\mu}_*^{-\prime}] + o_{\mathbb{P}}(1) = \boldsymbol{\iota}_q' \otimes \boldsymbol{\mu}_*^{-} + o_{\mathbb{P}}(1)$; and
- $T^{-1}\sum_{t=1}^{T} \boldsymbol{w}_t\boldsymbol{w}_t' = \mathbb{E}[\boldsymbol{w}_t\boldsymbol{w}_t'] + o_{\mathbb{P}}(1)$.

These limits imply that $T^{-1}\sum_{t=1}^{T} \boldsymbol{z}_{2t}\boldsymbol{z}_{2t}' = \mathbf{M}_{22} + o_{\mathbb{P}}(1)$, as desired. ■

Proof of Lemma 2.

(*i*) We note that:

- $T^{-2}\sum_{t=1}^{T} x_t^{+} = T^{-1}\sum_{t=1}^{T} \mu_*^{+}(t/T) + o_{\mathbb{P}}(1) \xrightarrow{\mathbb{P}} \frac{1}{2}\mu_*^{+}$;
- $T^{-3/2}\sum_{t=1}^{T} x_t = T^{-1}\sum_{t=1}^{T}(T^{-1/2}\sum_{i=1}^{t}\Delta x_i) \Rightarrow \int \mathcal{B}_x$ using that $T^{-1/2}\sum_{i=1}^{[T(\cdot)]}\Delta x_i \Rightarrow \int_0^{(\cdot)} d\mathcal{B}_x$;
- $T^{-3}\sum_{t=1}^{T} x_t^{+}x_t^{+} = T^{-1}\sum_{t=1}^{T} \mu_*^{+}\mu_*^{+}(t/T)^2 + o_{\mathbb{P}}(1) \xrightarrow{\mathbb{P}} \frac{1}{3}\mu_*^{+}\mu_*^{+}$;
- $T^{-5/2}\sum_{t=1}^{T} x_t^{+}x_t = T^{-1}\sum_{t=1}^{T} \mu_*^{+}(t/T)(T^{-1/2}\sum_{i=1}^{t}\Delta x_t) + o_{\mathbb{P}}(1) \Rightarrow \mu_*^{+}\int r\mathcal{B}_x$; and

- $T^{-2}\sum_{t=1}^{T} x_t x_t = T^{-1}\sum_{t=1}^{T}(T^{-1/2}\sum_{i=1}^{t}\Delta x_t)(T^{-1/2}\sum_{i=1}^{t}\Delta x_t) \Rightarrow \int \mathcal{B}_x^2$.

Therefore, $\widehat{\mathbf{Q}}_T \Rightarrow \boldsymbol{\mathcal{Q}}$, as desired.

(*ii*) We note that:

- $T^{-1/2}\sum_{t=1}^{T} u_t \Rightarrow \int d\mathcal{B}_u$ using that $T^{-1/2}\sum_{t=1}^{[T(\cdot)]} u_t \Rightarrow \int_0^{(\cdot)} d\mathcal{B}_u$;
- $T^{-3/2}\sum_{t=1}^{T} x_t^+ u_t = T^{-1/2}\sum_{t=1}^{T}\mu_*^+(t/T)u_t + o_{\mathbb{P}}(1) \Rightarrow \mu_*^+\int r d\mathcal{B}_u$; and
- $T^{-1}\sum_{t=1}^{T} x_t u_t = T^{-1/2}\sum_{t=1}^{T}(T^{-1/2}\sum_{i=1}^{t}\Delta x_i)u_t \Rightarrow \int \mathcal{B}_x d\mathcal{B}_u + \upsilon_*$ using the fact that $\upsilon_* := \lim_{T\to\infty} T^{-1}\sum_{t=1}^{T}\sum_{i=1}^{t}\mathbb{E}[\Delta x_i u_t]$ is finite.

Therefore, $\widehat{\mathbf{U}}_T \Rightarrow \boldsymbol{\mathcal{U}}$. ■

Proof of Corollary 1.

Given (A.7), the desired result follows from Lemma 4. ■

Proof of Theorem 1.

We note that $T\{(\widehat{\beta}_T^+ - \widehat{\beta}_T^-) - (\beta_*^+ - \beta_*^-)\} = O_{\mathbb{P}}(T^{-1/2})$ by the definition of $\widehat{\lambda}_T$. Therefore, the weak limit of $T(\widehat{\beta}_T^+ - \beta_*^+)$ is equivalent to that of $T(\widehat{\beta}_T^- - \beta_*^-)$. Furthermore, Corollary 1 implies that $T(\widehat{\beta}_T^- - \beta_*^-) \Rightarrow \mathbf{S}\boldsymbol{\mathcal{Q}}^{-1}\boldsymbol{\mathcal{U}}$, leading to the desired result. ■

Proof of Lemma 3.

Given Assumption 2, we note that $\widetilde{\upsilon}_T \xrightarrow{\mathbb{P}} \upsilon_*$ and $(\widetilde{\sigma}_T^{(1,1)})^{-1}\widetilde{\sigma}_T^{(1,2)} \xrightarrow{\mathbb{P}} \boldsymbol{\nu}_* := (\sigma_*^{(1,1)})^{-1}\sigma_*^{(1,2)}$. Therefore, if we let $\dot{u}_t := u_t - \Delta x_t \boldsymbol{\nu}_*$, $\widetilde{\mathbf{U}}_T = \widetilde{\mathbf{D}}_T^{-1}\sum_{t=1}^{T}\{\boldsymbol{q}_t\dot{u}_t - \mathbf{S}'\upsilon_*\} + o_{\mathbb{P}}(1)$, then $\widetilde{\mathbf{U}}_T \Rightarrow [\int d\mathcal{B}_{\dot{u}}, \mu_*^+\int r d\mathcal{B}_{\dot{u}}, \int \mathcal{B}_x d\mathcal{B}_{\dot{u}}]'$, where $\mathcal{B}_{\dot{u}}(\cdot) := \tau_*\mathcal{W}_u(\cdot)$. Therefore, $\widetilde{\mathbf{U}}_T \Rightarrow \widetilde{\boldsymbol{\mathcal{U}}}$. ■

Proof of Corollary 2.

Given that $\widetilde{\mathbf{D}}_T(\widetilde{\boldsymbol{\varrho}}_T - \boldsymbol{\varrho}_*) = [\widetilde{\mathbf{D}}_T^{-1}(\sum_{t=1}^{T}\boldsymbol{q}_t\boldsymbol{q}_t')\widetilde{\mathbf{D}}_T^{-1}]^{-1}\widetilde{\mathbf{U}}_T$, the desired result follows from Lemmas 2(*i*) and 3. ■

Proof of Theorem 2.

Given that $(\widetilde{\beta}_T^+ - \beta_*^+) - (\widetilde{\beta}_T^- - \beta_*^-) = \widetilde{\lambda}_T - \lambda_* = O_{\mathbb{P}}(T^{-3/2})$ and $(\widetilde{\beta}_T^- - \beta_*^-) = O_{\mathbb{P}}(T^{-1})$, it follows that $(\widetilde{\beta}_T^+ - \beta_*^+) = O_{\mathbb{P}}(T^{-1})$, implying that the weak limit of $T(\widetilde{\beta}_T^+ - \beta_*^+)$ is equivalent to that of $T(\widetilde{\beta}_T^- - \beta_*^-)$. Furthermore, Corollary 1 implies that $T(\widetilde{\eta}_T^- - \eta_*^-) = T(\widetilde{\beta}_T^- - \beta_*^-) \Rightarrow \mathbf{S}\boldsymbol{\mathcal{Q}}^{-1}\widetilde{\boldsymbol{\mathcal{U}}}$, leading to the desired result. ■

Proof of Lemma 4.

This result is easily obtained using the ergodic theorem and the multivariate central limit theorem. ■

Proof of Theorem 3.

(*i*) Given (A.8), we can combine Lemmas 4 (*i* and *ii*) to obtain the desired result.

(*ii*) If it further holds that $\mathbb{E}[e_t^2|\boldsymbol{h}_t] = \sigma_*^2$, then Lemma 4(*iii*) implies that $\boldsymbol{\Omega}_* = \sigma_*^2\boldsymbol{\Gamma}_*$. Therefore, Theorem 3(*i*) now implies that $\sqrt{T}(\widehat{\boldsymbol{\zeta}}_T - \boldsymbol{\zeta}_*) \overset{\text{A}}{\sim} N(\mathbf{0}, \sigma_*^2\boldsymbol{\Gamma}_*^{-1})$. ■

Proof of Lemma 5.

(*i*) We note that:

- $T^{-2}\sum_{t=1}^{T} t = \frac{1}{2} + o(1)$;
- $T^{-3/2}\sum_{t=1}^{T}\widehat{\boldsymbol{m}}_t = T^{-3/2}\sum_{t=1}^{T}\boldsymbol{m}_t - (T^{-2}\sum_{t=1}^{T} t)(T^{-3}\sum_{t=1}^{T} t^2)^{-1}(T^{-5/2}\sum_{t=1}^{T} t\boldsymbol{m}_t) = T^{-1}\sum_{t=1}^{T} T^{-1/2}(\sum_{i=1}^{t}\Delta\boldsymbol{m}_i) - (T^{-2}\sum_{t=1}^{T} t)(T^{-3}\sum_{t=1}^{T} t^2)^{-1}(T^{-1}\sum_{t=1}^{T}(t/T)T^{-1/2}\sum_{i=1}^{t}\Delta\boldsymbol{m}_i) \Rightarrow \int\boldsymbol{\mathcal{B}}_m - \frac{3}{2}\int r\boldsymbol{\mathcal{B}}_m$ using the fact that $T^{-1/2}\sum_{i=1}^{[T(\cdot)]}\Delta\boldsymbol{m}_i \Rightarrow \int_0^{(\cdot)} d\boldsymbol{\mathcal{B}}_m$;
- $T^{-3/2}\sum_{t=1}^{T}\boldsymbol{x}_t = T^{-1}\sum_{t=1}^{T}(T^{-1/2}\sum_{i=1}^{t}\Delta\boldsymbol{x}_i) \Rightarrow \int\boldsymbol{\mathcal{B}}_x$ by that $T^{-1/2}\sum_{i=1}^{[T(\cdot)]}\Delta\boldsymbol{x}_i \Rightarrow \int_0^{(\cdot)} d\boldsymbol{\mathcal{B}}_x$;
- $T^{-3}\sum_{t=1}^{T} t^2 = \frac{1}{3} + o(1)$;
- $T^{-5/2}\sum_{t=1}^{T} t\widehat{\boldsymbol{m}}_t = T^{-5/2}\sum_{t=1}^{T} t\boldsymbol{m}_t - T^{-5/2}(\sum_{t=1}^{T} t^2)(\sum_{t=1}^{T} t^2)^{-1}(\sum_{t=1}^{T} t\boldsymbol{m}_t) = \mathbf{0}$;
- $T^{-5/2}\sum_{t=1}^{T} t\boldsymbol{x}_t = T^{-1}\sum_{t=1}^{T}(t/T)(T^{-1/2}\sum_{i=1}^{t}\Delta\boldsymbol{x}_i) \Rightarrow \int r\boldsymbol{\mathcal{B}}_x$;
- $T^{-2}\sum_{t=1}^{T}\widehat{\boldsymbol{m}}_t\widehat{\boldsymbol{m}}_t' = T^{-2}\sum_{t=1}^{T}\boldsymbol{m}_t\boldsymbol{m}_t' - T^{-2}\sum_{t=1}^{T} t\boldsymbol{m}_t(\sum_{t=1}^{T} t^2)^{-1}\sum_{t=1}^{T} t\boldsymbol{m}_t' = T^{-1}\sum_{t=1}^{T}(T^{-1/2}\sum_{i=1}^{t}\Delta\boldsymbol{m}_i)(T^{-1/2}\sum_{i=1}^{t}\Delta\boldsymbol{m}_i)' - T^{-1}\sum_{t=1}^{T}((t/T)\,T^{-1/2}\sum_{i=1}^{t}\Delta\boldsymbol{m}_i)(T^{-3}\sum_{t=1}^{T} t^2)^{-1} T^{-1}\sum_{t=1}^{T}((t/T)T^{-1/2}\sum_{i=1}^{t}\Delta\boldsymbol{m}_i)' \Rightarrow \int\boldsymbol{\mathcal{B}}_m\boldsymbol{\mathcal{B}}_m' - 3\int r\boldsymbol{\mathcal{B}}_m\int r\boldsymbol{\mathcal{B}}_m'$;
- $T^{-2}\sum_{t=1}^{T}\boldsymbol{x}_t\widehat{\boldsymbol{m}}_t' = T^{-2}\sum_{t=1}^{T}\boldsymbol{x}_t\boldsymbol{m}_t' - T^{-2}\sum_{i=1}^{t} t\boldsymbol{x}_t(\sum_{i=1}^{t} t^2)^{-1}\sum_{t=1}^{T} t\boldsymbol{m}_t' = T^{-1}\sum_{t=1}^{T} T^{-1/2}\sum_{i=1}^{t}\Delta\boldsymbol{x}_i T^{-1/2}\sum_{i=1}^{t}\Delta\boldsymbol{m}_i' - T^{-1}\sum_{t=1}^{T}(t/T)\,T^{-1/2}\sum_{i=1}^{t}\Delta\boldsymbol{x}_i(T^{-3}\sum_{t=1}^{T} t^2)^{-1}(t/T)T^{-1/2}\sum_{i=1}^{t}\Delta\boldsymbol{m}_i' \Rightarrow \int\boldsymbol{\mathcal{B}}_x\,\boldsymbol{\mathcal{B}}_m' - 3\int r\boldsymbol{\mathcal{B}}_x\int r\boldsymbol{\mathcal{B}}_m'$;
- $T^{-2}\sum_{t=1}^{T}\boldsymbol{x}_t\boldsymbol{x}_t' = T^{-1}\sum_{t=1}^{T}(T^{-1/2}\sum_{i=1}^{t}\Delta\boldsymbol{x}_t)(T^{-1/2}\sum_{i=1}^{t}\Delta\boldsymbol{x}_t) \Rightarrow \int\boldsymbol{\mathcal{B}}_x\boldsymbol{\mathcal{B}}_x'$.

Therefore, $\ddot{\mathbf{R}}_T \Rightarrow \boldsymbol{\mathcal{R}}$, as desired.

(*ii*) We note that:

- $T^{-1/2}\sum_{t=1}^{T} u_t \Rightarrow \int d\mathcal{B}_u$ using the fact that $T^{-1/2}\sum_{t=1}^{[T(\cdot)]} u_t \Rightarrow \int_0^{(\cdot)} d\mathcal{B}_u$;
- $T^{-3/2}\sum_{t=1}^{T} tu_t = T^{-1/2}\sum_{t=1}^{T}(t/T)u_t + o_{\mathbb{P}}(1) \Rightarrow \int r d\mathcal{B}_u$;
- $T^{-1}\sum_{t=1}^{T}\widehat{\boldsymbol{m}}_t u_t = T^{-1}\sum_{t=1}^{T} u_t(\boldsymbol{m}_t - t(\sum_{t=1}^{T} t^2)^{-1}\sum_{t=1}^{T} t\boldsymbol{m}_t) = T^{-1}\sum_{t=1}^{T} u_t\boldsymbol{m}_t - T^{-3/2}$

$\sum_{t=1}^{T} u_t t(T^{-3}\sum_{t=1}^{T} t^2)^{-1}T^{-5/2}\sum_{t=1}^{T} t\boldsymbol{m}_t \Rightarrow \int \boldsymbol{\mathcal{B}}_m d\mathcal{B}_u + \boldsymbol{\upsilon}_{m*} - 3\int r d\mathcal{B}_u \int r\boldsymbol{\mathcal{B}}_m$ using the fact that $\boldsymbol{\upsilon}_{m*} := \lim_{T\to\infty} T^{-1}\sum_{t=1}^{T}\sum_{i=1}^{t}\mathbb{E}[\Delta \boldsymbol{m}_i u_t]$ is finite.

- $T^{-1}\sum_{t=1}^{T}\boldsymbol{x}_t u_t = T^{-1/2}\sum_{t=1}^{T}(T^{-1/2}\sum_{i=1}^{t}\Delta\boldsymbol{x}_i)u_t \Rightarrow \int \boldsymbol{\mathcal{B}}_x d\mathcal{B}_u + \boldsymbol{\upsilon}_{x*}$ using the fact that $\boldsymbol{\upsilon}_{x*} := \lim_{T\to\infty} T^{-1}\sum_{t=1}^{T}\sum_{i=1}^{t}\mathbb{E}[\Delta\boldsymbol{x}_i u_t]$ is finite.

Therefore, $\ddot{\mathbf{U}}_T \Rightarrow \ddot{\boldsymbol{\mathcal{U}}}$. ■

Proof of Corollary 3.

As the first claim follows in a straightforward fashion from Lemma 5, we instead focus on the proof of the second claim. Note that $T^{3/2}(\widehat{\xi}_T - \xi_{*T}) = O_{\mathbb{P}}(1)$ and $\xi_{*T} = \boldsymbol{\lambda}_*'\boldsymbol{\mu}_*^{+} + \boldsymbol{\lambda}_*'\sum t\boldsymbol{m}_t(\sum t^2)^{-1}$, so that $T^{3/2}(\widehat{\xi}_T - \boldsymbol{\lambda}_*'\boldsymbol{\mu}_*^{+} - \boldsymbol{\lambda}_*'\sum t\boldsymbol{m}_t(\sum t^2)^{-1}) = O_{\mathbb{P}}(1)$. Here, we note that $T^{1/2}\sum t\boldsymbol{m}_t(\sum t^2)^{-1} \Rightarrow \frac{1}{3}\int r\boldsymbol{\mathcal{B}}_m$. Therefore, it now follows that $T^{1/2}(\widehat{\xi}_T - \boldsymbol{\lambda}_*'\boldsymbol{\mu}_*^{+}) = T^{1/2}\boldsymbol{\lambda}_*'\sum t\boldsymbol{m}_t(\sum t^2)^{-1}) + O_{\mathbb{P}}(T^{-1}) \Rightarrow 3\boldsymbol{\lambda}_*'\int r\boldsymbol{\mathcal{B}}_m$. ■

Proof of Theorem 4.

This result is easily obtained from Corollary 3. ■

Proof of Lemma 6.

Given Assumption 3, note that $\bar{\boldsymbol{\upsilon}}_T \xrightarrow{\mathbb{P}} \ddot{\boldsymbol{\upsilon}}_* := [\boldsymbol{\upsilon}_{m*}', \boldsymbol{\upsilon}_{x*}']'$ and $(\bar{\boldsymbol{\Sigma}}_T^{(1,1)})^{-1}\bar{\boldsymbol{\sigma}}_T^{(1,2)} \xrightarrow{\mathbb{P}} \ddot{\boldsymbol{\nu}}_* := (\boldsymbol{\Sigma}_*^{(1,1)})^{-1}\boldsymbol{\sigma}_*^{(1,2)}$. Therefore, by letting $\mathring{u}_t := u_t - \boldsymbol{\ell}_t'\ddot{\boldsymbol{\nu}}_*$, $\bar{\mathbf{U}}_T = \ddot{\mathbf{D}}_T^{-1}\sum_{t=1}^{T}\{\boldsymbol{r}_t\mathring{u}_t - \bar{\mathbf{S}}'\ddot{\boldsymbol{\upsilon}}_*\} + o_{\mathbb{P}}(1)$, $\bar{\mathbf{U}}_T \Rightarrow [\int d\mathcal{B}_{\mathring{u}}^{\circ}, \int r d\mathcal{B}_{\mathring{u}}^{\circ}, \int \boldsymbol{\mathcal{B}}_m' d\mathcal{B}_{\mathring{u}}^{\circ} - 3\int r d\mathcal{B}_{\mathring{u}}^{\circ}\int r\boldsymbol{\mathcal{B}}_m', \int \boldsymbol{\mathcal{B}}_x' d\mathcal{B}_{\mathring{u}}^{\circ}]'$, where $\mathcal{B}_{\mathring{u}}^{\circ}(\cdot) := \ddot{\tau}\mathcal{W}_u(\cdot)$. Therefore, $\bar{\mathbf{U}}_T \Rightarrow \bar{\boldsymbol{\mathcal{U}}}$. ■

Proof of Theorem 5.

Given that $\ddot{\mathbf{D}}_T(\bar{\boldsymbol{\varpi}}_T - \bar{\boldsymbol{\varpi}}_{*T}) = (\ddot{\mathbf{D}}_T^{-1}(\sum_{t=1}^{T}\boldsymbol{r}_t\boldsymbol{r}_t')\ddot{\mathbf{D}}_T^{-1})^{-1}\bar{\mathbf{U}}_T$, Lemma 6 now proves the first claim. Second, note that $T[(\bar{\boldsymbol{\beta}}_T^{+} - \boldsymbol{\beta}_*^{+})', (\bar{\boldsymbol{\beta}}_T^{-} - \boldsymbol{\beta}_*^{-})']' = \ddot{\mathbf{S}}\ddot{\mathbf{D}}_T(\bar{\boldsymbol{\varpi}}_T - \bar{\boldsymbol{\varpi}}_{*T}) \Rightarrow \ddot{\mathbf{S}}\boldsymbol{\mathcal{R}}^{-1}\bar{\boldsymbol{\mathcal{U}}}$, as desired. ■

Proof of Theorem 6.

Corollary 2 implies that $T^{3/2}(\widetilde{\boldsymbol{\lambda}}_T - r) \Rightarrow \mathbf{S}\boldsymbol{\mathcal{Q}}^{-1}\widetilde{\boldsymbol{\mathcal{U}}}$ under H_0'', while Lemma 2(i) implies that $\widehat{\mathbf{Q}}_T := \widetilde{\mathbf{D}}_T^{-1}(\sum_{t=1}^{T}\boldsymbol{q}_t\boldsymbol{q}_t')\widetilde{\mathbf{D}}_T^{-1} \Rightarrow \boldsymbol{\mathcal{Q}}$. Furthermore, Assumption 2(i) implies that $\widetilde{\tau}_T^2 = \tau_*^2 + o_{\mathbb{P}}(1)$. Given the mixed normal distribution of the FM-OLS estimator for the long-run parameter in Corollary 2, it follows that $\mathcal{W}_T^{(\ell)} \overset{\text{A}}{\sim} \mathcal{X}_1^2$ under $\mathcal{H}_0''$.

In addition, we note that $\widetilde{\mathcal{W}}_T^{(\ell)} = (\widetilde{\mathbf{R}}\widetilde{\boldsymbol{\varrho}}_T - \mathbf{r})'\widetilde{\mathbf{D}}_T(\widetilde{\tau}_T^2\widetilde{\mathbf{R}}\widehat{\mathbf{Q}}_T^{-1}\widetilde{\mathbf{R}}')^{-1}\widetilde{\mathbf{D}}_T(\widetilde{\mathbf{R}}\widetilde{\boldsymbol{\varrho}}_T - \mathbf{r})$, and Theorem 2 implies that $\widetilde{\mathbf{D}}_T(\widetilde{\mathbf{R}}\widetilde{\boldsymbol{\varrho}}_T - \mathbf{r}) \overset{\text{A}}{\sim} N(\mathbf{0}, \tau_*^2\widetilde{\mathbf{R}}\boldsymbol{\mathcal{Q}}^{-1}\widetilde{\mathbf{R}}')$ conditional on $\sigma\{\mathcal{B}_x(r) : r \in (0,1]\}$ under H_0'''.

Given the condition that $\widehat{\mathbf{Q}}_T \Rightarrow \boldsymbol{\mathcal{Q}}$ and $\widetilde{\tau}_T^2 \xrightarrow{\mathbb{P}} \tau_*^2$, it now follows that $\widetilde{\mathcal{W}}_T^{(\ell)} \overset{\text{A}}{\sim} \mathcal{X}_2^2$ under H_0'''.

Given that $(\widetilde{\boldsymbol{\lambda}}_T - \boldsymbol{\lambda}_*) = O_{\mathbb{P}}(T^{-3/2})$, $\mathcal{W}_T^{(\ell)} = O_{\mathbb{P}}(T^3)$ under H_1''. Therefore, for any $c_T = o(T^3)$, $\mathbb{P}(\mathcal{W}_T^{(\ell)} > c_T) \to 1$. Furthermore, $(\widetilde{\beta}_T - \beta_*) = O_{\mathbb{P}}(T^{-1})$, implying that $\widetilde{\mathcal{W}}_T^{(\ell)} = O_{\mathbb{P}}(T^2)$ under H_1'''. Therefore, for any $\widetilde{c}_T = o(T^2)$, $\mathbb{P}(\widetilde{\mathcal{W}}_T^{(\ell)} > \widetilde{c}_T) \to 1$. This completes the proof. ■

Proof of Theorem 7.

Due to its similarity to the standard case, we omit the proof. ■

Proof of Theorem 8.

Due to its similarity to the standard case, we omit the proof. ■

A.3 A Simple Comparative Static Analysis

Here, we consider a simple comparative static analysis using the production function in Section 2.2, which is helpful in fixing the idea of the two different roles of the R&D activity. We describe the key roles of the capital converted from each type of R&D activity in terms of a complementary or substitutionary relationship with respect to physical capital, as follows:

$$y = \min[c, k + s], \tag{A.9}$$

where y, c, s, and k denote output, the capital converted from the innovative and managerial R&D expenditures and physical capital, respectively.

Suppose that the firm determines the optimal levels of capital by maximizing the profit level. We examine the following optimization problem:

$$\{c_*, k_*, s_*\} := \underset{c,k,s}{\arg\max}\ \min[c, k + s] - \kappa_0(c) - p_k k - p_s s,$$

where p_k and p_s denote the unit prices of k and s, respectively, and $\kappa_0(\cdot)$ denotes the cost function needed to convert innovative R&D activity to c. We let $\kappa_0'(\cdot) > 0$ and $\kappa_0''(\cdot) > 0$, and this particular cost function is assumed for the existence of the equilibrium.[2] Given the complementary production

[2]For the existence of the equilibrium, it is also possible to suppose a concave production function of c and a unit price for c, so that the optimization problem is modified to $\max_{c,k,s} \min[g(c), k + s] - p_c c - p_k k - p_s s$, where $g(\cdot)$ is such that

function between c and $a := k + s$, the optimization problem is solved in two stages: first, we suppose that c is given. Then, an efficient output is determined by letting $c = k + s$ to exploit the complementary relationship, letting $(k_*(c), s_*(c)) := \arg\max_{k,s} (k + s) - \kappa_0(c) - p_k k - p_s s$ such that $k + s = c$ and obtaining

$$(k_*(c), s_*(c)) = \begin{cases} (c, 0), & \text{if } p_k < p_s; \\ (0, c), & \text{if } p_k > p_s. \end{cases}$$

Second, we plug this optimal demand function back into the profit function and next optimize it with respect to c. That is,

$$c_* = \arg\max_c \ c - \kappa_0(c) - p_k k_*(c) - p_s s_*(c) = \arg\max_c \begin{cases} (1 - p_k)c - \kappa_0(c), & \text{if } p_k < p_s; \\ (1 - p_s)c - \kappa_0(c), & \text{if } p_k > p_s, \end{cases}$$

implying that from the first-order condition, the optimal c_* is such that $(1 - p_k) = \kappa_0'(c_*)$, if $p_k < p_s$; and $(1 - p_s) = \kappa_0'(c_*)$, if $p_k > p_s$. If we again plug this optimal level c_* back to $k_*(\cdot)$ and $s_*(\cdot)$, it follows that $(k_*, s_*) = (c_*, 0)$ if $p_k < p_s$; and $(k_*, s_*) = (0, c_*)$ if $p_k > p_s$.

The optimal demands for the capital respond to external shocks. We separately examine the complement and substitution effects by modifying the expenditure function. First, we suppose that $p_k < p_s$ with the initial cost function $\kappa_0(\cdot)$ and let $\kappa_0(\cdot)$ decrease to $\kappa_1(\cdot)$ such that $\kappa_0(\cdot) > \kappa_1(\cdot)$ with $\kappa_1'(\cdot) > 0$ and $\kappa_1''(\cdot) > 0$. By this supposition, the price for the innovative R&D activity uniformly decreases, and the optimal demand for c increases to c_{**} from c_* such that $(1 - p_k) = \kappa_1'(c_{**})$ and $(k_{**}, s_{**}) = (c_{**}, 0)$. Note that the demands for c and k move in the same direction but the demand for s remain the same, implying a complementary relationship between c and k.

Next, we examine a different static analysis. We suppose that $p_k < p_s^0$ initially but p_s decreases to p_s^1 such that $p_s^1 < p_k$ without modifying the cost function $\kappa_0(\cdot)$. By this decrease in p_s, the optimal demand for c remains the same, so that $c_{**} = c_*$ but the optimal demands for k and s shift $(k_{**}, s_{**}) = (0, c_*)$. That is, demands for s and k move in opposite directions, implying a substitutionary relationship between s and k.

$g'(\cdot) > 0$, $g''(\cdot) < 0$, and p_c is the unit price of c.

The response of the physical capital to the external shocks describes its core properties in relation to the R&D expenditure. The innovative R&D expenditure complements the physical capital, so that the production activity cannot extend its scope without investing in the innovative R&D activity. By having an environment favorable to innovative R&D activity, the firm can enhance its potential to produce more outputs by investing more physical capital. On the contrary, the managerial R&D expenditure substitutes the physical capital, so that the relative price of the physical capital to the capital converted from the managerial R&D activity determines the optimal level of the physical capital. If the output can be produced more efficiently by conducting the managerial R&D activity which is cheaper than the cost of the physical capital, the firm can enhance its production efficiency by substituting the managerial R&D activity for the physical capital.

A.4 A Further Singularity Problem under Single-Step Estimation

It is important to realize that the re-parameterization of the long-run relationship that we propose to resolve the singularity issue under 2-step estimation in (A.4) is insufficient to resolve the singularity issue involved in single-step NARDL estimation. In fact, efforts to estimate the short-run and the long-run parameters in a single step by combining (A.5) with (A.6) will encounter a further singularity problem, even if $k = 1$. Using the definitions of $\lambda_* := \beta_*^+ - \beta_*^-$ and $\eta_* := \beta_*^-$, it follows that $u_{t-1} = y_{t-1} - \lambda_* x_{t-1}^+ - \beta_* x_{t-1}$, such that:

$$\Delta y_t = \rho_* y_{t-1} + (\theta_*^+ - \theta_*^-) x_{t-1}^+ + \theta_*^- x_{t-1} + \gamma_* + \sum_{j=1}^{p-1} \varphi_{j*} \Delta y_{t-j} + \sum_{j=0}^{q-1} \left(\pi_{j*}^+ \Delta x_{t-j}^+ + \pi_{j*}^- \Delta x_{t-j}^- \right) + e_t,$$

where $\boldsymbol{\beta}_*^+ := -\theta_*^+ / \rho_*$ and $\boldsymbol{\beta}_*^- := -\theta_*^- / \rho_*$. Let:

$$\boldsymbol{\xi}_* := \left[\begin{array}{c:cc} \boldsymbol{\xi}_{1*}' & \boldsymbol{\xi}_{2*}' \end{array} \right]' := \left[\begin{array}{c:cc} \rho_* & \theta_* & \theta_*^- & \boldsymbol{\alpha}_{2*}' \end{array} \right]' \quad \text{and}$$

$$\boldsymbol{p}_t := \left[\begin{array}{c:cc} \boldsymbol{p}_{1t}' & \boldsymbol{p}_{2t}' \end{array} \right]' := \left[\begin{array}{c:cc} y_{t-1} & x_{t-1}^+ & x_{t-1} & \boldsymbol{z}_{2t}' \end{array} \right]'.$$

Note that $\boldsymbol{\xi}_{2*}$ and $\boldsymbol{p}_{2t}$ are identical to $\boldsymbol{\alpha}_{2*}$ and $\boldsymbol{z}_{2t}$, respectively, where $\theta_* := \theta_*^+ - \theta_*^-$. If we attempt to estimate the vector of unknown parameters, $\boldsymbol{\xi}_*$, in (A.3) by OLS, we obtain:

$$\widehat{\boldsymbol{\xi}}_T := \left(\sum_{t=1}^{T} \boldsymbol{p}_t \boldsymbol{p}_t'\right)^{-1} \left(\sum_{t=1}^{T} \boldsymbol{p}_t \Delta y_t\right).$$

We demonstrate that the inverse matrix in $\widehat{\boldsymbol{\xi}}_T$ is asymptotically singular in the following lemma:

Lemma A.1. *Given Assumption 1:*

(i) $\ddot{\mathbf{D}}_{1,T}^{-1} \left(\sum_{t=1}^{T} \boldsymbol{p}_{1t} \boldsymbol{p}_{1t}'\right) \ddot{\mathbf{D}}_{1,T}^{-1} \Rightarrow \boldsymbol{\mathcal{P}}_{11}$, *where* $\ddot{\mathbf{D}}_{1,T} := diag[T^{3/2}\mathbf{I}_2, T]$ *and:*

$$\boldsymbol{\mathcal{P}}_{11} := \begin{bmatrix} \frac{1}{3}\delta_*^2 & \frac{1}{3}\delta_*\mu_*^+ & \delta_* \int r\mathcal{B}_x \\ \frac{1}{3}\delta_*\mu_*^+ & \frac{1}{3}\mu_*^+\mu_*^+ & \mu_*^+ \int r\mathcal{B}_x \\ \delta_* \int r\mathcal{B}_x & \int r\mathcal{B}_x\mu_*^+ & \int \mathcal{B}_x^2 \end{bmatrix};$$

(ii) $\ddot{\mathbf{D}}_{1,T}^{-1} \left(\sum_{t=1}^{T} \boldsymbol{p}_{1t} \boldsymbol{p}_{2t}'\right) \ddot{\mathbf{D}}_{2,T}^{-1} \Rightarrow \boldsymbol{\mathcal{P}}_{12}$, *where* $\ddot{\mathbf{D}}_{2,T} := diag[T^{1/2}\mathbf{I}_{1+p+2q}]$ *and:*

$$\boldsymbol{\mathcal{P}}_{12} := \begin{bmatrix} \frac{1}{2}\delta_* & \frac{1}{2}\delta_*^2\boldsymbol{\iota}_{p-1}' & \frac{1}{2}\delta_*\boldsymbol{\iota}_q' \otimes \mu_*^+ & \frac{1}{2}\delta_*\boldsymbol{\iota}_q' \otimes \mu_*^- \\ \frac{1}{2}\mu_*^+ & \frac{1}{2}\delta_*\mu_*^+\boldsymbol{\iota}_{p-1}' & \frac{1}{2}\boldsymbol{\iota}_q' \otimes \mu_*^+\mu_*^+ & \frac{1}{2}\boldsymbol{\iota}_q' \otimes \mu_*^+\mu_*^- \\ \int \mathcal{B}_x & \delta_* \int \mathcal{B}_x\boldsymbol{\iota}_{p-1}' & \boldsymbol{\iota}_q' \otimes \int \mathcal{B}_x\mu_*^+ & \boldsymbol{\iota}_q' \otimes \int \mathcal{B}_x\mu_*^- \end{bmatrix}; \quad \textit{and}$$

(iii) $\ddot{\mathbf{D}}_{2,T}^{-1} \left(\sum_{t=1}^{T} \boldsymbol{p}_{2t} \boldsymbol{p}_{2t}'\right) \ddot{\mathbf{D}}_{2,T}^{-1} \xrightarrow{\mathbb{P}} \mathbf{P}_{22} := \mathbf{M}_{22}$. □

We omit the proof of Lemma A.1, as it can be easily derived from the proof of Lemma 1. Let $\ddot{\mathbf{D}}_T := \text{diag}[T^{3/2}\mathbf{I}_2, T, T^{1/2}\mathbf{I}_{1+p+2q}]$, then:

$$\ddot{\mathbf{D}}_T^{-1} \left(\sum_{t=1}^{T} \boldsymbol{p}_t \boldsymbol{p}_t'\right) \ddot{\mathbf{D}}_T^{-1} \Rightarrow \boldsymbol{\mathcal{P}} := \begin{bmatrix} \boldsymbol{\mathcal{P}}_{11} & \boldsymbol{\mathcal{P}}_{12} \\ \boldsymbol{\mathcal{P}}_{21} & \mathbf{P}_{22} \end{bmatrix},$$

where $\boldsymbol{\mathcal{P}}_{21} := \boldsymbol{\mathcal{P}}_{12}'$. Note that $\boldsymbol{\mathcal{P}}$ is singular, so it is difficult to obtain the limit distribution of $\widehat{\boldsymbol{\xi}}_T$ using the one-step approach even after applying the re-parameterization of the long- run levels relationship in (A.4).

A.5 Additional Monte Carlo Simulations

In this section, we provide additional simulation evidence. First, we set $k = 2$ and conduct simulations to examine the finite sample performance of the Wald test presented in Sections 4.3 and 4.4 of the manuscript. Next, we treat the cases of $k = 1$ and $k > 1$ separately and study the finite sample bias and mean squared error (MSE) of the parameters estimated by our two-step procedure, where the estimator for the long-run parameters is either OLS or FM-OLS (TOLS or FM-TOLS) and the estimator for the short-run parameters is OLS.

A.5.1 Monte Carlo Simulations when $k = 2$

We examine the finite sample performance of the Wald statistics in Sections 4.3 and 4.4 for $k = 2$. The data are generated using the NARDL(1,0) DGP: $\Delta y_t = \gamma_* + \rho_* u_{t-1} + \varphi_* \Delta y_{t-1} + \boldsymbol{\pi}_{0*}^{+\prime} \Delta \boldsymbol{x}_t^+ + \pi_{0*}^{-\prime} \Delta \boldsymbol{x}_t^- + e_t$, where $u_{t-1} := y_{t-1} - \alpha_* - \boldsymbol{\beta}_*^{+\prime} \boldsymbol{x}_{t-1}^+ - \boldsymbol{\beta}_*^{-\prime} \boldsymbol{x}_{t-1}^-$, $\Delta \boldsymbol{x}_t := \kappa_* \Delta \boldsymbol{x}_{t-1} + \sqrt{1-\kappa_*^2}\boldsymbol{v}_t$, and $(e_t, \boldsymbol{v}_t)' \sim \text{IID}N(\mathbf{0}_3, \mathbf{I}_3)$.

Testing the Long-Run Parameters We focus on the case where the FM-TOLS estimator is used. We generate the data by setting $(\alpha_*, \gamma_*, \rho_*, \varphi_*, \kappa_*) = (0, 0, -1, \varphi_*, 0.5)$, $(\boldsymbol{\beta}_*^{+\prime}, \boldsymbol{\beta}_*^{-\prime})' = (-1, 0.5, 0.75, -1.5)'$, and $(\boldsymbol{\pi}_{0*}^{+\prime}, \boldsymbol{\pi}_{0*}^{-\prime})' = (0.5, -0.5, -1, 1)'$. We test $\dot{H}_0^{(\ell)} : \boldsymbol{\iota}_2' \boldsymbol{\beta}_*^+ = -0.50$ and $\boldsymbol{\iota}_2' \boldsymbol{\beta}_*^- = -0.75$ vs. $\dot{H}_1^{(\ell)} : \boldsymbol{\iota}_2' \boldsymbol{\beta}_*^+ \neq -0.50$ or $\boldsymbol{\iota}_2' \boldsymbol{\beta}_*^- \neq -0.75$ while allowing φ_* to vary over -0.2, -0.1, 0, 0.1 and 0.2. The simulation results are reported in Table A.1. As T increases, the distribution of the Wald test statistic becomes well approximated by the chi-squared distribution with two degrees of freedom. For $\varphi_* = 0.3$, a larger sample size is required to achieve a satisfactory approximation.[3]

— Insert Table A.1 Here —

To examine the empirical power of the Wald test statistic, we test $\dot{H}_0^{(\ell)} : \boldsymbol{\iota}_2' \boldsymbol{\beta}_*^+ = -0.40$ and $\boldsymbol{\iota}_2' \boldsymbol{\beta}_*^- = -0.65$ vs. $\dot{H}_1^{(\ell)} : \boldsymbol{\iota}_2' \boldsymbol{\beta}_*^+ \neq -0.40$ or $\boldsymbol{\iota}_2' \boldsymbol{\beta}_*^- \neq -0.65$. Table A.2 shows that the Wald test statistic is consistent under the alternative hypothesis, irrespective of the value of φ_*.

— Insert Table A.2 Here —

[3] In this situation the use of resampling methods may be advisable.

Testing the Short-Run Parameters Here, we set $(\alpha_*, \gamma_*, \rho_*, \varphi_*, \kappa_*) = (0, 0, -1, \varphi_*, 0.5)$, $(\boldsymbol{\beta}_*^{+\prime}, \boldsymbol{\beta}_*^{-\prime})' = (-1, 0.5, 0.75, -1.5)'$, and $(\boldsymbol{\pi}_{0*}^{+\prime}, \boldsymbol{\pi}_{0*}^{-\prime})' = (0.5, 0.2, 0.5, 0.2)'$, while allowing φ_* to vary as before. We limit our attention to the case where we estimate the long-run parameters by the FM-TOLS estimator and compute $\widehat{u}_t$ prior to estimating the short-run parameters by OLS. We then test $\dot{H}_0^{(s)} : \boldsymbol{\pi}_{0*}^{+} - \boldsymbol{\pi}_{0*}^{-} = \mathbf{0}$ vs. $\dot{H}_1^{(s)} : \boldsymbol{\pi}_{0*}^{+} - \boldsymbol{\pi}_{0*}^{-} \neq \mathbf{0}$, using the Wald test with the heteroskedasticity consistent covariance estimator, $\widehat{\boldsymbol{\Omega}}_T$.

Table A.3 shows that the finite sample distribution of the Wald test statistic is well-approximated by the chi-squared distribution. For each significance level, its empirical level tends to the nominal level, once T reaches 1,000. In addition, the empirical levels display little sensitivity to φ_*, even for moderate T.

— Insert Table A.3 Here —

Finally, we examine the empirical power of the Wald test statistic. We work with the same DGP and test $\ddot{H}_0^{(s)} : \boldsymbol{\pi}_{0*}^{+} - \boldsymbol{\pi}_{0*}^{-} = 0.3\boldsymbol{\iota}$ vs. $\ddot{H}_1^{(s)} : \boldsymbol{\pi}_{0*}^{+} - \boldsymbol{\pi}_{0*}^{-} \neq 0.3\boldsymbol{\iota}$. We use the same Wald test statistic and report the simulation results in Table A.4. The empirical power of the test increases sharply with T and exhibits little sensitivity to the degree of autocorrelation measured by φ_*.

— Insert Table A.4 Here —

A.5.2 Monte Carlo Simulations with $k = 1$

In this section, we examine the bias and MSE of the single-step and two-step NARDL estimations. We generate simulated data using the same NARDL(1,0) DGP in Section 5 of the manuscript:

$$\Delta y_t = \gamma_* + \rho_* u_{t-1} + \varphi_* \Delta y_{t-1} + \pi_*^{+} \Delta x_t^{+} + \pi_*^{-} \Delta x_t^{-} + e_t,$$

where $u_{t-1} := y_{t-1} - \alpha_* - \beta_*^{+} x_{t-1}^{+} - \beta_*^{-} x_{t-1}^{-}$, $\Delta x_t := \kappa_* \Delta x_{t-1} + \sqrt{1 - \kappa_*^2} v_t$, and $(e_t, v_t)' \sim \text{IID}N(\mathbf{0}_2, \mathbf{I}_2)$. We set $(\alpha_*, \beta_*^{+}, \beta_*^{-}, \gamma_*, \rho_*, \varphi_*, \pi_*^{+}, \pi_*^{-}, \kappa_*) = (0, 2, 1, 0, -2/3, \varphi_*, 1, 1/2, 1/2)$ and we allow the sample size, T, and the parameter φ_* to vary. Note that Δx_t is generated by an AR(1) process with normally distributed disturbances and that u_t is both serially correlated and contemporaneously correlated with Δx_t.

Next, we specify the following long-run and short-run models:

$$y_t = \alpha + \lambda x_t^+ + \eta x_t + u_t \quad \text{and} \quad \Delta y_t = \gamma + \rho \widehat{u}_{t-1} + \varphi_1 \Delta y_{t-1} + \pi_0^+ \Delta x_t^+ + \pi_0^- \Delta x_t^- + e_t,$$

where $\widehat{u}_t := y_t - \widehat{\alpha}_T - \widehat{\lambda}_T x_t^+ - \widehat{\eta}_T x_t$. We estimate these models in two steps. In the first step, we estimate the parameters of the long-run relationship using either OLS or FM-OLS. In the second step, we estimate the short-run parameters by OLS. In each case, we evaluate the performance of the estimators by comparing their finite sample bias and MSE. We calculate the bias as follows:

$$\text{Bias}_T(\beta_*^+) := R^{-1} \sum_{j=1}^{R} (\widehat{\beta}_{T,j}^+ - \beta_*^+) \quad \text{and} \quad \text{Bias}_T(\varphi_*) := R^{-1} \sum_{j=1}^{R} (\widehat{\varphi}_{T,j} - \varphi_*),$$

where R is the number of replications used in the simulation experiment, $\widehat{\beta}_T^+$ is obtained in the first step by OLS or FM-OLS and $\widehat{\varphi}_T$ is obtained in the second-step by OLS. Likewise, we calculate the finite sample MSE of $\widehat{\beta}_T^+$ and $\widehat{\varphi}_T$ as:

$$\text{MSE}_T(\beta_*^+) := R^{-1} \sum_{j=1}^{R} (\widehat{\beta}_{T,j}^+ - \beta_*^+)^2 \quad \text{and} \quad \text{MSE}_T(\varphi_*) := R^{-1} \sum_{j=1}^{R} (\widehat{\varphi}_{T,j} - \varphi_*)^2.$$

The finite sample bias and MSE of the estimated parameters based on $R = 5,000$ replications of the simulation experiments are reported in Tables A.5 and A.6, respectively. To conserve space, we do not report the finite sample bias or MSE for the intercepts, α and γ, but these results are available from the authors on request.

— Insert Tables A.5 and A.6 Here —

First, consider the long-run parameter estimators obtained in the first step. The finite sample bias of the FM-OLS estimator is substantially smaller than that of the first-step OLS estimator. Recall that FM-OLS yields normally distributed estimators for the long-run parameters, β_*^+ and β_*^-. Consequently, in most cases, we find that the finite sample bias of the FM-OLS estimator is close to zero, because $T(\widetilde{\beta}_T^+ - \beta_*^+)$ and $T(\widetilde{\beta}_T^- - \beta_*^-)$ are asymptotically mixed-normally distributed around zero. By contrast, the OLS estimator is not asymptotically distributed around zero and exhibits non-negligible bias. In addition, our simulation results indicate that the FM-OLS estimator is often more efficient

than its OLS counterpart, resulting in a smaller MSE as the sample size increases. This tendency is particularly apparent for small and/or negative values of φ_*, although it is likely to be different for other nuisance parameters. Taken as a whole, these results strongly favor the use of FM-OLS in the first step.

Now, consider the short-run parameter estimators obtained by OLS in the second step. We find that the finite sample biases of the second step OLS estimators of the dynamic parameters become negligible as the sample size increases. This is true irrespective of whether we use OLS or FM-OLS in the first step, although the smallest biases are obtained in almost all cases when the first-step estimator is FM-OLS. The MSEs of the second-step OLS estimators are similar irrespective of the use of OLS or FM-OLS in the first step. Even for a small sample of just 50 observations, the bias is minor in all cases. This is an encouraging observation because many existing applications of the NARDL model rely on small datasets, constrained by the low sampling frequency and limited history of many macroeconomic databases.

A.5.3 Monte Carlo Simulations when $k = 2$

In this section, we generate simulated data using the following NARDL(1,0) DGP, which is the same DGP as in Section A.5.1 of the manuscript:

$$\Delta y_t = \gamma_* + \rho_* u_{t-1} + \varphi_* \Delta y_{t-1} + \boldsymbol{\pi}_{0*}^{+\prime} \Delta \boldsymbol{x}_t^+ + \pi_{0*}^{-\prime} \Delta \boldsymbol{x}_t^- + e_t,$$

where $u_{t-1} := y_{t-1} - \alpha_* - \boldsymbol{\beta}_*^{+\prime} \boldsymbol{x}_{t-1}^+ - \boldsymbol{\beta}_*^{-\prime} \boldsymbol{x}_{t-1}^-$, $\Delta \boldsymbol{x}_t := \kappa_* \Delta \boldsymbol{x}_{t-1} + \sqrt{1-\kappa_*^2}\boldsymbol{v}_t$, and $(e_t, \boldsymbol{v}_t)' \sim$ IID$N(\mathbf{0}_3, \mathbf{I}_3)$. We set $(\alpha_*, \gamma_*, \rho_*, \varphi_*, \kappa_*) = (0, 0, -1, \varphi_*, 0.5)$, $(\boldsymbol{\beta}_*^{+\prime}, \boldsymbol{\beta}_*^{-\prime})' = (-1, 0.5, 0.75, -1.5)'$, and $(\boldsymbol{\pi}_{0*}^{+\prime}, \boldsymbol{\pi}_{0*}^{-\prime})' = (0.5, -0.5, -1, 1)'$. As before, we allow T and φ_* to vary and examine the effect of different degrees of serial correlation.

We next specify the long-run and short-run models as: $y_t = \alpha + \boldsymbol{\lambda}' \boldsymbol{x}_t^+ + \boldsymbol{\eta} \boldsymbol{x}_t + u_t$ and $\Delta y_t = \gamma + \rho \widehat{u}_{t-1} + \varphi_1 \Delta y_{t-1} + \boldsymbol{\pi}_0^+ \Delta \boldsymbol{x}_t^+ + \boldsymbol{\pi}_0^- \Delta \boldsymbol{x}_t^- + e_t$, where $\widehat{u}_t$ is the regression residual obtained from the first step estimation. In the first step, we estimate the long-run parameters by TOLS or FM-TOLS, and then subsequently estimate the short-run parameters by OLS. As in the case with $k = 1$, we evaluate the performance of the estimators by studying their respective finite sample bias and MSE, which are

obtained using $R = 5,000$ replications. The results are reported in Tables A.7 and A.8.

— Insert Tables A.7 and A.8 Here —

We first examine the long-run parameter estimators obtained in the first step. As T increases, the finite sample bias of the FM-TOLS estimator becomes smaller than that of the TOLS estimator. Recall that FM-OLS yields normally distributed estimators for the long-run parameters, $\boldsymbol{\beta}_*^+$ and $\boldsymbol{\beta}_*^-$. Consequently, we find that the finite sample bias of the FM-TOLS estimator approaches zero much faster than the TOLS estimator as T increases. In addition, the FM-TOLS estimator becomes more efficient than the TOLS estimator as T increases, resulting in a smaller MSE at larger sample sizes. These results favor the use of the FM-TOLS estimator in samples of small to moderate size.

We finally consider the short-run dynamic parameter estimators obtained by OLS. We find that the finite sample biases of the OLS estimator become negligible as the sample size rises. This is true irrespective of the use of either TOLS or FM-TOLS in the preceding step. Likewise, the MSEs of the OLS estimators of the dynamic parameters are similar irrespective of whether we use TOLS or FM-TOLS in the first step, particularly as the sample size becomes larger.

A.6 Additional Empirical Evidence

In Table A.9, we report the descriptive statistics of both the R&D ratio to GDP and the log of GPDI. As we detail below, they are not stationary. The descriptive statistics reveal that the differenced R&D ratio is more standard than the differenced log of GPDI in the sense that the first has the characteristics of a normal distribution centered at zero, whereas the latter is more widely distributed, centered at a non-zero value with a negative skew and notable excess kurtosis. These different characteristics may imply that their interrelationship cannot be fully explained by a simple linear model.

— Insert Table A.9 Here —

We apply Phillips and Perron's (1988) unit root test to both series. We test the unit root hypothesis both including and excluding the time trend. The results are reported in Table A.10. Irrespective of the presence of the time trend, the unit-root hypothesis cannot be rejected, implying that both series are unit root nonstationary. Furthermore, the time trend in the Phillips and Perron equation for unit

root testing is statistically significant for the log of GPDI but insignificant for the R&D ratio to GDP, implying that the log of GPDI is a unit root process with a time drift, while the R&D ratio to GDP is a unit root process without a time drift, viz., $\mathbb{E}[\Delta r_t] = 0$ but $\mathbb{E}[\Delta i_t] > 0$. This aspect implies that their relationship has to be investigated by a model that explains the presence of the time trend, such as the NARDL model.

— Insert Table A.10 Here —

Lastly, we replicate the NARDL estimation exercise from the main text using the single-step NARDL estimator popularized by SYG. The cumulative dynamic multipliers obtained from the single-step parameter estimates reported in Figure A.1 are very similar to those obtained from the two-step estimates in Figure A.1, indicating that both estimation procedures yield similar results in practice.

— Insert Figure A.1 Here —

φ_*	sample size	100	250	500	1,000	3,000	5,000
-0.20	1%	44.58	17.42	7.64	3.48	1.20	1.42
	5%	58.30	32.32	18.08	10.60	5.56	5.64
	10%	65.52	40.84	26.28	17.64	10.98	10.68
-0.10	1%	42.96	18.12	8.12	3.32	1.48	1.24
	5%	57.82	31.10	19.04	10.76	6.02	5.48
	10%	65.34	39.20	26.66	17.48	11.64	10.34
0.00	1%	42.50	16.78	8.44	4.30	1.42	1.28
	5%	56.38	29.90	19.20	11.62	5.80	5.60
	10%	64.06	38.70	28.20	18.74	11.36	10.76
0.10	1%	41.24	16.18	8.56	4.02	1.68	1.16
	5%	56.14	30.00	19.30	11.32	6.68	5.80
	10%	63.30	38.78	27.12	19.24	12.50	10.88
0.20	1%	40.68	14.64	8.34	4.22	2.12	1.34
	5%	53.64	28.22	18.44	11.70	6.74	5.82
	10%	61.40	37.22	26.22	18.58	12.22	11.32

Table A.1: EMPIRICAL LEVELS OF THE WALD TEST FOR LONG-RUN SYMMETRY. The FM-TOLS estimator is used in the first step. The data is generated as follows: $\Delta y_t = -u_{t-1} + \varphi_* \Delta y_{t-1} + \boldsymbol{\pi}_{0*}^{+\prime} \Delta \boldsymbol{x}_t^+ + \boldsymbol{\pi}_{0*}^{-\prime} \Delta \boldsymbol{x}_t^- + e_t$, where $u_t := y_t - \boldsymbol{\beta}_*^{+\prime} \boldsymbol{x}_t^+ - \boldsymbol{\beta}_*^{-\prime} \boldsymbol{x}_t^-$, $\Delta \boldsymbol{x}_t = 0.5 \Delta \boldsymbol{x}_{t-1} + \sqrt{1 - 0.5^2} \boldsymbol{v}_t$, and $(e_t, \boldsymbol{v}_t')' \sim \text{IID} N(\mathbf{0}_3, \mathbf{I}_3)$. $\dot{H}_0^{(\ell)} : \boldsymbol{\iota}_2' \boldsymbol{\beta}_*^+ = -0.5$ and $\boldsymbol{\iota}_2' \boldsymbol{\beta}_*^- = -0.75$ vs. $\dot{H}_1^{(\ell)} : \boldsymbol{\iota}_2' \boldsymbol{\beta}_*^+ \neq -0.5$ or $\boldsymbol{\iota}_2' \boldsymbol{\beta}_*^- \neq -0.75$. The simulation results are obtained using $R = 5,000$ replications. When $\varphi_* = 0.2$ and $n = 10,000$, the empirical levels are 1.18%, 5.52%, and 10.50% for the empirical levels 1%, 5%, and 10%, respectively.

φ_*	sample size	100	200	300	400	500
-0.20	1%	47.46	70.16	90.44	98.10	99.74
	5%	62.40	80.76	94.26	99.00	99.88
	10%	70.16	85.42	96.18	99.32	99.92
-0.10	1%	48.76	71.48	91.24	98.04	99.68
	5%	62.14	81.50	94.80	99.08	99.84
	10%	70.28	86.02	96.42	99.36	99.86
0.00	1%	47.32	70.54	90.56	98.20	99.78
	5%	61.72	81.70	94.02	99.12	99.94
	10%	69.78	86.56	95.44	99.46	99.94
0.10	1%	46.36	69.20	90.22	98.06	99.86
	5%	60.26	79.82	94.00	98.98	99.96
	10%	67.16	84.56	95.86	99.36	99.98
0.20	1%	43.10	63.52	88.70	97.58	99.44
	5%	56.98	75.22	93.74	98.88	99.78
	10%	65.50	80.66	95.68	99.18	99.88

Table A.2: EMPIRICAL POWER OF THE WALD TEST FOR LONG-RUN SYMMETRY (IN PERCENT). The FM-TOLS estimator is used in the first step. The data is generated as follows: $\Delta y_t = -u_{t-1} + \varphi_* \Delta y_{t-1} + \boldsymbol{\pi}_{0*}^{+\prime} \Delta \boldsymbol{x}_t^+ + \boldsymbol{\pi}_{0*}^{-\prime} \Delta \boldsymbol{x}_t^- + e_t$, where $u_t := y_t - \boldsymbol{\beta}_*^{+\prime} \boldsymbol{x}_t^+ - \boldsymbol{\beta}_*^{-\prime} \boldsymbol{x}_t^-$, $\Delta \boldsymbol{x}_t = 0.5 \Delta \boldsymbol{x}_{t-1} + \sqrt{1 - 0.5^2} \boldsymbol{v}_t$, and $(e_t, \boldsymbol{v}_t')' \sim \text{IID} N(\mathbf{0}_3, \mathbf{I}_3)$. $\ddot{H}_0^{(\ell)} : \boldsymbol{\iota}_2' \boldsymbol{\beta}_*^+ = -0.4$ and $\boldsymbol{\iota}_2' \boldsymbol{\beta}_*^- = -0.65$ vs. $\ddot{H}_1^{(\ell)} : \boldsymbol{\iota}_2' \boldsymbol{\beta}_*^+ \neq -0.4$ or $\boldsymbol{\iota}_2' \boldsymbol{\beta}_*^- \neq -0.65$. The simulation results are obtained using $R = 5,000$ replications.

φ_*	sample size	100	200	400	600	800	1,000
-0.20	1%	10.92	3.98	2.10	1.88	1.42	1.06
	5%	22.80	11.20	7.20	6.60	6.40	5.62
	10%	32.52	17.88	13.38	12.12	11.40	10.56
-0.10	1%	10.58	3.72	2.02	1.34	1.20	1.22
	5%	22.50	11.12	7.56	6.36	6.06	5.84
	10%	32.18	18.66	13.38	12.28	11.38	10.94
0.00	1%	10.90	3.92	2.00	1.54	1.48	1.28
	5%	23.34	11.80	7.90	6.36	6.64	5.50
	10%	31.46	19.30	13.96	11.36	12.46	10.50
0.10	1%	10.80	3.98	2.00	1.36	1.44	1.26
	5%	22.60	11.96	7.36	6.54	6.46	5.40
	10%	30.78	18.68	12.74	12.38	12.16	10.82
0.20	1%	10.26	3.76	2.38	1.70	1.50	1.38
	5%	23.06	11.68	7.76	6.58	6.28	5.72
	10%	32.16	19.26	14.02	12.28	11.68	10.68

Table A.3: EMPIRICAL LEVELS OF THE WALD TEST FOR SHORT-RUN SYMMETRY (IN PERCENT). The FM-TOLS estimator is used in the first step and OLS is used in the second step. The data is generated as follows: $\Delta y_t = -u_{t-1} + \varphi_* \Delta y_{t-1} + \boldsymbol{\pi}_{0*}^{+\prime} \Delta \boldsymbol{x}_t^+ + \boldsymbol{\pi}_{0*}^{-\prime} \Delta \boldsymbol{x}_t^- + e_t$, where $u_t := y_t - \boldsymbol{\beta}_*^{+\prime} \boldsymbol{x}_t^+ - \boldsymbol{\beta}_*^{-\prime} \boldsymbol{x}_t^-$, $\Delta \boldsymbol{x}_t = 0.5 \Delta \boldsymbol{x}_{t-1} + \sqrt{1 - 0.5^2} \boldsymbol{v}_t$, and $(e_t, \boldsymbol{v}_t')' \sim \text{IID} N(\mathbf{0}_3, \mathbf{I}_3)$. $\dot{H}_0^{(s)} : \boldsymbol{\pi}_{0*}^+ - \boldsymbol{\pi}_{0*}^- = \mathbf{0}_2$ vs. $\dot{H}_1^{(s)} : \boldsymbol{\pi}_{0*}^+ - \boldsymbol{\pi}_{0*}^- \neq \mathbf{0}_2$. The simulation results are obtained using $R = 5,000$ replications.

φ_*	sample size	100	200	400	600	800	1,000
-0.20	1%	20.74	21.68	40.30	61.64	76.56	86.20
	5%	36.78	40.48	62.66	80.90	90.96	95.76
	10%	46.58	51.82	73.06	87.76	95.04	98.26
-0.10	1%	21.56	22.94	41.36	61.54	76.68	86.96
	5%	37.70	41.56	63.86	80.14	91.18	95.40
	10%	46.98	52.92	74.76	87.70	95.16	97.72
0.00	1%	21.04	23.38	42.32	61.96	76.86	86.66
	5%	36.70	42.28	64.08	81.12	90.50	95.58
	10%	46.52	53.74	74.38	88.60	94.46	97.34
0.10	1%	20.86	24.26	41.74	61.58	76.62	87.28
	5%	37.22	42.92	63.96	81.92	90.42	95.84
	10%	46.84	54.56	74.36	88.70	94.80	97.94
0.20	1%	20.48	23.32	42.08	62.02	76.58	86.82
	5%	36.56	42.84	63.60	80.88	90.20	95.28
	10%	46.76	53.20	73.78	87.98	94.48	97.42

Table A.4: EMPIRICAL POWER OF THE WALD TEST FOR SHORT-RUN SYMMETRY (IN PERCENT). The FM-TOLS estimator is used in the first step and OLS is used in the second step. The data is generated as follows: $\Delta y_t = -u_{t-1} + \varphi_* \Delta y_{t-1} + \boldsymbol{\pi}_{0*}^{+\prime} \Delta \boldsymbol{x}_t^+ + \boldsymbol{\pi}_{0*}^{-\prime} \Delta \boldsymbol{x}_t^- + e_t$, where $u_t := y_t - \boldsymbol{\beta}_*^{+\prime} \boldsymbol{x}_t^+ - \boldsymbol{\beta}_*^{-\prime} \boldsymbol{x}_t^-$, $\Delta \boldsymbol{x}_t = 0.5 \Delta \boldsymbol{x}_{t-1} + \sqrt{1 - 0.5^2} \boldsymbol{v}_t$, and $(e_t, \boldsymbol{v}_t')' \sim \text{IID} N(\mathbf{0}_3, \mathbf{I}_3)$. $\ddot{H}_0^{(s)} : \boldsymbol{\pi}_{0*}^+ - \boldsymbol{\pi}_{0*}^- = 0.3 \boldsymbol{\iota}_2$ vs. $\ddot{H}_1^{(s)} : \boldsymbol{\pi}_{0*}^+ - \boldsymbol{\pi}_{0*}^- \neq 0.3 \boldsymbol{\iota}_2$. The simulation results are obtained using $R = 5,000$ replications.

	Sample Size	50		100		150		200		250	
	First Step	OLS	FM-OLS	OLS	FM-OLS	OLS	FM-OLS	OLS	FM-OLS	OLS	FM-OLS
φ_*	Second Step	OLS	OLS	OLS	OLS	OLS	OLS	OLS	OLS	OLS	OLS
-0.50	β_*^+	-0.263	-0.130	-0.140	-0.038	-0.095	-0.017	-0.072	-0.010	-0.058	-0.006
	β_*^-	-0.269	-0.038	-0.140	-0.009	-0.095	-0.004	-0.071	-0.002	-0.058	-0.001
	ρ_*	-0.101	-0.083	-0.036	-0.029	-0.022	-0.017	-0.015	-0.012	-0.012	-0.009
	φ_*	0.112	0.074	0.055	0.028	0.036	0.016	0.028	0.012	0.023	0.009
	π_*^+	-0.062	-0.022	-0.026	0.004	-0.018	0.007	-0.012	0.005	-0.010	0.006
	π_*^-	-0.107	-0.038	-0.044	-0.008	-0.032	-0.008	-0.024	-0.006	-0.020	-0.005
-0.25	β_*^+	-0.185	-0.073	-0.098	-0.020	-0.066	-0.007	-0.050	-0.002	-0.040	-0.001
	β_*^-	-0.192	0.004	-0.099	0.002	-0.066	0.003	-0.050	0.004	-0.041	0.003
	ρ_*	-0.084	-0.070	-0.030	-0.026	-0.018	-0.017	-0.012	-0.012	-0.011	-0.010
	φ_*	0.088	0.044	0.048	0.016	0.033	0.008	0.025	0.006	0.020	0.004
	π_*^+	-0.042	-0.002	-0.024	0.002	-0.017	0.003	-0.010	0.005	-0.009	0.005
	π_*^-	-0.069	-0.011	-0.032	-0.005	-0.026	-0.007	-0.019	-0.004	-0.015	-0.003
0.00	β_*^+	-0.112	-0.033	-0.057	-0.010	-0.037	-0.001	-0.027	0.000	-0.022	0.002
	β_*^-	-0.117	0.023	-0.057	0.004	-0.037	0.005	-0.027	0.005	-0.022	0.004
	ρ_*	-0.081	-0.069	-0.035	-0.034	-0.024	-0.023	-0.017	-0.016	-0.013	-0.012
	φ_*	0.051	0.016	0.028	0.007	0.019	0.003	0.015	0.001	0.011	0.000
	π_*^+	-0.035	-0.010	-0.018	-0.006	-0.009	0.001	-0.008	0.000	-0.006	0.002
	π_*^-	-0.047	-0.007	-0.026	-0.011	-0.017	-0.007	-0.015	-0.007	-0.009	-0.003
0.25	β_*^+	-0.024	0.000	-0.009	-0.006	-0.006	-0.003	-0.004	-0.001	-0.004	-0.001
	β_*^-	-0.027	0.024	-0.010	-0.003	-0.007	-0.001	-0.004	0.000	-0.004	-0.001
	ρ_*	-0.072	-0.068	-0.035	-0.036	-0.022	-0.023	-0.017	-0.018	-0.014	-0.014
	φ_*	0.015	0.001	0.006	0.002	0.005	0.001	0.003	0.000	0.003	0.000
	π_*^+	-0.001	-0.004	-0.004	-0.011	0.001	-0.004	-0.003	-0.007	-0.001	-0.005
	π_*^-	-0.024	-0.022	-0.007	-0.015	-0.007	-0.012	-0.004	-0.008	-0.005	-0.008
0.50	β_*^+	0.065	0.015	0.034	-0.023	0.024	-0.016	0.018	-0.013	0.014	-0.011
	β_*^-	0.062	-0.004	0.034	-0.035	0.024	-0.021	0.017	-0.016	0.014	-0.012
	ρ_*	-0.046	-0.046	-0.022	-0.019	-0.015	-0.013	-0.011	-0.010	-0.008	-0.007
	φ_*	-0.016	-0.008	-0.009	0.002	-0.005	0.003	-0.004	0.002	-0.003	0.002
	π_*^+	0.023	-0.017	0.011	-0.021	0.010	-0.012	0.006	-0.012	0.005	-0.009
	π_*^-	0.026	-0.019	0.013	-0.021	0.007	-0.017	0.005	-0.012	0.004	-0.010

Table A.5: FINITE SAMPLE BIAS. This table reports the finite sample bias associated with our two-step estimation procedure, both in the case where OLS is used in the first step and in the case where FM-OLS is used in the first step. In all cases, OLS is used in the second step. The data is generated as follows: $\Delta y_t = -(2/3)u_{t-1} + \varphi_* \Delta y_{t-1} + \Delta x_t^+ + (1/2)\Delta x_t^- + e_t$, where $u_t := y_t - 2x_t^+ - x_t^-$, $\Delta x_t = 0.5\Delta x_{t-1} + \sqrt{1-0.5^2}v_t$, and $(e_t, v_t)' \sim \text{IID}N(\mathbf{0}_2, \mathbf{I}_2)$. The simulation results are obtained using $R = 5,000$ replications.

	Sample Size	50		100		150		200		250	
	First Step	OLS	FM-OLS	OLS	FM-OLS	OLS	FM-OLS	OLS	FM-OLS	OLS	FM-OLS
φ_*	Second Step	OLS	OLS	OLS	OLS	OLS	OLS	OLS	OLS	OLS	OLS
-0.50	β_*^+	0.104	0.057	0.029	0.009	0.013	0.003	0.007	0.001	0.005	0.001
	β_*^-	0.120	0.129	0.029	0.010	0.014	0.003	0.007	0.001	0.005	0.001
	ρ_*	0.026	0.024	0.006	0.006	0.003	0.003	0.002	0.002	0.002	0.002
	φ_*	0.020	0.013	0.006	0.004	0.003	0.002	0.002	0.001	0.002	0.001
	π_*^+	0.153	0.134	0.062	0.053	0.037	0.032	0.025	0.022	0.019	0.017
	π_*^-	0.180	0.152	0.062	0.053	0.038	0.032	0.026	0.022	0.020	0.017
-0.25	β_*^+	0.060	0.034	0.016	0.006	0.007	0.002	0.004	0.001	0.003	0.001
	β_*^-	0.068	0.096	0.016	0.007	0.007	0.002	0.004	0.001	0.003	0.001
	ρ_*	0.023	0.022	0.007	0.007	0.004	0.004	0.003	0.003	0.002	0.002
	φ_*	0.016	0.011	0.007	0.004	0.004	0.003	0.003	0.002	0.002	0.002
	π_*^+	0.136	0.125	0.055	0.051	0.034	0.031	0.023	0.021	0.018	0.017
	π_*^-	0.140	0.130	0.056	0.050	0.033	0.030	0.023	0.021	0.018	0.017
0.00	β_*^+	0.032	0.023	0.007	0.004	0.003	0.001	0.002	0.001	0.001	0.000
	β_*^-	0.036	0.045	0.007	0.005	0.003	0.001	0.002	0.001	0.001	0.000
	ρ_*	0.022	0.021	0.008	0.008	0.005	0.005	0.003	0.003	0.003	0.003
	φ_*	0.011	0.010	0.005	0.004	0.003	0.003	0.002	0.002	0.002	0.002
	π_*^+	0.126	0.121	0.050	0.048	0.031	0.030	0.022	0.022	0.018	0.017
	π_*^-	0.128	0.126	0.050	0.048	0.030	0.029	0.023	0.022	0.018	0.017
0.25	β_*^+	0.015	0.018	0.002	0.003	0.001	0.001	0.001	0.001	0.000	0.000
	β_*^-	0.015	0.034	0.003	0.004	0.001	0.001	0.001	0.001	0.000	0.000
	ρ_*	0.019	0.019	0.007	0.007	0.004	0.004	0.003	0.003	0.002	0.002
	φ_*	0.007	0.009	0.004	0.004	0.002	0.002	0.002	0.002	0.001	0.001
	π_*^+	0.116	0.117	0.047	0.046	0.030	0.029	0.021	0.021	0.017	0.017
	π_*^-	0.112	0.114	0.047	0.047	0.030	0.030	0.022	0.022	0.017	0.017
0.50	β_*^+	0.022	0.020	0.004	0.004	0.002	0.002	0.001	0.001	0.001	0.001
	β_*^-	0.022	0.033	0.004	0.007	0.002	0.002	0.001	0.001	0.001	0.001
	ρ_*	0.011	0.011	0.005	0.004	0.003	0.003	0.002	0.002	0.002	0.002
	φ_*	0.007	0.007	0.003	0.003	0.002	0.002	0.001	0.001	0.001	0.001
	π_*^+	0.116	0.115	0.045	0.046	0.030	0.030	0.021	0.021	0.017	0.017
	π_*^-	0.113	0.111	0.046	0.047	0.029	0.029	0.021	0.021	0.017	0.017

Table A.6: FINITE SAMPLE MEAN SQUARED ERROR (MSE) OF THE ESTIMATORS. This table reports the finite sample MSE associated with our two-step estimation procedure, both in the case where OLS is used in the first step and in the case where FM-OLS is used in the first step. In all cases, OLS is used in the second step. The data is generated as follows: $\Delta y_t = -(2/3)u_{t-1} + \varphi_* \Delta y_{t-1} + \Delta x_t^+ + (1/2)\Delta x_t^- + e_t$, where $u_t := y_t - 2x_t^+ - x_t^-$, $\Delta x_t = 0.5\Delta x_{t-1} + \sqrt{1-0.5^2}v_t$, and $(e_t, v_t)' \sim \text{IID}N(\mathbf{0}_2, \mathbf{I}_2)$. The simulation results are obtained using $R = 5,000$ replications.

	Sample Size	50		100		200		300		400		500	
	First Step	TOLS	FM-TOLS	TOLS	FM-TOLS	TOLS	FM-TOLS	TOLS	FM-TOLS	TOLS	FM-TOLS	TOLS	FM-TOLS
φ_*	Second Step	OLS	OLS	OLS	OLS	OLS	OLS	OLS	OLS	OLS	OLS	OLS	OLS
-0.20	β^+_{1*}	0.393	0.685	0.199	0.248	0.093	0.069	0.063	0.037	0.047	0.020	0.038	0.012
	β^+_{2*}	-0.329	-0.691	-0.162	-0.264	-0.080	-0.072	-0.053	-0.042	-0.039	-0.024	-0.031	-0.015
	β^-_{1*}	-0.426	-0.790	-0.207	-0.289	-0.100	-0.079	-0.067	-0.043	-0.049	-0.024	-0.040	-0.015
	β^-_{2*}	0.549	1.025	0.272	0.384	0.136	0.106	0.090	0.059	0.066	0.033	0.052	0.019
	ρ_*	-0.024	0.009	-0.007	-0.023	-0.002	-0.029	-0.001	-0.019	-0.001	-0.015	0.000	-0.011
	φ_*	0.018	0.053	0.007	0.044	0.002	0.025	0.001	0.015	0.001	0.010	0.001	0.007
	π^+_{1*}	0.009	0.214	0.003	0.078	0.000	0.025	0.000	0.011	0.000	0.007	0.000	0.004
	π^+_{2*}	-0.016	-0.288	-0.006	-0.113	-0.002	-0.027	-0.001	-0.014	-0.001	-0.007	-0.001	-0.002
	π^-_{1*}	-0.005	-0.233	0.001	-0.075	0.001	-0.019	0.000	-0.008	0.000	-0.006	0.000	-0.002
	π^-_{2*}	0.000	0.240	-0.003	0.085	-0.002	0.024	-0.001	0.014	-0.001	0.008	-0.001	0.004
-0.10	β^+_{1*}	0.390	0.694	0.190	0.259	0.090	0.075	0.059	0.040	0.044	0.021	0.034	0.015
	β^+_{2*}	-0.318	-0.683	-0.153	-0.265	-0.074	-0.078	-0.048	-0.043	-0.037	-0.024	-0.029	-0.016
	β^-_{1*}	-0.414	-0.779	-0.198	-0.293	-0.098	-0.086	-0.062	-0.047	-0.047	-0.025	-0.037	-0.018
	β^-_{2*}	0.522	0.999	0.252	0.384	0.121	0.111	0.080	0.062	0.059	0.034	0.047	0.022
	ρ_*	-0.158	0.019	-0.063	-0.016	-0.026	-0.026	-0.016	-0.017	-0.012	-0.013	-0.009	-0.011
	φ_*	0.124	0.050	0.068	0.042	0.034	0.024	0.024	0.015	0.017	0.010	0.013	0.007
	π^+_{1*}	0.073	0.227	0.017	0.079	0.003	0.024	0.001	0.013	0.003	0.008	-0.001	0.006
	π^+_{2*}	-0.109	-0.280	-0.048	-0.111	-0.021	-0.031	-0.010	-0.012	-0.010	-0.009	-0.008	-0.003
	π^-_{1*}	-0.030	-0.222	0.005	-0.071	0.004	-0.022	0.010	-0.009	0.004	-0.008	0.007	-0.005
	π^-_{2*}	-0.017	0.233	-0.036	0.088	-0.032	0.033	-0.026	0.016	-0.018	0.011	-0.015	0.008
0.00	β^+_{1*}	0.379	0.698	0.173	0.264	0.083	0.078	0.053	0.042	0.040	0.026	0.031	0.016
	β^+_{2*}	-0.317	-0.686	-0.146	-0.267	-0.071	-0.081	-0.047	-0.045	-0.034	-0.026	-0.028	-0.017
	β^-_{1*}	-0.409	-0.811	-0.186	-0.310	-0.092	-0.090	-0.058	-0.049	-0.044	-0.030	-0.034	-0.019
	β^-_{2*}	0.501	1.014	0.232	0.391	0.111	0.116	0.075	0.065	0.055	0.038	0.044	0.025
	ρ_*	-0.141	0.033	-0.057	-0.007	-0.025	-0.021	-0.014	-0.015	-0.011	-0.013	-0.008	-0.010
	φ_*	0.112	0.044	0.061	0.040	0.032	0.023	0.021	0.015	0.017	0.010	0.013	0.007
	π^+_{1*}	0.084	0.237	0.015	0.089	0.003	0.027	0.002	0.016	0.001	0.011	-0.002	0.006
	π^+_{2*}	-0.106	-0.287	-0.043	-0.118	-0.023	-0.029	-0.014	-0.014	-0.009	-0.012	-0.007	-0.007
	π^-_{1*}	-0.041	-0.239	0.011	-0.086	0.008	-0.025	0.010	-0.013	0.007	-0.009	0.007	-0.008
	π^-_{2*}	-0.027	0.226	-0.045	0.094	-0.033	0.037	-0.023	0.019	-0.019	0.016	-0.015	0.009
0.10	β^+_{1*}	0.345	0.729	0.169	0.272	0.077	0.083	0.049	0.048	0.036	0.030	0.029	0.019
	β^+_{2*}	-0.306	-0.706	-0.148	-0.291	-0.067	-0.085	-0.042	-0.049	-0.032	-0.030	-0.026	-0.020
	β^-_{1*}	-0.389	-0.829	-0.182	-0.311	-0.086	-0.095	-0.053	-0.054	-0.040	-0.034	-0.033	-0.022
	β^-_{2*}	0.476	1.059	0.223	0.411	0.101	0.122	0.066	0.071	0.049	0.043	0.039	0.029
	ρ_*	-0.125	0.051	-0.050	0.005	-0.020	-0.018	-0.014	-0.012	-0.010	-0.011	-0.007	-0.009
	φ_*	0.101	0.035	0.055	0.038	0.029	0.022	0.021	0.013	0.015	0.010	0.012	0.007
	π^+_{1*}	0.056	0.258	0.018	0.092	0.004	0.036	0.001	0.019	-0.001	0.014	-0.001	0.008
	π^+_{2*}	-0.105	-0.294	-0.042	-0.129	-0.019	-0.035	-0.008	-0.020	-0.009	-0.014	-0.007	-0.007
	π^-_{1*}	-0.022	-0.239	0.013	-0.081	0.010	-0.029	0.012	-0.014	0.009	-0.015	0.006	-0.008
	π^-_{2*}	-0.027	0.265	-0.041	0.100	-0.033	0.042	-0.022	0.026	-0.019	0.018	-0.014	0.011
0.20	β^+_{1*}	0.338	0.747	0.150	0.283	0.069	0.089	0.044	0.052	0.033	0.031	0.027	0.022
	β^+_{2*}	-0.313	-0.754	-0.138	-0.282	-0.063	-0.091	-0.040	-0.051	-0.031	-0.031	-0.025	-0.021
	β^-_{1*}	-0.373	-0.850	-0.174	-0.323	-0.077	-0.101	-0.050	-0.059	-0.037	-0.035	-0.030	-0.024
	β^-_{2*}	0.461	1.086	0.203	0.423	0.091	0.131	0.059	0.075	0.044	0.046	0.034	0.032
	ρ_*	-0.110	0.068	-0.045	0.011	-0.019	-0.013	-0.012	-0.011	-0.009	-0.010	-0.006	-0.008
	φ_*	0.086	0.026	0.049	0.033	0.026	0.020	0.018	0.013	0.014	0.008	0.011	0.006
	π^+_{1*}	0.061	0.263	0.016	0.108	-0.003	0.033	-0.002	0.025	0.001	0.015	0.001	0.012
	π^+_{2*}	-0.112	-0.327	-0.043	-0.119	-0.022	-0.042	-0.010	-0.020	-0.007	-0.013	-0.008	-0.011
	π^-_{1*}	-0.014	-0.243	0.007	-0.094	0.016	-0.031	0.011	-0.023	0.008	-0.015	0.007	-0.010
	π^-_{2*}	-0.025	0.277	-0.043	0.108	-0.035	0.046	-0.025	0.028	-0.022	0.020	-0.016	0.014

Table A.7: FINITE SAMPLE BIAS. This table reports the finite sample bias associated with our two-step estimation procedure, both in the case where the TOLS is used in the first step and in the case where the FM-TOLS is used in the first step. In all cases, OLS is used in the second step. The data is generated as follows: $\Delta y_t = -u_{t-1} + \varphi_* \Delta y_{t-1} + \boldsymbol{\pi}^{+\prime}_{0*} \Delta \boldsymbol{x}^+_t + \boldsymbol{\pi}^{-\prime}_{0*} \Delta \boldsymbol{x}^-_t + e_t$, where $u_t := y_t - \boldsymbol{\beta}^{+\prime}_* \boldsymbol{x}^+_t - \boldsymbol{\beta}^{-\prime}_* \boldsymbol{x}^-_t$, $\Delta \boldsymbol{x}_t = 0.5 \Delta \boldsymbol{x}_{t-1} + \sqrt{1 - 0.5^2} \boldsymbol{v}_t$, and $(e_t, \boldsymbol{v}'_t)' \sim \text{IID} N(\mathbf{0}_3, \mathbf{I}_3)$. The simulation results are obtained using $R = 5,000$ replications.

	Sample Size	50		100		200		300		400		500	
	First Step	TOLS	FM-TOLS	TOLS	FM-TOLS	TOLS	FM-TOLS	TOLS	FM-TOLS	TOLS	FM-TOLS	TOLS	FM-TOLS
φ_*	Second Step	OLS	OLS	OLS	OLS	OLS	OLS	OLS	OLS	OLS	OLS	OLS	OLS
-0.20	β^+_{1*}	0.427	1.201	0.105	0.193	0.024	0.019	0.011	0.006	0.006	0.002	0.004	0.001
	β^+_{2*}	0.397	1.254	0.091	0.197	0.022	0.020	0.010	0.007	0.005	0.003	0.003	0.001
	β^-_{1*}	0.471	1.436	0.105	0.219	0.026	0.022	0.011	0.007	0.006	0.003	0.004	0.001
	β^-_{2*}	0.537	1.865	0.126	0.293	0.031	0.028	0.014	0.009	0.008	0.003	0.005	0.002
	ρ_*	0.001	0.047	0.000	0.011	0.000	0.003	0.000	0.002	0.000	0.001	0.000	0.001
	φ_*	0.001	0.020	0.000	0.006	0.000	0.002	0.000	0.001	0.000	0.001	0.000	0.001
	π^+_{1*}	0.008	0.547	0.001	0.133	0.000	0.031	0.000	0.017	0.000	0.011	0.000	0.009
	π^+_{2*}	0.008	0.614	0.001	0.135	0.000	0.033	0.000	0.017	0.000	0.011	0.000	0.008
	π^-_{1*}	0.008	0.587	0.001	0.128	0.000	0.031	0.000	0.017	0.000	0.011	0.000	0.008
	π^-_{2*}	0.007	0.511	0.001	0.122	0.000	0.032	0.000	0.018	0.000	0.011	0.000	0.009
-0.10	β^+_{1*}	0.445	1.257	0.098	0.192	0.023	0.019	0.010	0.006	0.005	0.002	0.003	0.001
	β^+_{2*}	0.378	1.234	0.087	0.192	0.020	0.019	0.008	0.007	0.005	0.002	0.003	0.001
	β^-_{1*}	0.438	1.438	0.098	0.224	0.024	0.022	0.010	0.008	0.006	0.003	0.003	0.001
	β^-_{2*}	0.509	1.812	0.114	0.289	0.027	0.028	0.011	0.010	0.006	0.003	0.004	0.002
	ρ_*	0.043	0.041	0.010	0.010	0.003	0.003	0.002	0.002	0.001	0.001	0.001	0.001
	φ_*	0.024	0.018	0.008	0.006	0.003	0.002	0.001	0.001	0.001	0.001	0.001	0.001
	π^+_{1*}	0.382	0.549	0.102	0.130	0.036	0.031	0.020	0.017	0.014	0.011	0.010	0.009
	π^+_{2*}	0.378	0.569	0.111	0.133	0.035	0.032	0.020	0.017	0.014	0.011	0.010	0.009
	π^-_{1*}	0.355	0.565	0.102	0.126	0.034	0.031	0.020	0.017	0.013	0.011	0.010	0.009
	π^-_{2*}	0.341	0.507	0.105	0.126	0.037	0.032	0.021	0.018	0.014	0.012	0.011	0.009
0.00	β^+_{1*}	0.429	1.254	0.088	0.190	0.020	0.020	0.008	0.006	0.005	0.003	0.003	0.001
	β^+_{2*}	0.371	1.350	0.077	0.196	0.019	0.020	0.008	0.007	0.004	0.003	0.003	0.001
	β^-_{1*}	0.440	1.516	0.093	0.235	0.021	0.024	0.009	0.008	0.005	0.003	0.003	0.001
	β^-_{2*}	0.476	1.933	0.099	0.305	0.023	0.030	0.010	0.010	0.006	0.004	0.004	0.002
	ρ_*	0.037	0.042	0.009	0.009	0.003	0.003	0.001	0.002	0.001	0.001	0.001	0.001
	φ_*	0.021	0.018	0.007	0.006	0.002	0.002	0.001	0.001	0.001	0.001	0.001	0.001
	π^+_{1*}	0.365	0.549	0.099	0.127	0.034	0.030	0.019	0.017	0.013	0.012	0.010	0.009
	π^+_{2*}	0.352	0.609	0.096	0.132	0.033	0.031	0.019	0.017	0.013	0.012	0.009	0.009
	π^-_{1*}	0.343	0.559	0.102	0.124	0.033	0.030	0.020	0.017	0.013	0.012	0.010	0.009
	π^-_{2*}	0.332	0.505	0.098	0.122	0.035	0.031	0.020	0.017	0.014	0.012	0.010	0.009
0.10	β^+_{1*}	0.397	1.286	0.084	0.209	0.017	0.021	0.007	0.007	0.004	0.003	0.003	0.001
	β^+_{2*}	0.372	1.294	0.078	0.219	0.017	0.022	0.007	0.007	0.004	0.003	0.002	0.001
	β^-_{1*}	0.416	1.551	0.087	0.238	0.019	0.026	0.008	0.008	0.004	0.003	0.003	0.002
	β^-_{2*}	0.461	2.088	0.097	0.323	0.020	0.032	0.009	0.011	0.005	0.004	0.003	0.002
	ρ_*	0.030	0.041	0.007	0.009	0.002	0.002	0.001	0.001	0.001	0.001	0.001	0.001
	φ_*	0.018	0.016	0.006	0.006	0.002	0.002	0.001	0.001	0.001	0.001	0.001	0.001
	π^+_{1*}	0.340	0.539	0.095	0.131	0.032	0.031	0.018	0.017	0.013	0.012	0.010	0.009
	π^+_{2*}	0.336	0.567	0.091	0.143	0.032	0.031	0.018	0.017	0.013	0.012	0.010	0.009
	π^-_{1*}	0.317	0.553	0.091	0.126	0.032	0.032	0.020	0.018	0.013	0.011	0.010	0.009
	π^-_{2*}	0.318	0.532	0.095	0.126	0.032	0.032	0.020	0.018	0.014	0.012	0.011	0.009
0.20	β^+_{1*}	0.388	1.444	0.074	0.210	0.016	0.023	0.006	0.008	0.004	0.003	0.002	0.001
	β^+_{2*}	0.392	1.475	0.072	0.209	0.015	0.022	0.006	0.008	0.004	0.003	0.002	0.001
	β^-_{1*}	0.412	1.707	0.080	0.257	0.017	0.027	0.007	0.009	0.004	0.003	0.002	0.002
	β^-_{2*}	0.460	2.209	0.091	0.342	0.018	0.034	0.007	0.012	0.004	0.004	0.003	0.002
	ρ_*	0.025	0.040	0.006	0.009	0.002	0.002	0.001	0.001	0.001	0.001	0.001	0.001
	φ_*	0.015	0.015	0.005	0.005	0.002	0.002	0.001	0.001	0.001	0.001	0.001	0.001
	π^+_{1*}	0.320	0.555	0.086	0.136	0.030	0.032	0.018	0.018	0.012	0.011	0.009	0.009
	π^+_{2*}	0.336	0.613	0.090	0.137	0.032	0.033	0.018	0.017	0.013	0.011	0.010	0.009
	π^-_{1*}	0.323	0.561	0.089	0.136	0.031	0.031	0.017	0.017	0.012	0.012	0.010	0.009
	π^-_{2*}	0.307	0.532	0.092	0.125	0.033	0.033	0.019	0.018	0.013	0.012	0.010	0.009

Table A.8: FINITE SAMPLE MEAN SQUARED ERROR (MSE) OF THE ESTIMATORS. This table reports the finite sample MSE associated with our two-step estimation procedure, both in the case where the TOLS is used in the first step and in the case where the FM-TOLS is used in the first step. In all cases, OLS is used in the second step. The data is generated as follows: $\Delta y_t = -u_{t-1} + \varphi_* \Delta y_{t-1} + \boldsymbol{\pi}^{+\prime}_{0*} \Delta \boldsymbol{x}^+_t + \boldsymbol{\pi}^{-\prime}_{0*} \Delta \boldsymbol{x}^-_t + e_t$, where $u_t := y_t - \boldsymbol{\beta}^{+\prime}_* \boldsymbol{x}^+_t - \boldsymbol{\beta}^{-\prime}_* \boldsymbol{x}^-_t$, $\Delta \boldsymbol{x}_t = 0.5 \Delta \boldsymbol{x}_{t-1} + \sqrt{1 - 0.5^2} \boldsymbol{v}_t$, and $(e_t, \boldsymbol{v}'_t)' \sim \text{IID} N(\mathbf{0}_3, \mathbf{I}_3)$. The simulation results are obtained using $R = 5,000$ replications.

	$\Delta \log$ GPDI	Δ(R&D/GDP)
Mean	0.009	0.004
Median	0.009	0.001
Maximum	0.110	0.082
Minimum	-0.176	-0.082
Standard Deviation	0.039	0.028
Skewness	-0.752	0.190
Excess Kurtosis	2.701	0.256
Sample Size	240	240

Table A.9: DESCRIPTIVE STATISTICS. Descriptive statistics are computed over 240 quarters from 1960Q1 to 2019Q4. GPDI is measured in US Dollars at 2012 prices and seasonally adjusted. R&D and GDP are seasonally adjusted nominal values.

PP test	$\log$ GPDI	R&D/GDP
PP test w/o trend	-1.138	-1.946
p-value	0.701	0.311
PP test w/ trend	-3.198	-2.255
p-value	0.087	0.457

Table A.10: PHILLIPS AND PERRON'S (1988) UNIT-ROOT TEST STATISTICS. Two Phillips and Perron test statistics are computed, one including and the other excluding a time trend. When the time trend is included, it is statistically significant for the log of GPDI but not for R&D intensity. The lag lengths are selected by the SIC when estimating the ADF equations.

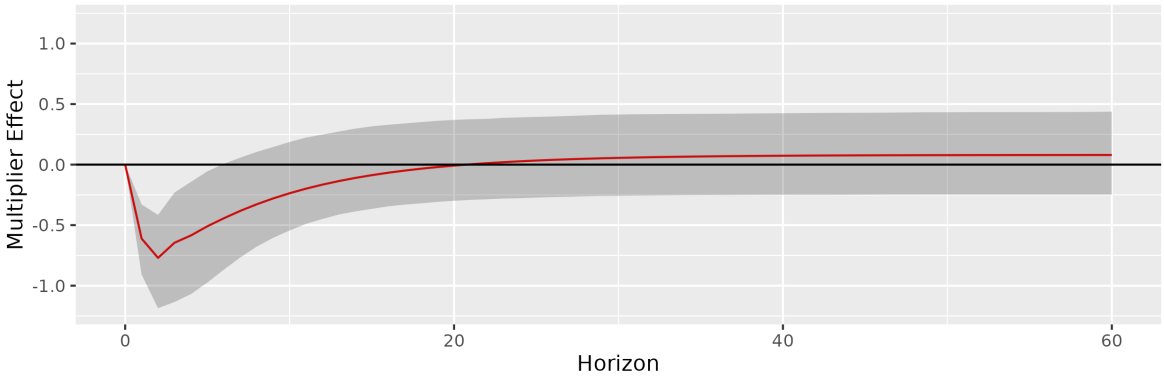

(a) Cumulative response of i_{t+h} to a +1 unit shock to r_t^+ in period 1

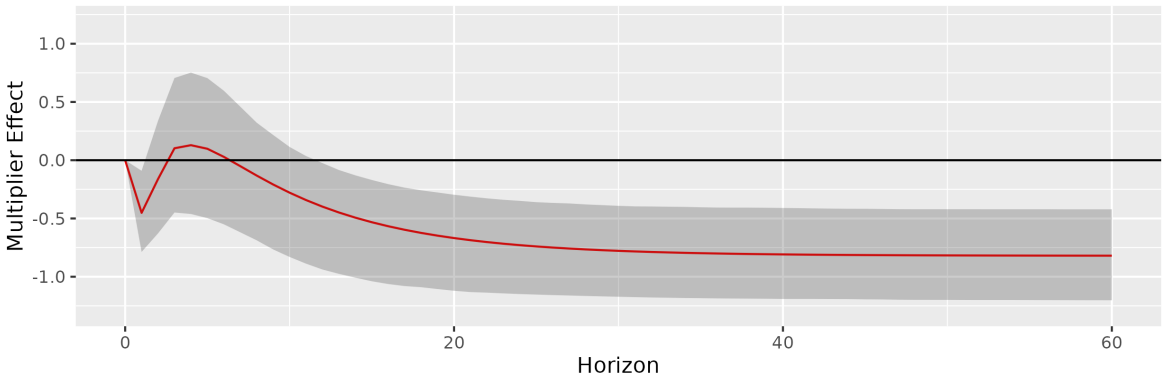

(b) Cumulative response of i_{t+h} to a +1 unit shock to r_t^- in period 1

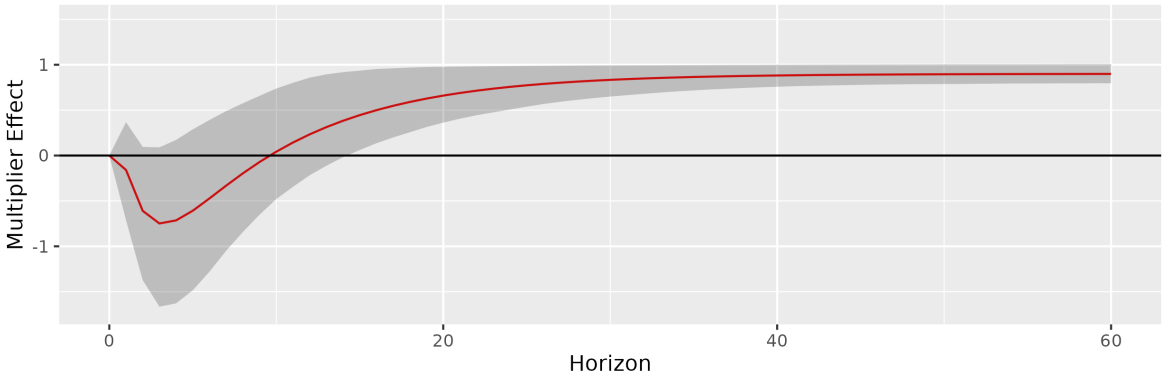

(c) Asymmetry across horizons

Figure A.1: CUMULATIVE DYNAMIC MULTIPLIERS (SINGLE-STEP). Panels (a) and (b) present the cumulative dynamic multiplier effects with respect to unit shocks to r_t^+ and r_t^-, respectively, occurring in period 1. Panel (c) shows the asymmetry at each horizon, i.e., the value of the cumulative dynamic multiplier effect in panel (b) subtracted from the corresponding value in panel (a). Empirical 95% confidence intervals obtained from 5,000 replications of a moving block bootstrap procedure are reported throughout.